DIGITAL COMPUTATION OF TRANSIENTS AND SAFETY TESTING OF MINE ELECTRICAL POWER SYSTEMS

Prepared for

UNITED STATES DEPARTMENT OF THE INTERIOR
BUREAU OF MINES

by

WEST VIRGINIA UNIVERSITY
MORGANTOWN, WEST VIRGINIA 26506

Annual Report for June 24, 1975 to June 23, 1976

on

Grant No. G0144137

July, 1976

OFR 41-77

DIGITAL COMPUTATION OF TRANSIENTS AND SAFETY TESTING OF MINE ELECTRICAL POWER SYSTEMS

Prepared for

UNITED STATES DEPARTMENT OF THE INTERIOR
BUREAU OF MINES

by

WEST VIRGINIA UNIVERSITY
MORGANTOWN, WEST VIRGINIA 26506

Annual Report for June 24, 1975 to June 23, 1976

on

Grant No. G0144137

July, 1976

DISCLAIMER NOTICE

"The views and conclusions contained in this document are those of the authors and should not be interpreted as necessarily representing the official policies of the Interior Department's Bureau of Mines or the U. S. Government."

1. Report No.	2.	3. Recipient's Accession No.

4. Title and Subtitle	5. Report Date
Digital Computation of Transients and Safety Testing of Mine Electrical Power Systems	Submitted September, 1976
	6.

7. Author(s)	8. Performing Organization Report No.
Eldon Keith Stanek	

9. Performing Organization Name and Address	10. Project/Task/Work Unit No.
Department of Electrical Engineering West Virginia University Morgantown, WV 26506	11. Contract or Grant No. G0144137

12. Sponsoring Organization Name and Address	13. Type of Report
Office of the Assistant Director - Mining Bureau of Mines Department of the Interior Washington, D.C. 20241	Annual report for June 24, 1975 to June 23, 1976
	14.

15. Supplementary Notes

16. Abstract

This annual report deals with four distinct tasks related to research on the safety and reliability of mine electrical power systems. Task one is to develop tests and the associated instrumentation to detect incipient faults on a mine or any low-voltage power system. Task two is a dual effort related to the digital prediction of electrical transients on mine power systems and laboratory testing of transient suppression devices. Task three is also a dual effort. This task consists of both theoretical and laboratory work to assess both the reliability and the fail-safe characteristics of several items of protective equipment used in mine power systems. Task four consists of an effort to use programmable calculators and/or computer terminals to check overcurrent protective device coordination.

17. Originator's Key Words		18. Availability Statement
Mine Power Systems Insulation Testing Digital Computation of Transients Transient Suppression Relay/Fuse Coordination	Fail-Safe Reliability	

19. U. S. Security Classif. of the Report	20. U. S. Security Classif. of This Page	21. No. of Pages	22. Price
N/A	N/A		

FOREWORD

This report was prepared by West Virginia University, Engineering Experiment Station, Morgantown, West Virginia under USBM Grant No. G0144137. The grant was initiated under the Coal Mine Health and Safety Research Program. It was administered under the technical direction of the Pittsburgh Mining and Safety Research Center with Mr. G. J. Conroy acting as the technical project officer. Mr. A. G. Young was the contract administrator for the Bureau of Mines.

This report is a summary of the work recently completed as part of this grant during the period 6-24-75 to 6-23-76. This report was submitted by the authors 8-9-76.

This technical report has been reviewed and approved.

TABLE OF CONTENTS

CHAPTER I

PERIODIC INSPECTION OF MINE POWER SYSTEMS

1.1 INTRODUCTION

The tests outlined in last year's annual report were performed on mine power systems as well as pieces of equipment in the laboratory. Time was also spent in building up test equipment. Statistical means were also devised to analyze the test data.

Enough data have not been accumulated to make a final assessment of the capabilities of each test to detect incipient faults. This is partly due to the fact that visits could not be arranged to different mines on a regular basis. This difficulty is being overcome and there is at least one mine (Federal #2 at Blacksville) where some of the tests have been carried out on a regular basis and test data compared. The comparison is shown in Appendix A of Chapter I.

The status of various tests is described below.

1.2 INSULATION RESISTANCE TESTING

1.2.1 Test Results

The insulation resistance tests were carried out both in the laboratory as well on various pieces of electrical equipment in different mines. Typical results obtained are indicated in Tables 1.1 thru 1.7.

Table 1.1

Windings of an Old DC Machine (Laboratory)

Applied Voltage (volts)	Insulation Resistance (MΩ)					
	A to frame	F to frame	S to frame	F to A	F to S	S to A
100	70	100	0	200	150	60
250	50	90	0	140	90	40
500	43	85	0	130	85	92
1000	40	84	0	120	84	36

Legend: A = armature winding
F = shunt field winding
S = series field winding

Table 1.2

Used Cable (Laboratory)

Applied voltage (volts)	Insulation Resistance (MΩ)		
	Phase a to b	Phase b to c	Phase a to c
100	∞	∞	∞
250	500	∞	500
500	500	∞	500
1000	450	1500	450

Table 1.3

Main Cable Outgoing to Shear (Delmont Mine)

Applied voltage (volts)	Insulation Resistance (MΩ)				
	Phase a to b	Phase c to b	Phase b to G*	Phase c to G	Phase a to G
100	∞	∞	∞	∞	∞
250	600	500	250	100	180
500	600	500	240	90	150
1000	500	400	230	80	150

G* = ground

Table 1.4

Circuit Breaker No. 1 (Delmont Mine)

Applied Voltage (volts)	Insulation Resistance (MΩ)		
	Phase c to G	Phase b to G	Phase a to G
100	∞	∞	∞
250	35	25	20
500	30	22	20
1000	30	18	17

Table 1.5

Circuit Breaker No. 2. (Delmont Mine)

Applied voltage (volts)	Insulation Resistance (MΩ)		
	Phase c to G	Phase b to G	Phase a to G
100	∞	∞	∞
250	375	375	400
500	350	350	350
1000	320	340	350

Table 1.6

Miner Outgoing Cable (Delmont Mine)

Applied voltage (volts)	Insulation Resistance (MΩ)			
	Phase b to c	Phase c to G	Phase b to G	Phase a to G
100	∞	∞	∞	∞
250	400	350	350	300
500	400	300	300	300
1000	400	300	300	300

Table 1.7

Roof Bolter Cable (Delmont Mine)

Applied voltage (volts)	Insulation Resistance (MΩ)		
	Phase b to c	Phase a to c	Phase c to G
100	∞	∞	∞
250	100	100	100
500	90	90	85
1000	80	80	80

1.2.2 Analysis of Insulation Resistance Data

Results for a defective dc machine are shown in Table 1.1. As can be seen from Table 1.1, as the applied voltage is increased the insulation resistance decreases appreciably. For example, the insulation resistance of the armature windings to frame is 70 MΩ at 100 volts and it is only 40 MΩ at 1000 volts, a drop of almost 43%. Insulation resistance of shunt field windings to armature windings is 200 MΩ at 100 volts and it is 120 MΩ at 1000 volts, a drop of 40%. This is an indication of insulation weakness. This insulation weakness could also be noted in the other types of tests, which were carried out on the windings of this machine.

It is clear that this dc machine has a short from the series field to the frame. This is not the type of problem that the tests are designed to detect. Hopefully, the periodic tests will detect problems before they develop into complete short circuits.

The insulation resistance of a used cable is shown in Table 1.2. As the applied voltage is increased the insulation resistance does not decrease appreciably. For example, the insulation resistance of phase a to b is 500 MΩ at 250 and 450 at 1000 volts, a drop of 10%, therefore, the insulation is sound.

Tables 1.3 thru 1.7 give the insulation resistances of different pieces of equipment in a mine. All of these equipments appear to have sound insulation.

A large volume of data on insulation resistances were gathered on other pieces of equipment. All of these devices appear to be sound with typical values of cables being in the neighborhood of 100 MΩ and above. Minimum values for circuit breakers appear to be about 20 MΩ.

Based on a large volume of data, in the step-voltage test, a drop of 30% (or more) of insulation resistance at higher voltage is an indication of insulation weakness, even though the readings may be higher than the suggested minimum safe values (insulation resistance should be approximately one megohm for each 1000 volts of operating voltage, with a minimum value of one megohm).

The insulation resistance readings, should preferably be corrected to a base temperature, such as 20°C, or all the readings should be taken at approximately the same temperature. One rule of thumb is for every 10°C increase in temperature the resistance should be halved, or for every 10°C decrease, the resistance should be doubled.

For example a two megohm resistance at 20°C reduces to 1/2 megohm at 40°C. This can more precisely be done using temperature correction factors table.[1]

Commonly used dc test voltages for routine maintenance are as follows:

Equipment ac rating	dc tests voltage
Up to 100 volts	100 and 250 volts
440 to 550 volts	500 and 1000 volts
2400 volts	1000 to 2500 volts, or higher
4160 volts and above	1000 to 5000 volts, or higher

1.3 POWER FACTOR MEASUREMENT

1.3.1 Introduction to Insulation Power Factor

During the past year, the electronic power factor meter was built. Also a capacitance and dissipation factor bridge was purchased.

This bridge is a compact instrument designed to accurately measure the capacitance and dissipation factor (cotangent of the power factor angle = cot θ = cos θ/sin $\theta \approx$ cos θ for θ near 90°), of electrical insulating materials. The instrument can be used for measurements of cable insulation, transformer insulation, generator and motor coil insulation, bushing and switchgear insulation and capacitance. This bridge has the following features.

a. A phase-sensitive detector allows independent balancing of capacitance and dissipation factor controls.

b. 100 Hz excitation uses a tuned, synchronous detector to overcome power frequency interference problems.

c. The device provides 3-terminal tests on ungrounded samples, 3-terminal tests on grounded samples, and 2-terminal tests on permanently grounded samples.

d. Low-30-volt operation reduces shock hazard, and size and weight of the instrument.

The complete specifications are given in Appendix B.

The only disadvantages with the bridge are that it does not allow measurements at variable voltage or frequency. These measurements can be carried out using the electronic power factor meter.

1.3.2 Laboratory and Field Results

Capacitance, dissipation factor and power factor measurements were carried out in the mines or laboratory on numerous pieces of equipment. Typical results are shown in Tables 1.8 through 1.14.

Table 1.8

Capacitance and Dissipation Factor Measurement of an "Old" Induction Motor Windings

Connection	Capacitance (in pF)	Dissipation Factor (percent)	Calculated Power Factor (percent)
T6,T7,T8 to T2, T5	584.5	22.84	22.26
T6,T7,T8 to T1,T4	527.6	21.83	21.32
T6,T7,T8 to T3,T6	560.9	22.14	21.61
T2,T5 to T1,T4	259.6	21.19	20.73
T2,T5 to T3,T6	269.2	21.73	21.23
T3,T6 to T1,T4	310.2	22.31	21.77
T6,T7,T8 to frame	2225.4	21.21	20.74
T2,T5 to frame	898.4	22.29	21.75
T1,T4 to frame	864.8	21.44	20.96
T3,T6 to frame	898.2	21.75	21.25

Legend: T1,T2,T3,T4,T5,T6,T7, and T8 are various windings arrangements of an induction motor.

Table 1.9

Capacitance and Dissipation Factor Measurement of an "Old" DC Machine Windings

Connection	Capacitance (pF)	Dissipation Factor (percent)	Calculated Power Factor (percent)
A to frame	2243.5	21.65	21.16
F to frame	1050.8	19.50	19.14
A to S	Short	Short	Short
A to F	1055.6	19.39	19.03

Legend: A = armature winding
F = shunt field winding
S = series field winding

Table 1.10

Capacitance and Dissipation Factor Measurement of a "new" cable (200 feet)

Connection	Capacitance (μF)	Dissipation Factor (percent)	Calculated Power Factor (percent)
B to R	1.0395×10^{-2}	4.51	4.50
B to Y	9.921×10^{-3}	3.90	3.89
R to Y	1.459×10^{-2}	5.35	5.34
Y to G	1.5156×10^{-2}	6.27	6.25
R to G	2.0328×10^{-2}	6.14	6.12
B to G	1.5116×10^{-2}	6.06	6.04

Legend: B = Black
R = Red
Y = Yellow
G = Ground

Table 1.11

Capacitance and Dissipation Factor Measurement of an "old" cable (30 feet)

Connection	Capacitance (μF)	Dissipation Factor (percent)	Calculated Power Factor (percent)
a to b	1.4138×10^3	8.52	8.49
a to c	2.097×10^3	9.32	9.28
b to c	3.425×10^3	7.07	7.05
a to G	2.066×10^3	8.97	8.93
b to G	3.426×10^3	7.00	6.98
c to G	2.34×10^3	9.20	9.16

Legend: a = phase a
b = phase b
c = phase c
G = ground conductor

Table 1.12

Capacitance and Dissipation Factor of an Outgoing Distribution Cable to Shaft 6-Type G

Connection	Capacitance (μF)	Dissipation Factor (percent)	Calculated Power Factor (percent)
a to b	.05431	6.79	6.77
a to c	.05348	6.79	6.77
b to c	.05348	6.79	6.77
c to G	.09204	9.48	9.43
b to G	.09245	9.03	8.99
a to G	.09310	9.10	9.06

Legend: a = phase a
b = phase b
c = phase c
G = ground conductor

Table 1.13

Power Factor Measurement of a "new" cable (200 feet)
(using electronic pF meter)

Applied Voltage 500 volts

Connection	Power Factor (percent)
B to R	4.5
B to Y	4.5
R to Y	4.5
Y to G	6.12
R to G	6.12
B to G	6.12

Legend: B = Black
R = Red
Y = Yellow
G = Ground Conductor

Table 1.14

Power Factor Measurement of an old Cable 30 feet

Applied Voltage 500 volts

Connection	Power Factor (percent)
R to B	8.5
R to Y	8.5
Y to B	8.5
R to G	9.0
Y to G	9.0
B to G	9.0

1.3.3 Analysis of Dissipation Factor and Power Factor Data

Some of the typical results obtained from a large volume of data gathered on a variety of electrical equipment both in mines and in the laboratory has been presented. Table 1.9 is a significant result since it shows a shorted winding (armature to series field) as well as apparently sound insulation between various windings and the frame in an old dc machine. It should be noted that not only was one winding shorted to another but also all of the dissipation factors were significantly higher than in sound machines.

Similar analysis of dissipation factors measured for old and new cables pointed up significantly higher values for old and worn cable samples. Based completely on an empirical approach it was concluded that a dissipation factor in excess of 20% is an indicator of questionable insulation integrity.

1.4 HARMONIC DETECTION

1.4.1 Introduction To Harmonic Detection

It was indicated in the last year's report that insulation deterioration might cause audio frequency harmonics to be present in the charging current waveform. This suggested a method for detecting incipient faults by performing spectrum analysis of the waveform. However, it could not be experimentally verified because of the unavailability of suitable measuring equipment.

This year a low-frequency tuning section for a spectrum analyzer available at WVU was procured. A spectrum analyzer is a swept receiver that provides a CRT display of signal amplitude versus frequency. It displays the Fourier components of a given waveform.

Tests were carrried out at elevated voltage levels on a variety of equipment in the laboratory. Typical spectrum analysis displays for various equipment are shown in Fig. 1.1.

1.4.2 Analysis of Spectrum Analyzer Display

All the tests were carried out at 4 kV ac. The settings of the spectrum analyzer were as follows:

Bandwidth	3 kHZ
Scanwidth	10 kHZ/Div. Thus the entire width of screen corresponds to 100 kHz.
Scan Time	50 msec.

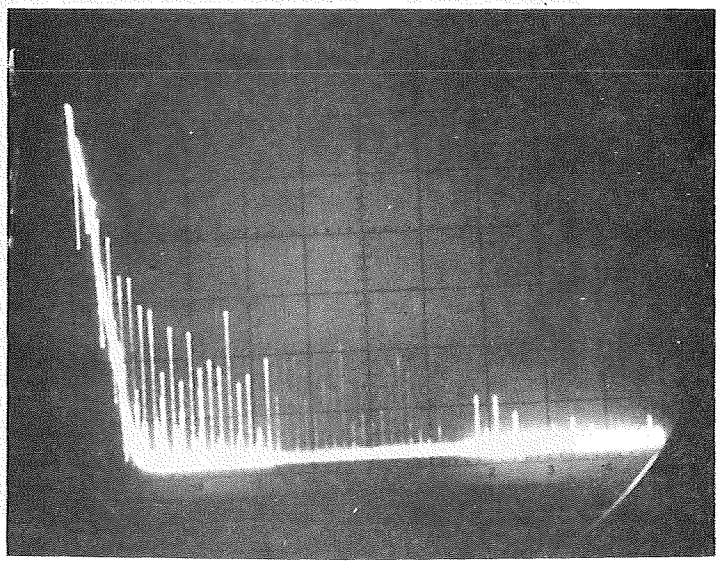

a) Old Induction Motor

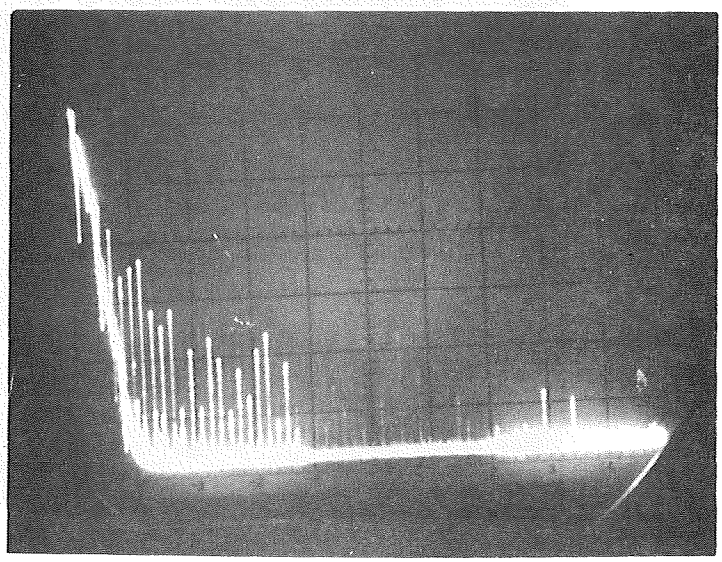

b) Old dc Machine

Fig. 1.1. Spectrum Analyzer Display for Various Pieces of Equipment.

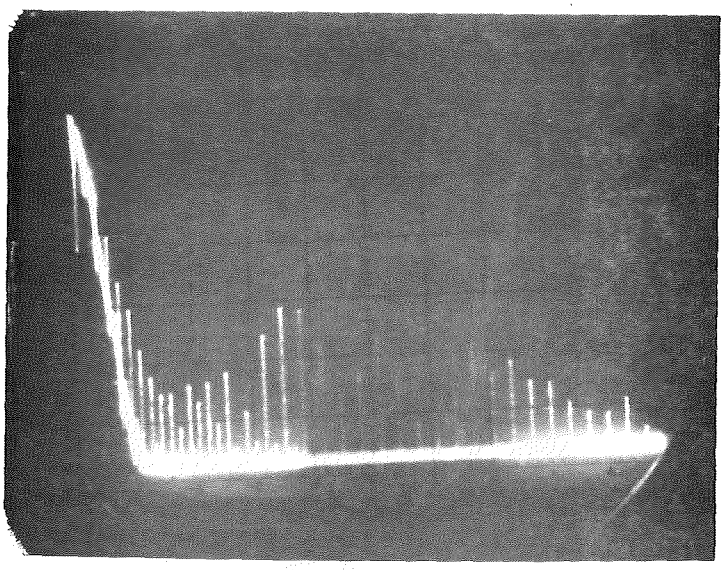

c) Old Cable

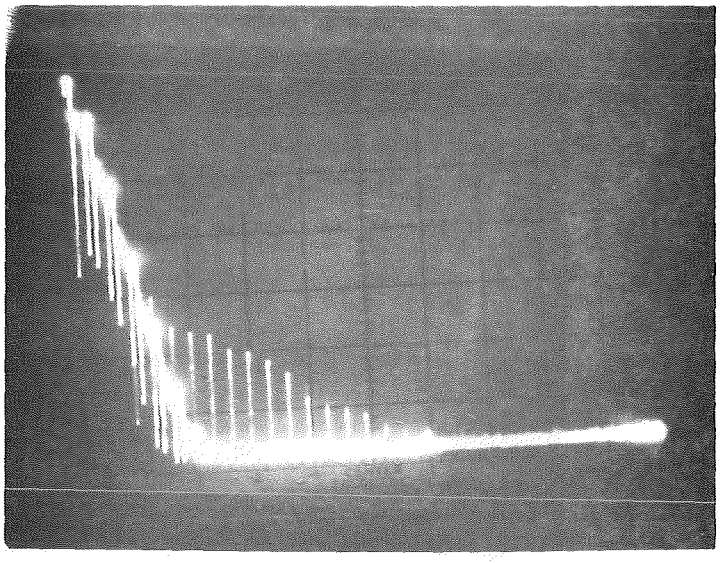

d) New Sound Cable

Fig. 1.1. Spectrum Analyzer Display for Various Pieces of Equipment.

If one studies Fig. 1.1 closely, in all the cases harmonics were pronounced upto about 50 kHZ. While, for the new cable no harmonics beyond about 50 kHZ were present, harmonics were noted upto 70-80 kHz for the old dc and ac machines and upto about 95 kHz for the old cables.

Since as yet, a large volume of test data are not available, firm conclusions cannot be drawn. However, it can safely be deduced that there is some correlation between high frequency harmonics and the condition of the insulation of any system. The threshold level appears to be around 50 kHZ. Still extensive tests have to be carried out to determine optimum test voltages, relation between test voltage and harmonic content and also between insulation life and the frequency level of harmonics.

1.5 HIGH VOLTAGE TESTING

1.5.1 Test Results

During the year a 30 kV ac/dc test set was purchased. The set was built according to the specifications outlined in last year's annual report. The tests mentioned in that report were carried out in the laboratory on the following pieces of equipment:

1. New portable cables, 1000 V grade insulation, in 300 ft lengths.

2. Used cables of various lengths.

3. Windings of an old induction motor and an old dc machine.

Some of the results obtained are plotted in Figs. 1.2 thru 1.5. The humidity measurements were carried out because the leakage current showed a marked dependance on humidity. It may be pointed out here that while many samples were tested over a prolonged period of time only typical results are shown here.

If one studies the curves closely, the leakage current in the case of cables showed no definite trend (Figs. 1.2 and 1.3). The large variations obtained could not be attributed to any definite cause. In fact tests carried out the same day at 30 minute intervals showed different results. On the other hand, the characteristics in the case of induction motor and dc machine windings showed definite consistency. (Figs. 1.4 and 1.5). No doubt, there were large changes due to changes in humidity, but they were uniform. In fact, tests carried out on the same day showed no marked change unlike the case of cable insulation.

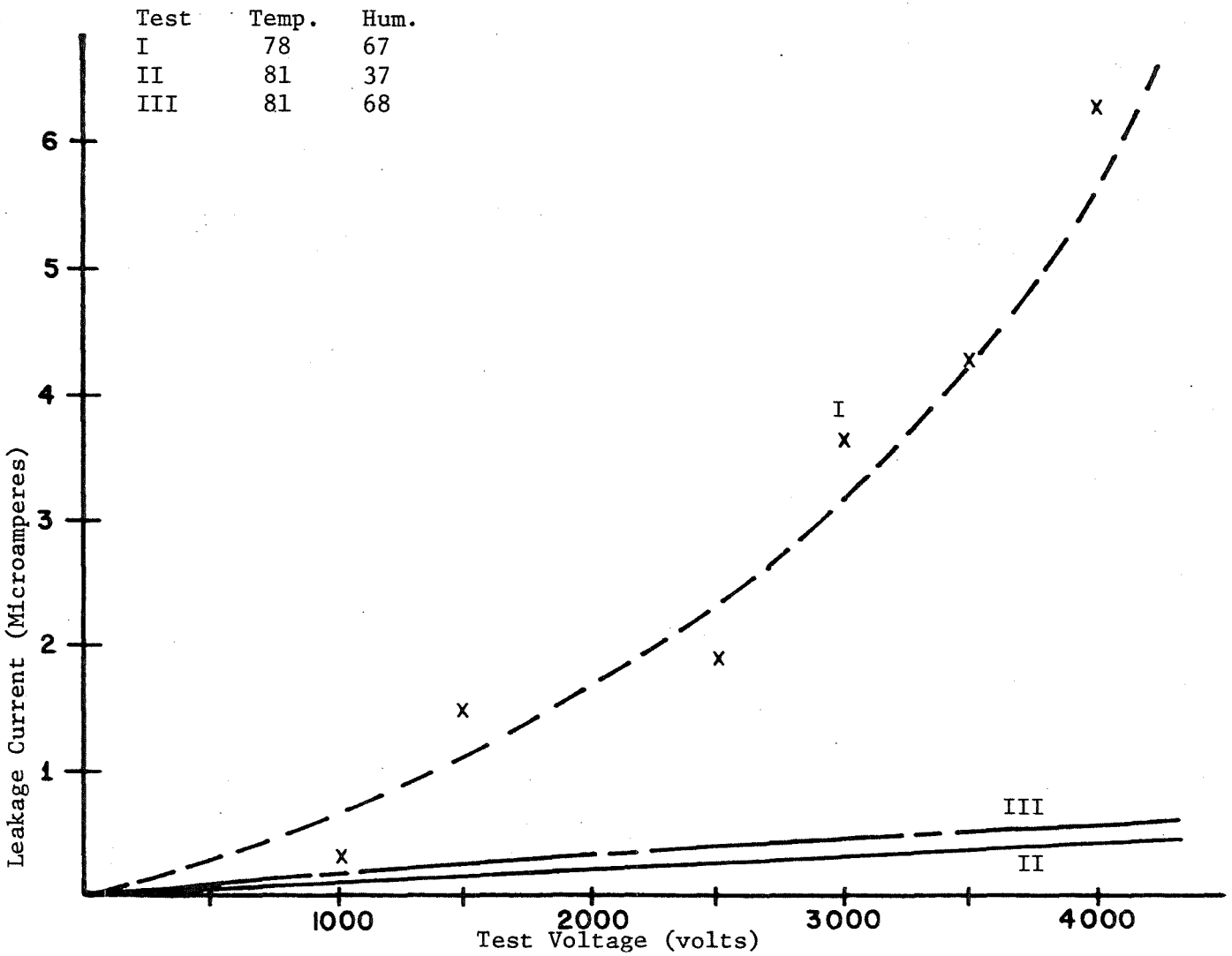

Fig. 1.2. Leakage Current Characteristics of New Portable Cable 300 ft. long.

Test	Temp.(°F)	Hum(%)
I	79	38
II	76.5	69
III	80	68
IV	81.5	67

Tests III & IV Carried Out on the Same Day at 30 Min. Intervals.

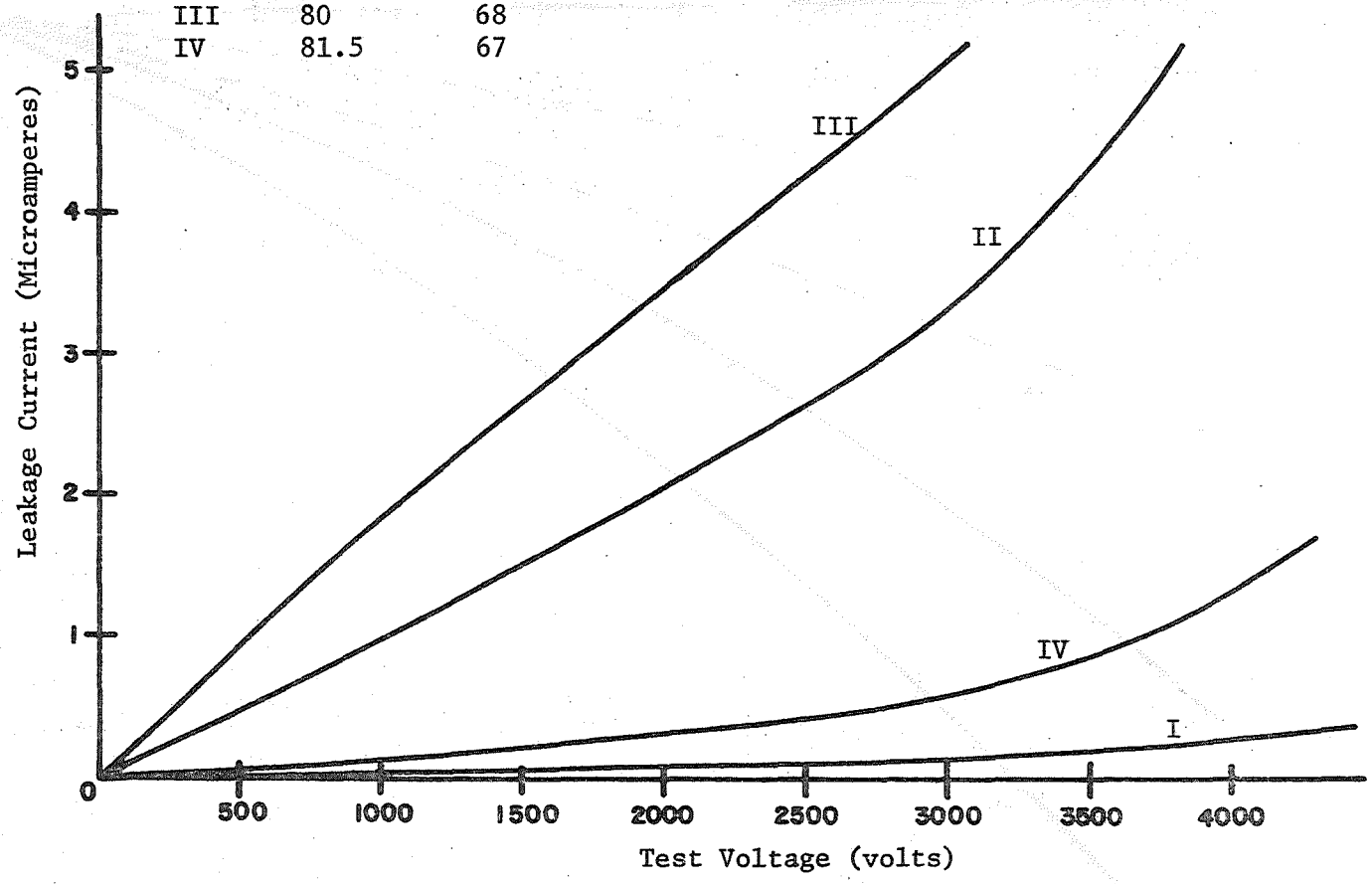

Fig. 1.3. Leakage Current Characteristics of an Old Cable 30 ft. Long.

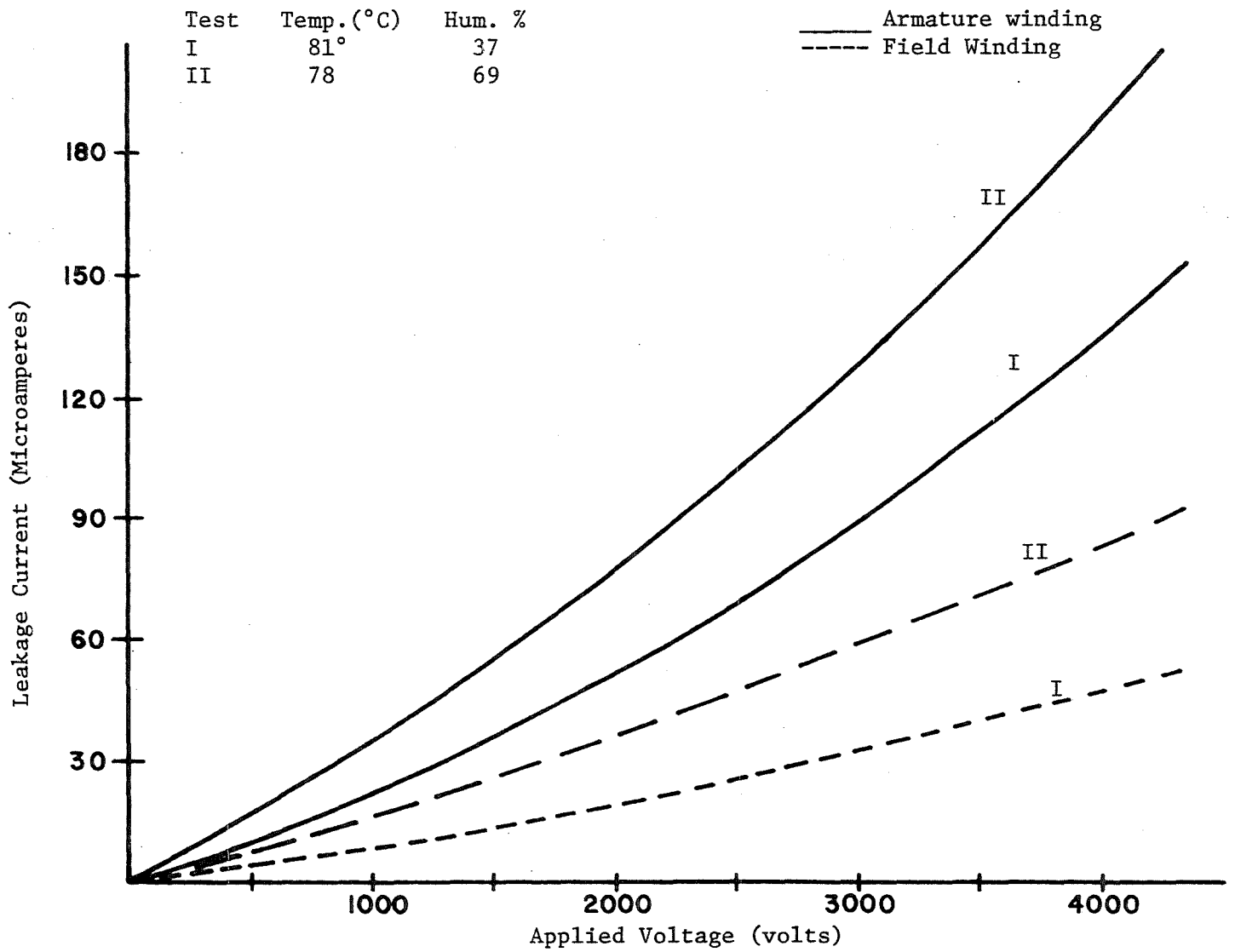

Fig. 1.4. Leakage Current Characteristics of Old dc Machine Windings.

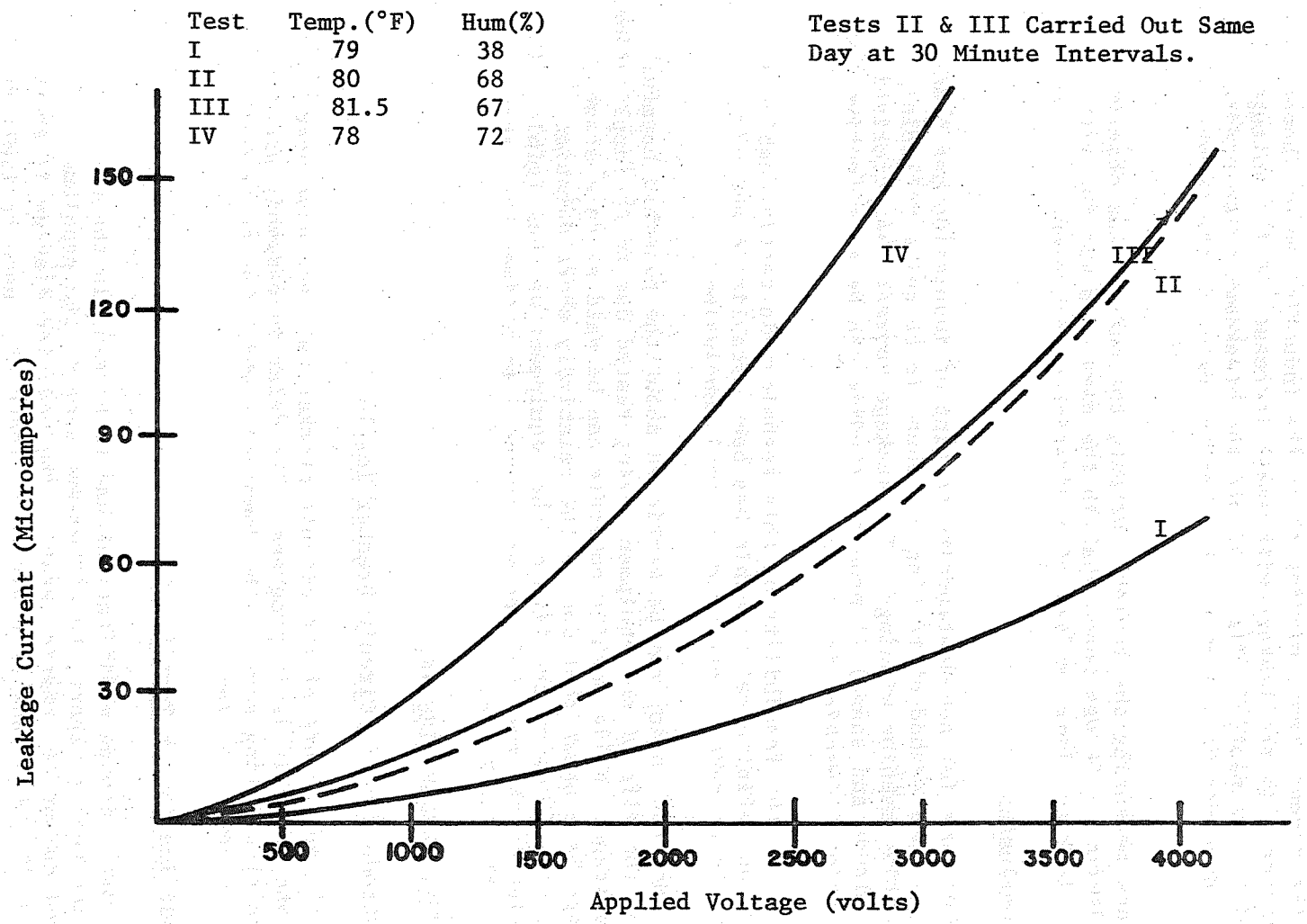

Fig. 1.5. Leakage Current Characteristics of Old Induction Motor Winding.

On the seventh test, winding II of the induction motor showed a marked increase in the leakage with small increase in the voltage. The results were plotted (Fig. 1.5) and the breakdown value predicted from the curve was very near to the observed value of the breakdown voltage.

Besides measuring the leakage current, the current was observed on an oscilloscope. It was found that in the case of a winding with excessive leakage, large spikes of ionization were present.

1.5.2 Conclusions

A procedure for non-destructive testing of insulation has been presented. This method of testing was found to be quite reliable for evaluating machine windings. The leakage current characteristics (both magnitude and shape) if properly studied can be an effective tool for evaluation of machine insulation.

As far as the feasibility of this technique in testing cables is concerned, no definite relationship has been established and more tests have to be made to arrive at a final conclusion.

One important point may be mentioned about the possible harmful effects on the life of the equipment being tested due to the application of high voltage. While nothing concrete can be said at this stage, experiments have shown that due to the relatively short duration of tests, the effect on the life of the equipment was negligible. The 'safe' value of the test voltage was around 2 to 3 times the rated voltage of the insulation.

1.6 CIRCUIT BREAKER TESTING

1.6.1 Introduction to Circuit Breaker Testing

All the components of the circuit breaker test set have been procured and assembly is in progress. The delay in assembly was due to difficulty ordering some of the components which had to be built according to specifications.

1.6.2 Modification in Test Set Up

Some minor design modifications had to be made in the test set up from last year's report, to circumvent some of the problems encountered during the testing stage. The modified diagram is shown in Fig. 1.6.'I' is a bank of 6 air-cored inductors used to limit the test current to the circuit breaker. By using various series-parallel combinations of the inductors, any desired value of the current in steps of around 400A up to 5000A may be obtained. 'SG' is a spark

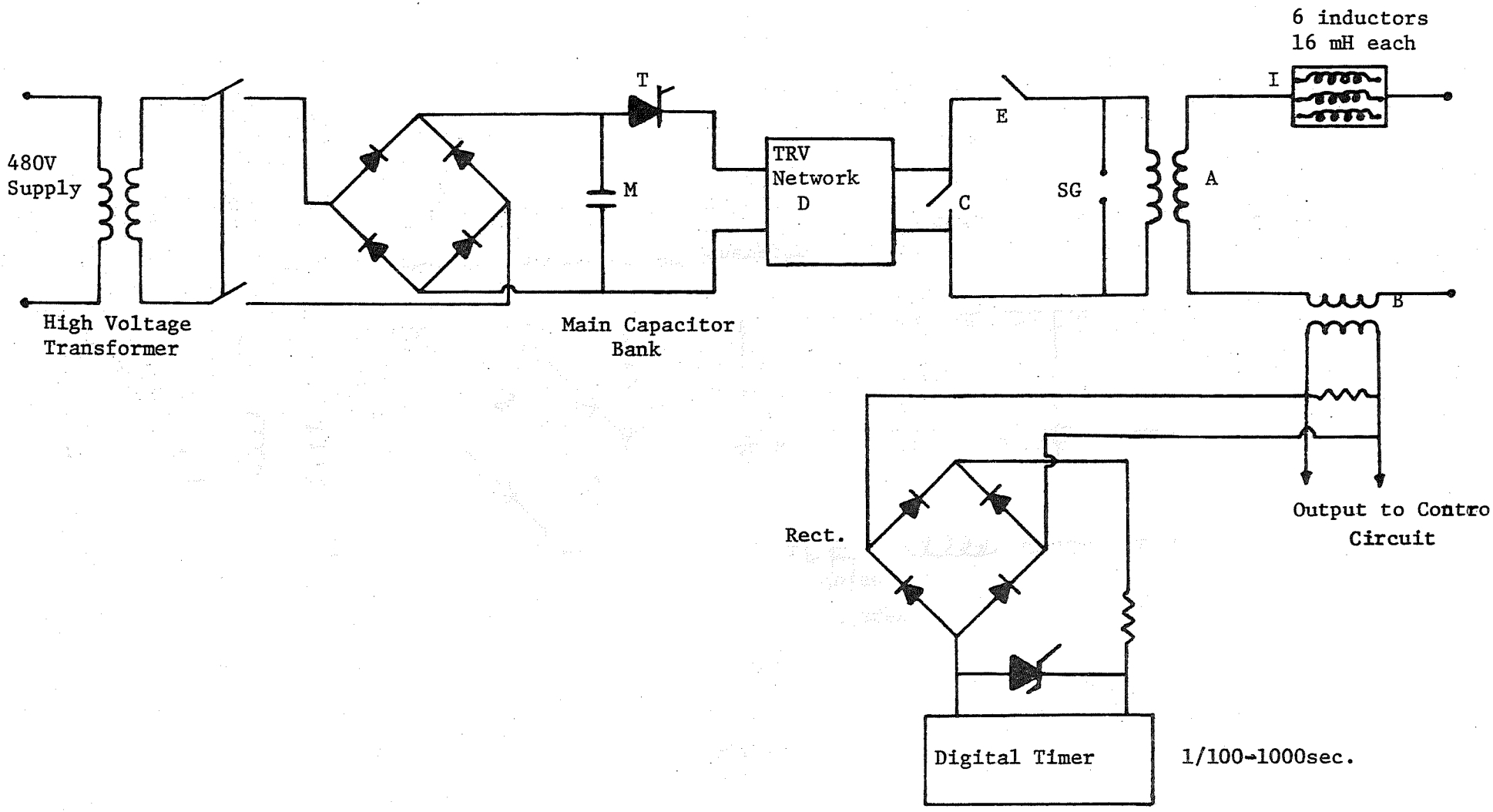

Fig. 1.6. Modified Set-Up of Synthetic Test Circuit.

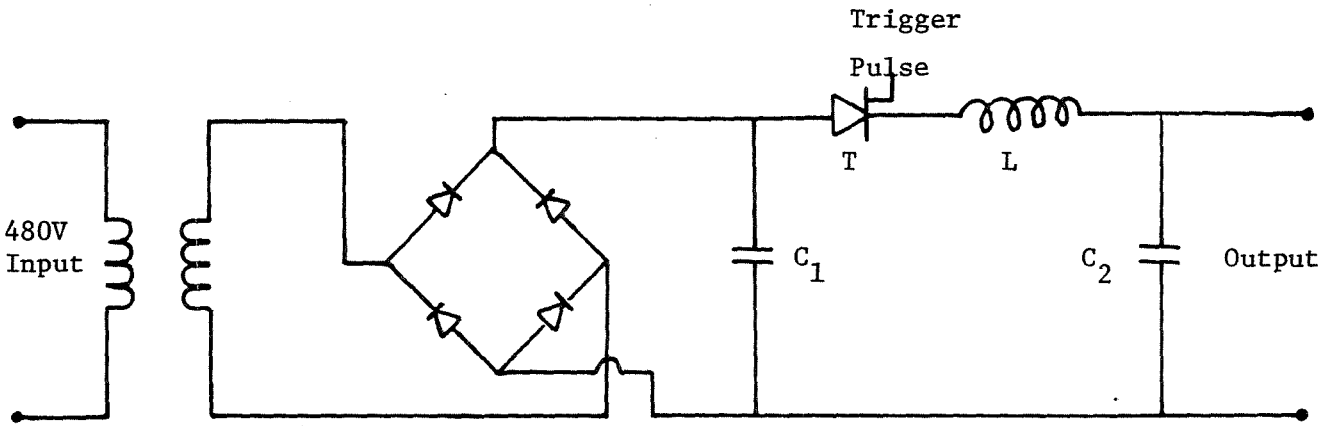

Fig. 1.7. Schematic Diagram of TRV Generator.

gap used to protect the low-voltage source in case the auxiliary breaker 'E' breaks down before the main breaker 'C'. A very sensitive digital timer has also been incorporated to measure the tripping time of the circuit breaker very accurately. The range is 1/100 to 1000 seconds.

The circuit used to shape the transient recovery voltage (TRV) is shown in Fig. 1.7. The various components are designed to give the required peak and frequency of the transient recovery voltage.

The output voltage is given by

$$V_0 = V_{in} [C_1/C_1+C_2][1 - \text{Cos}\,(t/\sqrt{LC})] \qquad (1.1)$$

where:

V_0 = open-circuit output voltage

V_{in} = charging voltage of capacitor C_1

$C = C_1/C_1+C_2$

The triggering circuit for the Thyristor T is shown in Fig. 1.8. Normally Transistor T_1, is non-conducting and the capacitor C is charged to the supply voltage. After a pulse is applied to the base of the transistor, it starts conducting and the capacitor C is discharged through the primary of the pulse transformer T_2. The output of the pulse transformer is fed to the gate of the thyristor T.

The complete specifications and design criteria of the various components for the circuit breaker test set are given in Appendix C.

1.7 INFRA-RED TESTING

1.7.1 Test Results

To carry out this test a sensitive infra-red detector was borrowed from the USBM. The device has temperature scales of 200° absolute and ±10°C differential. The temperature sensitivity is 0.4°C which is sufficient for the type of measurements needed. The complete specifications are given in Appendix D.

This test was carried out on actual mine systems as well as old cables in the laboratory. Preliminary results from the field tests were quite encouraging. Some hot spots ranging from 5° to 10°C were

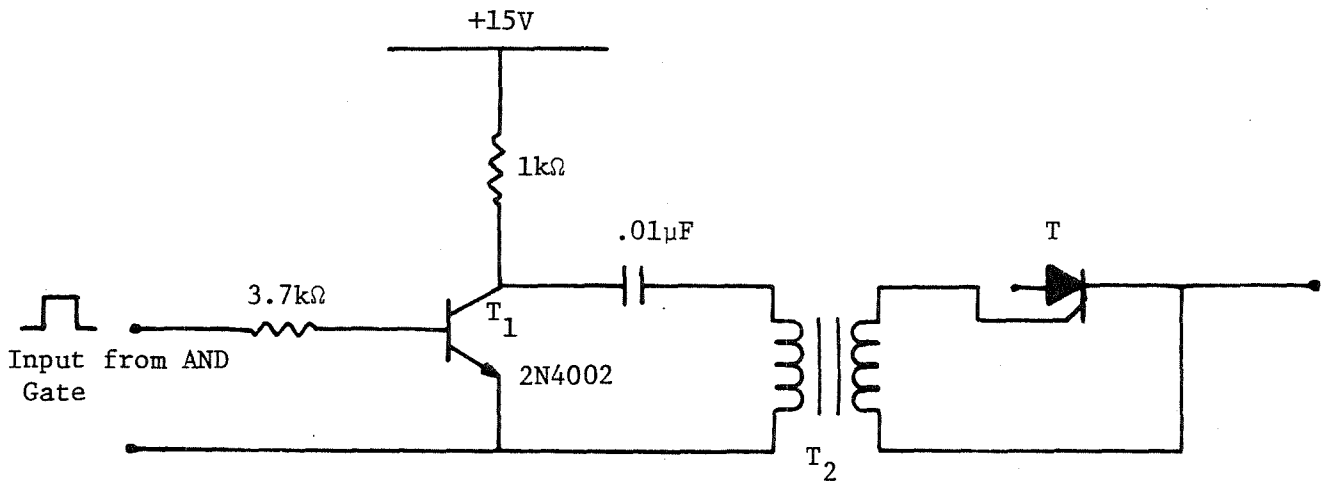

Fig. 1.8. Triggering Circuit for Thyristor T.

found on a length of trailing cable, which seemed to be a good candidate for incipient faults. But, unfortunately before the next set of measurements were made the cable was mechanically damaged and taken out of service. A lot of other difficulties were encountered in carrying out this test on loaded mine power systems which include:

a. Some of the cables are spooled for some portion of their lengths. Also in many places cables are bunched together, making testing of individual cables difficult.

b. The only loaded portions of the system are near the face of the mine. But since there is a lot of activity in that region (to and from movement of shuttle cars, etc.) there is hardly any time left for making measurements.

While nothing concrete can be done about the first problem, ways were designed to circumvent the second. The most feasible was to connect a dummy load to the system. Initially a resistive or inductive load was proposed but the idea was rejected because of the excessive size of the load. A simpler procedure was designed which is shown in Fig. 1.9.

The voltage-drop values at full load current are tabulated in Table 1.15 for various sizes of cables generally found in mine systems.

From the table:

Maximum voltage drop occurs for 1/0 cable = 11.21 V
Hence, the rated voltage of transformer T_2 should be = 11.21 V
Twelve volts is the closest standard rating. The circuit should be able to supply full-load current for the largest size cable (=500 MCM)

I_{FL} (cable) = 290 A

Hence transformer T_2 secondary current = $\frac{290}{\sqrt{3}}$ = 167 A

Therefore, the transformer rating = $3 \times 12 \times 167 \times 10^{-3} \simeq 6$ kVA
This is the rating for a three-phase bank. If single-phase units are used each will be rated 2 kVA.

Transformer T_2 primary line-to-neutral voltage = 240 V. Thus, the transformation ratio = $\frac{240}{12}$ = 20. And the primary current = $\frac{167}{20}$ = 8.37 A $\simeq$ 10A

One can conclude that the continuously variable autotransformer should be rated at three-phase, 480 V, 10 A.

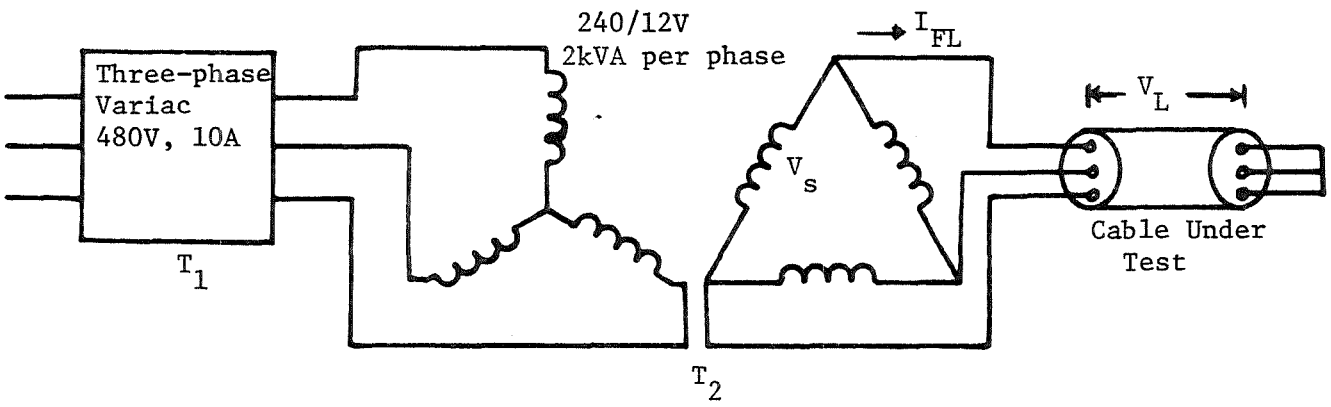

Fig. 1.9. High Current Circuit for Infra-Red Test.

Table 1.15

Voltage Drops for Various Sizes of Cables

Cable Size (AWG or MCM)	Full load Current (A) (I_{FL})	Resistance Ω/500 ft. (R)	Voltage Drop per phase (V) $V_L=I_{FL}xR$	Transformer T_2 Secondary Voltage (V) $V_s=\sqrt{3}\ V_L$
1/0	120	.054	6.48	11.21
2/0	135	.043	5.81	10.06
3/0	155	.034	5.27	9.12
4/0	180	.027	4.86	8.41
250	200	.0235	4.70	8.13
300	220	.0193	4.25	7.34
350	235	.0167	3.92	6.79
400	250	.0145	3.63	6.28
500	290	.0117	3.39	5.86

1.7.2 Conclusions Related to Infra-Red Testing

A method of detecting incipient faults using an infra-red technique has been discussed. Some difficulties have been encountered in carrying out this test in an actual mine environment and ways have been devised to circumvent most of the problems.

However, the feasibility of this testing technique has to be determined by systematic collection of test data from field tests and correlating them with the useful life of insulation systems. It is hoped that eventually, if enough data are accumulated, it may be possible to use statistical methods in predicting incipient faults using this technique.

1.8 INSULATING LIQUID TESTING

1.8.1 Introduction To Insulating Liquids Testing

Mineral oil is the most frequently used insulating medium besides kraft paper and resin-bounded paper for converter transformers, smoothing reactors, bushings, and the auxiliary equipment of converter stations; it plays an important part in the insulation of high voltage between conductors as well as to earth. It is also used as an arc quencher in low- and high-voltage circuit breakers.

The electrical strength of an insulating oil depends on the electrode configuration and the degreee of purity of the liquid. In addition, the type of test voltage, its duration, pressure and temperature play an active part; for small gap spacings, the material, its pretreatment, and the surface conditions of the electrodes are of additional importance. With the removal of even the smallest impurities, the electrical strength can be brought up to very high values. However, there is little sense in purifying the oil to this extreme condition because on filling the apparatus in which it is to be used it will be immediately contaminated to a certain degree. The breakdown values will be appreciably lower with a higher content of foreign particles, as must be expected with lack of care in handling the oil. The values nevertheless, should be representative for oil in a newly manufactured piece of high voltage equipment.

The development of the breakdown itself depends, to a great extent on the test condition. Under the action of long duration voltages and not absolutely pure oil, it can be assumed that the breakdown is initiated by a chain-like build-up of dust or thread-like particles along the field lines between the electrodes. As a result of their high dielectric constant and conductivity, these particles will be drawn into positions of highest field intensity where they either end, or agglomerating cause a bridging of the

space between the electrodes. In quasi-homogeneous fields with direct voltage, the conditions for the occurrence of such bridges are more favorable than with alternating voltages in a diverging field. With alternating voltages, of course, the driving impulses acting on the suspended particles are much smaller because of the continuous polarity reversals and, in the field of a spike, for example, spark over is preceded by predischarges which lead to strong movements or eddies in the oil, thus making a bridging of the gap more difficult.

The breakdown field strength is appreciably lower in a plain or uniform field with direct voltage than with alternating voltage, but not so when the electrodes are sharp or bent.

1.8.2 Description of Test Equipment

Associated Research Oil Testing Hypot Model 4521 has been acquired which is specifically designed for testing the dielectric breakdown strength of insulating liquids in accordance with ASTMD877 using disc electrodes, and D1816 using VDE electrodes. In accordance with ASTM requirements, this 60kV-2kVA oil test set employs a center-tap-grounded high voltage power supply terminated in two cradle-type terminals. The voltage control is motor driven to secure a uniform rate of voltage rise, providing repeatability of test results. Oil cups are equipped with one-inch disc electrodes complete with .1" gap gauge to meet ASTM D877 and VDE electrodes complete with .80" gap gauge and motor driven stirrer to meet ASTM D18.16. The standard method of test for dielectric breakdown voltage of insulating liquids is given in the standards book by "The American Society for Testing and Material."

1.9 ACCELERATED LIFE TEST

1.9.1 Introduction to Aging Theory

Accelerated life testing of products and materials is used to get information quickly, related to life distribution. Accelerated testing is achieved by subjecting the test units to conditions that are more severe than the normal ones. This results in shorter lives than would be observed under normal conditions. The results obtained at the more severe or accelerated conditions are then extrapolated to the normal conditions to obtain an estimate of the life distribution under normal conditions. Such testing provides a savings in time and expense compared with testing under normal conditions.[9]

The purpose of this effort is to make periodic insulation tests on scaled-down versions of mine equipment, to age this equipment by overload and to see which periodic tests best show the effects of aging on that equipment. The overloading experiments must be designed to shorten the actual working lifetime of the equipment, until failure is eventually reached. However, this shortened life must be able to provide enough data sets to be able to correlate statistically the data effectively.

It was decided that a large data base could be accumulated by performing the periodic tests on equipment which could be aged in a controlled laboratory situation where small scale samples of electrical equipment could be alternately tested and aged.

Because it was desirable to approximate as closely as possible the mechanism of aging in mine equipment, thermal aging was chosen as the aging method. This method was chosen because the most likely modes of failure for electrical equipment are deterioration of solid insulation due to overheating and/or mechanical damage to the insulation.

Another mode of failure is the deterioration of the conductor to the point that the local series resistance would increase. This effect could cause local heating in the conductor which could cause conductor or insulation melting. Since these effects are basically thermal phenomena, thermal aging is again indicated as a superior method.

Now, the question arises as to how the thermal aging test should be done. Overcurrent heating was chosen as the best alternative, since overcurrent aging may produce mechanical effects due to both magnetic forces and thermal expansion forces. Furthermore, heating by internal methods tests the heat dissipating ability of the insulation. If the material fails to dissipate heat properly, a hot spot in the insulation will occur.

However, overcurrent aging is not without its problems. First, a source with the necessary current capability must be found. If a variable autotransformer is used, the voltage is set to a specific value which produces a desired current. As the experiment continues, the resistance of the conductor increases with increasing temperature. Also, thermal conductivity may be a function of temperature for certain materials. These phenomena may tend to cause a "thermal runaway", when a constant voltage setting is maintained, especially if the inductive reactance is limiting the current. Therefore, it was desirable to protect sources from large undesired overcurrents with fuses or circuit breakers. The magnitudes of currents were required to produce a given temperature rise is also an important factor. Fortunately, they can be obtained from electrical equipment design books.

1.9.2 Transformer Aging

There are several problems one is faced with when trying to design an aging experiment for a specific transformer. The first problem is selecting the temperature the equipment should be maintained at to shorten its life to a given number of hours. Another problem is to find the correct amount of current needed to produce a given temperature rise. Figure 1.10 is a graph of typical lifetimes versus temperature for various insulation classes.[6] This graph was utilized when selecting aging times and temperatures. Transformers rated 0.5 kVA, 480/240 - 240/120 V, single phase 60 Hz, with class B insulation were used in the experiment. For these transformers rated current = $\frac{\text{rated kVA}}{\text{applied volts}} \times 10^{-3} = 2.085\text{A}$ (1.2)

Therefore, two per unit current equals 4.17A. At 2 p.u. loading: Total losses if core losses are neglected = $2I^2R = 104.17$ watts. Losses per unit surface area are therefore Watts/sq. in. = $\frac{104.17 \text{ watts}}{4(5")(6") + (5")(5")} =$

$0.7184 \text{ watts/in}^2$

If the graph of Figure 1.11 is linearly extrapolated, a temperature rise of 77°C is predicted.[5]

$$\frac{44}{0.35}(0.7184) = 90.31°\text{C}$$

This would produce a case temperature of 90.31° + 25° = 115.31°C

In order to minimize current requirements, it was decided to connect the 240-240 transformers primary of one transformer to the secondary of the next. In this way, voltage could be applied at one end and a short at the other end, causing overcurrent conditions simultaneously in all six transformers. This connection is in Figure 1.12. It was realized that due to excitation currents, the current in the transformer at the source end would probably be greater than the current at the shorted end, but this could be compensated for by switching the source end and shorted end periodically during the overall aging cycle.

The results of the initial aging cycle were as follows:

Total aging time: 2 hours 40 minutes

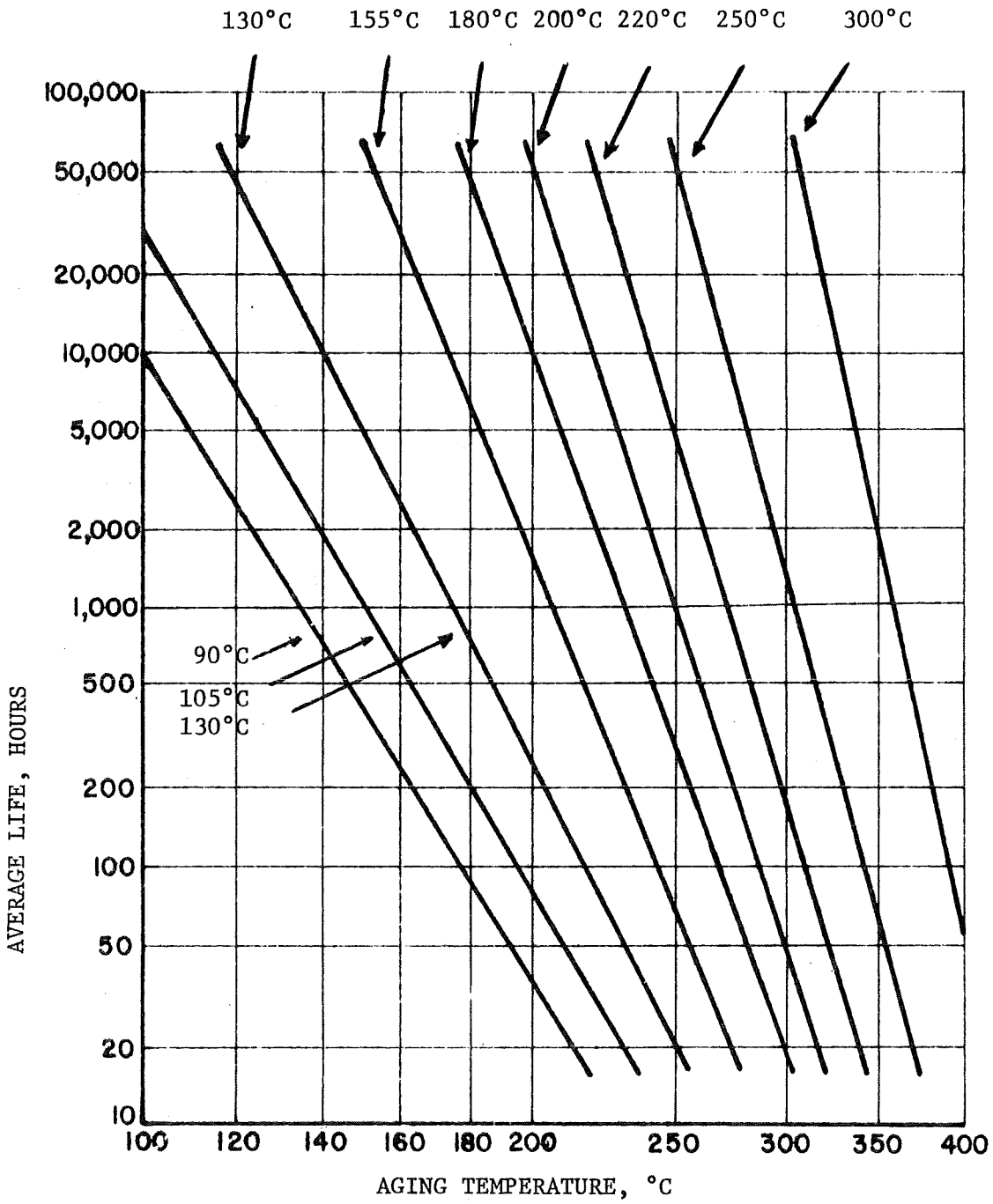

Fig. 1.10. Aging Temperatures Plotted Against Average Life for Electrical Insulating Materials and Systems (Note: Intercepts at the 20,000-hr Level Conform to Temperature Indices for Classes From 105° to 300°C, the Intercept for Class 90°C Falling Outside the Graph; the Line for Polyurethene Enamel Illustrates Occassional Divergence from The Usual Relationship Between Activation Energy and Resistance to Aging).

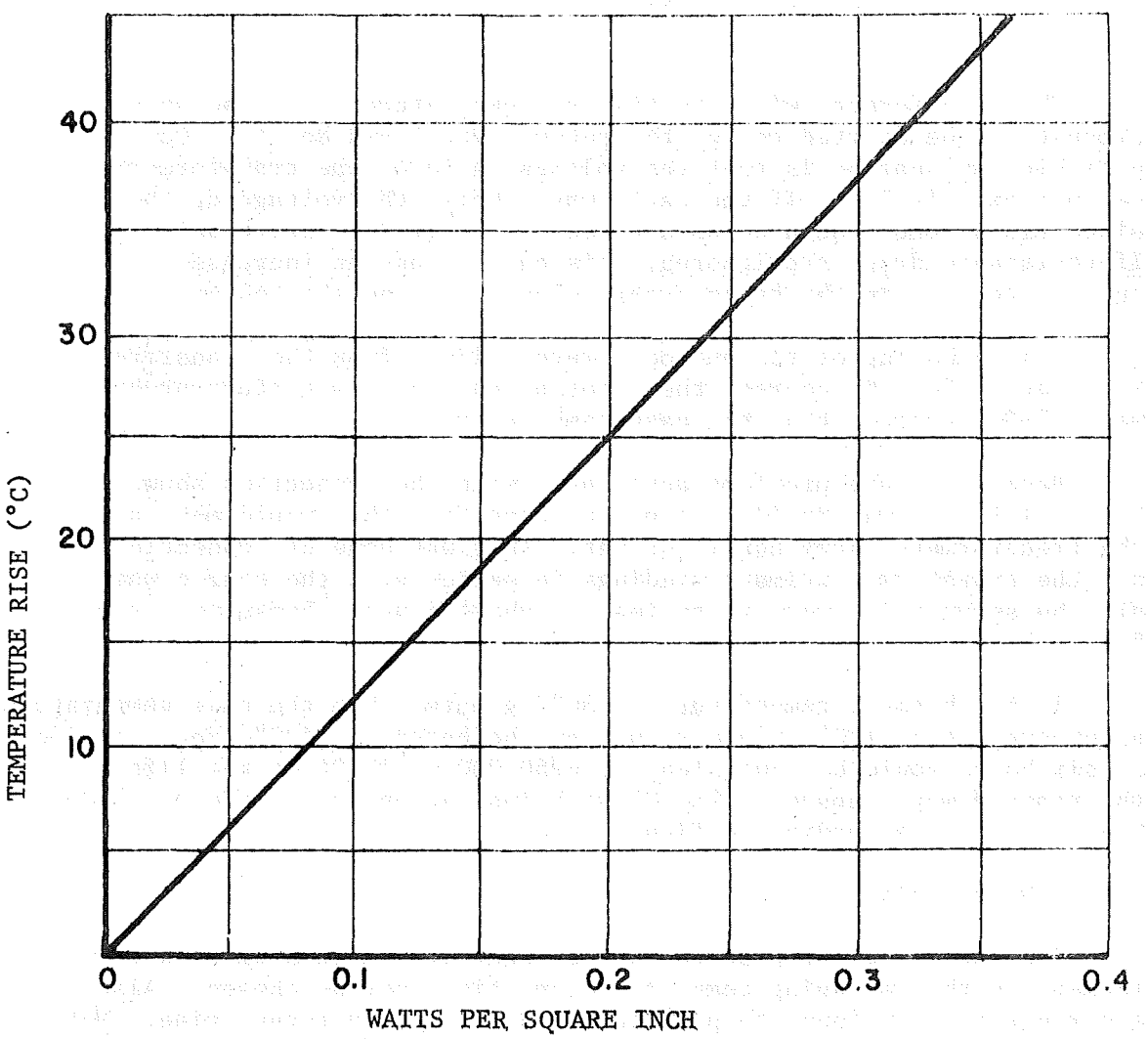

Fig. 1.11. Relation Between Temperature-Rise and Dissipation of The Exposed Surface of a Small, Gray-Painted Transformer Tank in Still Air.

Temperatures of case at shutdown:
Transformer No. 1: 80°C
Transformer No. 6: 140°C
Current: 2 p.u.

The transformers with the highest temperatures were the ones closest to the shorted end of the set-up (No. 6 and No. 5). One possible explanation is that the voltage ratio of the transformers was not exactly 1:1. If the ratio was 1.05:1, the voltage at the sixth transformer could be as high as $(1.05)^6(240) = 321.6$ volts. If resistance drops are ignored, this could cause an increased current to flow in the transformers closest to the shorted end.

Some bubbling of tar and odor were evident from the transformer No. 6 at 140°C. Of course, the internal hotspot temperature probably was 20°-30° greater than the case temperature.

Because of the problems associated with the connection shown in Figure 1.12, it was decided to use a connection that would make all the transformers carry equal current. This was done by connecting all the transformer primary windings in series with the source while all the secondaries were in series and shorted upon themselves. (See Figure 1.13).

If the hotspot temperature is 30°C greater than the case temperature, a temperature of 120°C would result at the hotspot. 120°C for a period of six hours would be equivalent to 6/50,000 = 0.012% of the life of the transformer elapsed. (The Class B insulation has a life of 50,000 hours at 120°C according to Figure 1.10).

1.9.3 Motor Aging

The same types of problems are evident with motors as with transformers in that an aging temperature and time must be chosen. Also, a current must be found to produce the desired temperature rise. Motors rated 1/2 hp, 115 V, 60 Hz, split-phase, 8.4A, with class A insulation were used. It was decided to age the motors in a locked rotor configuration.

A formula for the expected temperature rise is given as follows:

$$t = \frac{40000W}{(3000+V)\,DL} \qquad (1.3)$$

where t: temperature rise (°C)
W: total dissipated power (watts)
V: peripheral velocity of rotor (RPM)
D: outside diameter of case (in)
L: axial length of rotor (in)

By applying a known voltage to the typical sample in the locked rotor state, current measurement can be made. From these measurements, the dissipated power per motor can be estimated. Since the rotors are

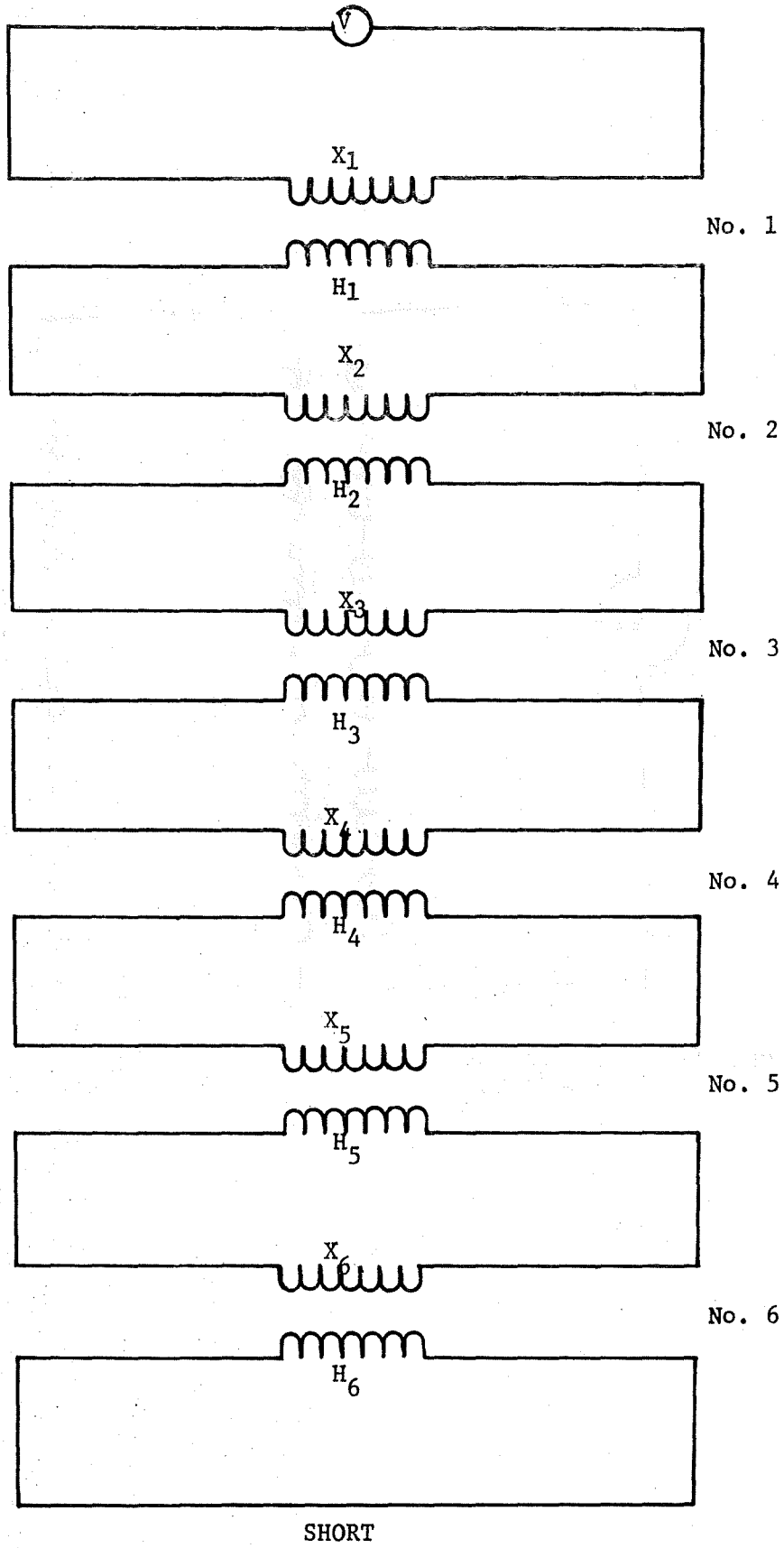

Fig. 1.12. Initial Connections of Transformers for Accelerated Life Tests.

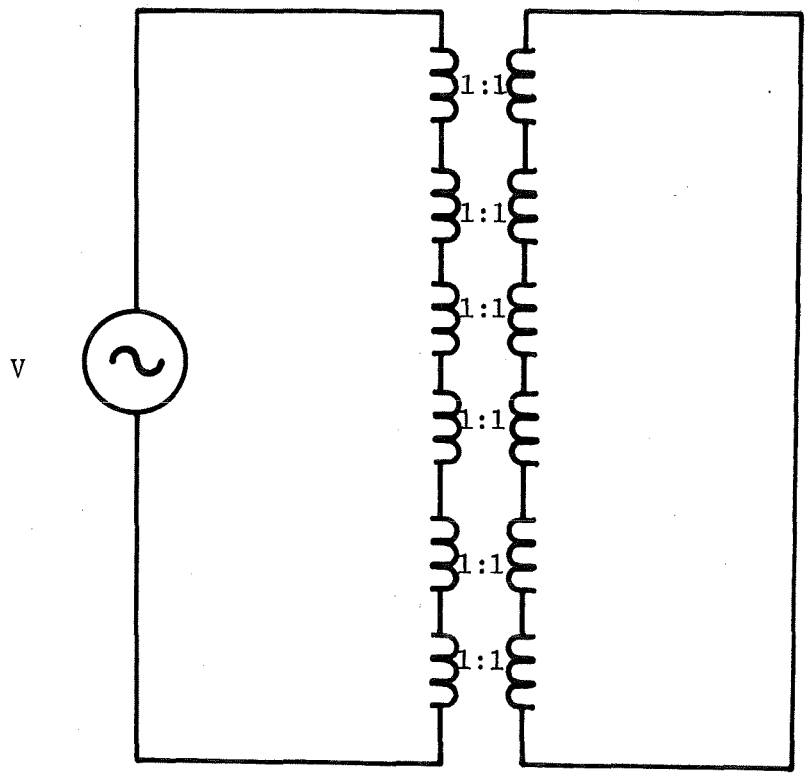

Fig. 1.13. Connections of Transformers for Accelerated Life Tests.

blocked, all the input power must appear as losses. The motor voltage was 27.5V and motor current was 10A. The power is

$$p = VI \cos\theta \tag{1.4}$$

Assuming a power factor of 0.8 for a typical motor, the power is 220W. Substituting the above values into the equation 1.3 and using D = 6.5 in and L = 6 in, one obtains a temperature rise of 75.21°C. The case temperature is thus, 100.21°C

The set-up of Fig. 1.14 was used to perform the aging experiment. The six motors are connected in a three-phase delta with two motors in series in each leg. The actual aging tests produced a temperature of 98.6°C in the operating time of one half hour that it was connected with a current of ten amperes. The aging times and temperatures are tabulated in Table 1.16.

The expended life time can be found by substituting the values of Table 1.16 into the following formula.

$$\text{Expended life} = \Sigma \frac{\text{Aging time at temperature T}}{\text{Life time at temperature T}} \tag{1.5}$$

Substituting the aging times and temperatures for Table 1.16 one gets a total expended life of 0.0716%.

1.9.4 Cable Aging

Cables of size #2(AWG), 3 conductors, type G-GC, with class A insulation, rated 2000V have a capability of approximately 115 Amperes per phase. Therefore, test equipment which has relatively high current capability is needed. From practical experience gathered in carrying out the experiments, it was decided that a current capability slightly greater than 2.0 per unit would be adequate. A supply was connected Wye-Delta with three 240-32V power transformers. The current capability when the bank is fed from a variable autotransformer with 20A rating is 20 $\sqrt{3}$ 240/32 = 259.8 Amps. This value is greater than 2.0 per unit.

The cables were connected in a Wye configuration as in Fig. 1.15 Short lengths of #2AWG TWH wire were used as "Jumpers" between the individual ten feet lengths of cable. All connections were made with #2 stranded solderless wire connectors for ease of dissassembly when periodic testing is required. With this connection, the contact resistance may be of the same order of magnitude as the conductor resistance of the cables. Therefore, it becomes important to monitor the temperature distribution of the cables to prevent large contact resistances from causing hotspots.

The data shown in Table 1.17 are the cable aging times and temperatures which were measured on the outside of the sheath. The temperature on the inside of the insulation may be approximated using the following equation

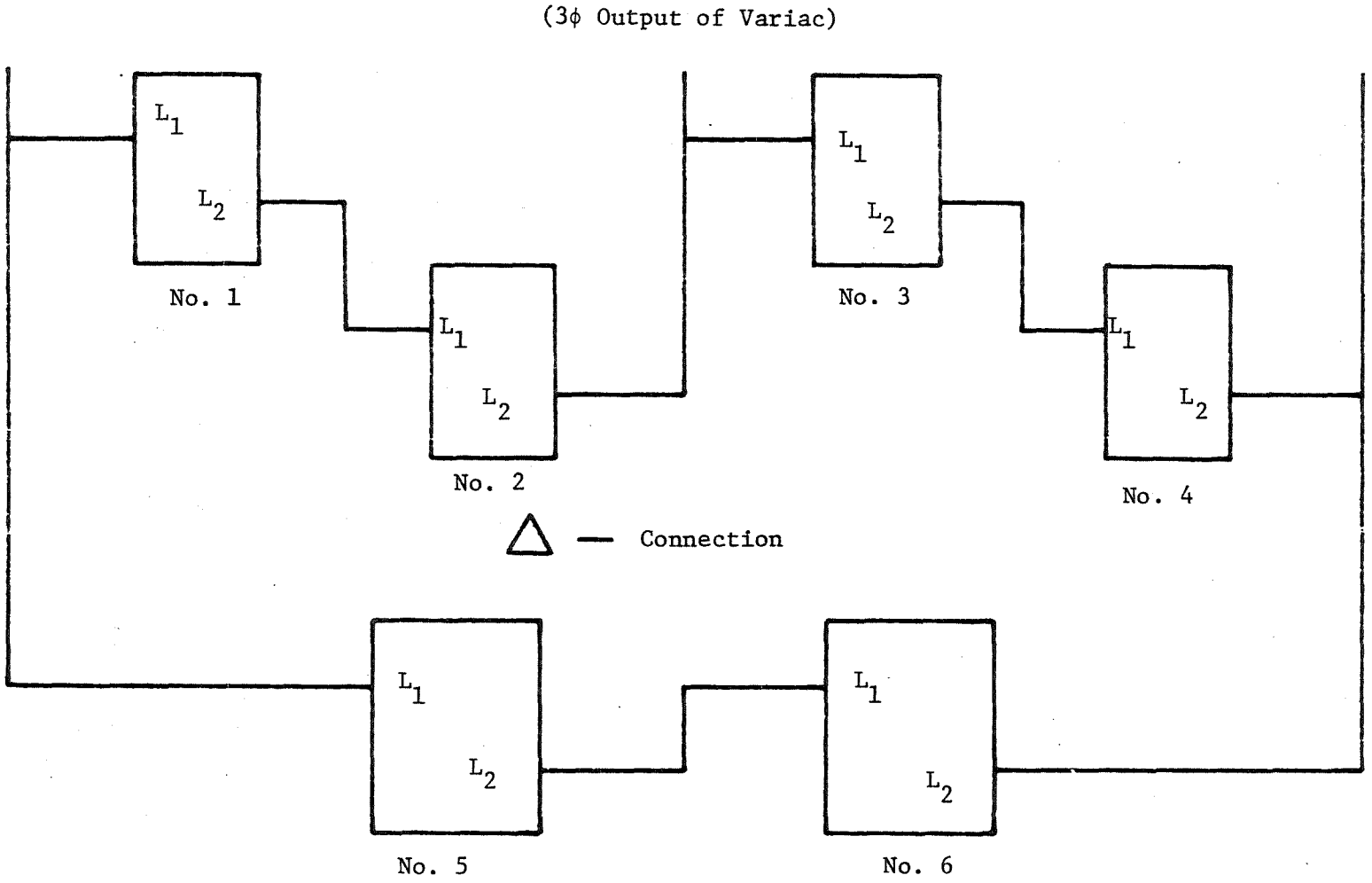

Fig. 1.14. Motor Aging Set-Up.

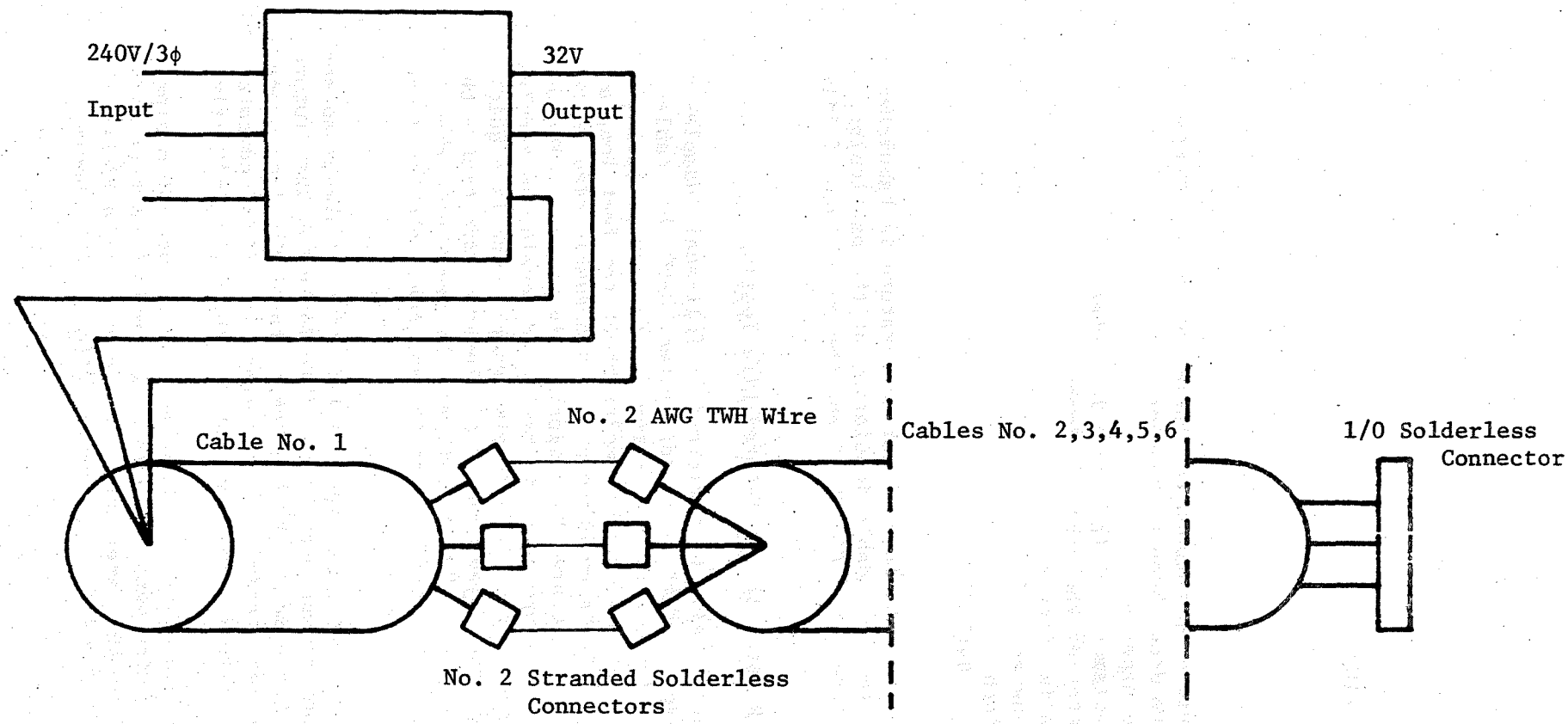

Fig. 1.15. Cable Aging Set-Up.

$$T_1 = \frac{\alpha k I^2 \log_{10}(D/d)}{A} \tag{1.6}$$

where

$$\alpha = \frac{234.5 + T}{309.5} \tag{1.7}$$

and

T_1 = temperature drop through the inside of the insulation in °C.
T = temperature drop through the sheath in °C.
I = current in Amperes.
D = insulated diameter of the cable in inches.
d = bare diameter of the cable in inches.
A = cable area in circular mils.
K = thermal constant = 76.7
1 mil = 10^{-3} inch
1 circular mil = $\frac{\pi x (10^{-3})^2}{4}$ inch^2

In Table 1.18, the calculated inner temperature is tabulated as well as the life of the 90°C cable insulation at the particular temperature as extrapolated from Fig. 1.10 and the percentage of life expended.

1.9.5 Conclusions Related to Accelerated Life Testing

The tests should ideally be performed on full-scale samples of mine electrical equipment such as; motors rated 10-200 hp, cables several hundred feet long, etc. The actual tests were performed on fractional horsepower motors, cable samples about ten feet long and 1/2 kVA transformers. It is understood that the sample size is too small to yield results that are statistically significant. The use of a small sample size is appealing in trying to develop an accelerated life test because after all, reducing sample size is a quick way of meeting one of the objectives of accelerated life test - the reduction of test expenses. However, it must be remembered that the correlation between actual industry samples and small samples is an important future task.

In the tests described, the expended life time is always so small that the tests are not saving much time. This indicates that future testing needs to be performed at higher temperatures for longer periods of time if any appreciable aging is to be expected. This indicates a bit of caution in designing and carrying out the tests initially.

These three tests are still in progress. Each type of equipment will be tested after fifty hours of aging. Analyzing the test data is an important part of the experiment. The plan is to achieve temperatures that will produce 10% expended life in fifty hours.

Table 1.16

Motor Aging Times and Temperatures

Current	Elapsed Time	Approximate Temperatures
10A	0.5 hr	98.6°C
5A	5.75 hr	75°C
5A	2.67 hr	68°C
8A	1.25 hr	100°C
8A	1.75 hr	115°C

Table 1.17

Cable Aging Times and Temperatures

Current	Elapsed Time	Sheath Temperature
155A	3.83 hr	48.7°C
155A	1.25 hr	49°C
200A	3.5 hr	75°C
175A	2.25 hr	60°C
175A	3.5 hr	60°C

Table 1.18

Calculated Values

Temperatures	Life Time for Class B Insulation	Expended Life
53.94°C	100000 hr	0.0038%
54.24°C	100000 hr	0.0013%
80.24°C	30000 hr	0.0117%
65.24°C	70000 hr	0.0032%
65.24°C	70000 hr	0.0050%
	Total:	0.0250%

1.10 STATISTICAL METHODS FOR ANALYZING DATA

1.10.1 Available Techniques

A wide range of existing techniques can be applied to the analysis of the field and accelerated life test data previously described. These techniques are described in detail in Reference 8 and other texts on statistics and probability. Some of the techniques that have been studied for use in the correlation of data to component failures include linear and nonlinear regression analysis and correlation coefficients, multiple linear regression analysis and multiple correlation coefficients. The goal of this statistical analysis is to verify the ability to determine incipient faults by the tests being conducted. It is expected that some of the tests being conducted will be discarded on the basis of these analyses.

APPENDIX A

COMPARISON OF TEST DATA FROM FEDERAL #2 MINE AT BLACKSVILLE

A.1 INSULATION RESISTANCE TESTS

The tests were carried out using a Biddle Megger

TABLE A.1

#24 Shuttle Car Cable, #2/3C Conductor Flat

Voltage	Insulation Resistance (MΩ) 100V			250 V			500 V			1000V		
Test	I	II	III	I	II	III	I	II	III	I	II	III
Connection												
L_1-G	8	7	3.2	7	5	3.4	6	4.5	1.8	6	4	1.6
L_2-G	5	4	3.2	3.5	2.5	3.3	4	4	1.8	4	4	1.7
L_3-G	5	10	3.6	4.5	7.5	2.9	4	6	2.6	4	5	2.3
L_1-L_2*	-	-	-	-	-	-	-	-	-	-	-	-
L_1-L_3	8	14	3.8	7.5	7.5	3.4	7	9.5	3.2	6	7	2.9
L_2-L_3	9	13	4.8	7.5	7.5	3.5	7	9	3.2	6	7	2.9

*Starter Coil or Control Transformer in Circuit.

TABLE A.2

AUXILIARY FAN, #6-3 GGC

	Insulation Resistance (MΩ)											
Voltage	100V			250V			500V			1000V		
Test	I	II	III	I	II	III	I	II	III	I	II	III
Connection												
L_1-G	400	∞	160	500	400	130	410	380	130	300	400	120
L_2-G	200	∞	250	250	200	87	200	150	80	180	120	66
L_3-G	500	∞	∞	500	400	145	400	300	115	400	240	100
L_1-L_2	400	∞	∞	500	250	500	300	250	175	200	250	160
L_1-L_3	500	∞	∞	500	250	225	400	250	180	400	210	155
L_2-L_3	400	∞	∞	375	500	175	450	480	150	200	400	130

A.2 CAPACITANCE AND DISSIPATION FACTOR

These tests were carried out using a Biddle Capacitance and Dissipation Factor Bridge.

TABLE A.3

#24 Shuttle Car Cable, #2/3 Contactor Flat

Connection	Capacitance (μF)			Dissipation Factor (%)		
	I	II	III	I	II	III
L_1-G	.041	-	.0422	23.67	-	8.13
L_2-G	.063	-	.0399	> 30	-	7.00
L_3-G	.0192	-	.0390	6.74	-	6.87
L_1-L_2	-	-	.0392	-	-	15.68
L_1-L_3	.0417	-	.0392	10.86	-	15.60
L_2-L_3	.0407	-	.0375	10.67	-	14.69

TABLE A.4

AUXILIARY FAN, #6-3 GGC

Connection	Capacitance (μF)			Dissipation Factor (%)		
	I	II	III	I	II	III
L_1-G	.0306	-	.031	3.92	-	3.07
L_2-G	.0307	-	.031	3.88	-	3.70
L_3-G	.0292	-	.0295	3.80	-	3.07
L_1-L_2	.0188	-	.032	1.30	-	4.83
L_1-L_3	.0176	-	.0317	1.19	-	5.06
L_2-L_3	.0180	-	.0319	1.19	-	5.53

A.3 NOTES

1. Tests I, II, and III were made on March 8, May 8 and June 12, respectively.

2. The location in mine was 6 left.

3. L_1, L_2, L_3 indicate phase conductors while G indicates the ground.

4. Instruments used were Megger and Capacitance/Dissipation Factor Bridge.

5. While many cables were tested, the data presented here is a representative sample of the same.

6. Careful analysis of the data shows that the insulation of the #24 shuttle car cable is progressively deteriorating and can be expected to break down in the near future. The same type of behavior was exhibited by the #25 shuttle car cable and the Miner cable which is not shown. On the other hand, the auxiliary fan cable shows sound insulation, although the values of the insulation resistance are gradually falling down . They are still much higher than the minimum safe values. The same is true of the Roof Bolter Cable.

7. Dissipation factor measurements could not be made in Test II because of a malfunction in the bridge.

8. Measurements could not be made on motors because of access problems. It needs to be studied.

9. All cables tested were 500-550 ft. in length.

APPENDIX B

SPECIFICATIONS OF DISSIPATION

FACTOR BRIDGE

Measuring capacitance: 5 pF to 1.2 μF in 12 ranges.
Range: 200/500/1000 pF at full scale.
0.002/0.005/0.01/0.02/0.05/0.1/2.0/0.5/1.2 μF at full scale.
Accuracy: 0.2% of reading plus 5 pF.
Resolution: 0.01% of range selected.
Measuring Dissipation Factor:
Range: 0-1/10/20% of D.F. at full scale
Accuracy: 0.03/0.3/0.5% D.F. at full scale
Resolution: 0.001/0.01/10/01% D.F. at full scale

APPENDIX C

SPECIFICATIONS OF THE CIRCUIT BREAKER TEST SET

C.1 PURPOSE

The purpose the circuit breaker test set is to carry out high current tests on circuit breakers in mines to determine their effective interrupting capability.

There are a lot of commercially available test sets for carrying out short circuit tests on circuit breakers. However, most of the test sets are designed to test the trip mechanism rather than arc interruption capability, which is the determining factor in the overall performance of the circuit breaker.

This test set, designed and currently being fabricated at WVU has the capability of performing arc interruption tests on circuit breakers, besides being capable of performing all routine tests done by the presently available test sets.

The test set has to be portable to be easily carried around for making field tests of circuit breakers installed in mine systems. This posed major design limitations on the size and thereby the current capability of the set.

Keeping in view these limitations the set was designed for a current level of 5000 A.

C.2 COMPONENTS OF THE TEST SET

The electrical layout of the test set is shown in Fig. C.1. The specifications of the various components in the set are described below.

C.2.1 Main Enclosure (A)

The main enclosure is used to house the high power part of the circuit including the main high current transformer, current limiting inductors, transient recovery voltage network, control circuit breakers and switches and current transformers.

The overall size of the enclosure is 36" x 24" x 18" deep and is made out of 12 gauge steel.

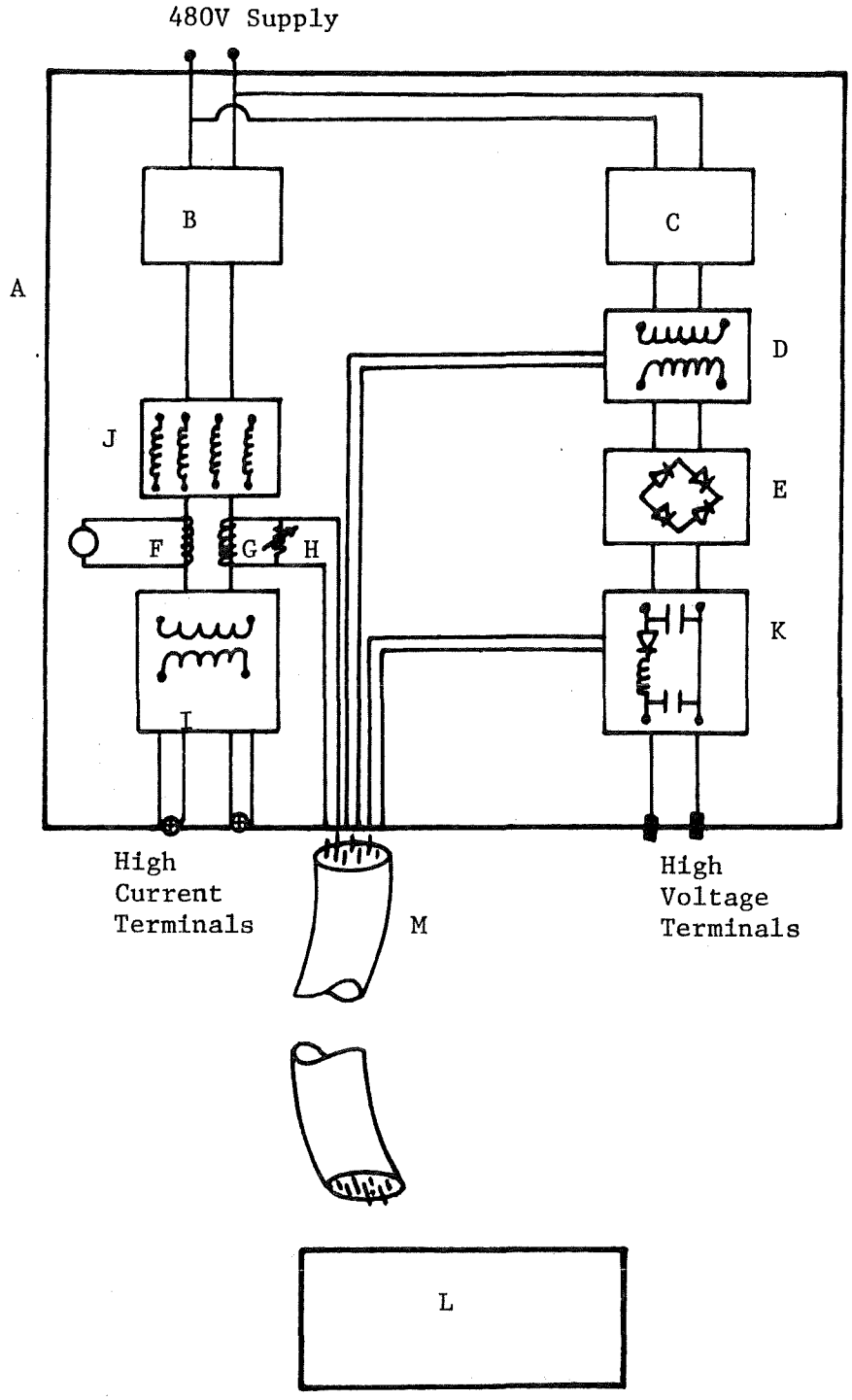

Fig. C.1. Layout of the Circuit Breaker Test Set.

C.2.2 Circuit Breaker(B)

This device is used to switch the high current part of the circuit. It is rated at 480 V, 100 A.

C.2.3 Control Switch (C)

It controls the high voltage part of the circuit. It is rated at 480 V, 5 A.

C.2.4 Control Transformer(D)

It provides the 120 V power supply for the electronic circuits as well as the voltage for charging up the T.R.V. network. It is rated at 480/120-240 V, 250 VA.

C.2.5 Rectifier (E)

It rectifies the ac voltage to charge up the main capacitor bank. It is rated at maximum peak reverse voltage of 1200 V, at an operating current of 0.75 A.

C.2.6 Current Transformer(F)

This is used to measure the current level of the test set in conjunction with an ammeter. The current transformer is rated at 300/5 A, 2 VA while the meter is 300 A, 0.007 Ω.

C.2.7 Current Transformer (G)

This current transformer is rated at 250/5 A, 15 VA and is used to provide the signal for the triggering control circuit, as well as a signal for actuating the digital timer which measures the interruption time of the circuit breaker. It has to be used in conjunction with potentimeter H which is rated at 25 Ω, 25 watts.

It is very important to set the potentiometer H according to the level of the test current. The reason is that the level of the voltage should be around 3.75 - 5 V to actuate the relay which in turn actuates the digital timer.

For example, to calculate the potentiometer setting for the minimum expected value of output test current (≃200 A).

Transformer "I" primary current = $\frac{200}{15}$ = 13.3 A

CT 'G' secondary current = $\frac{13.3}{50}$ = .266 A

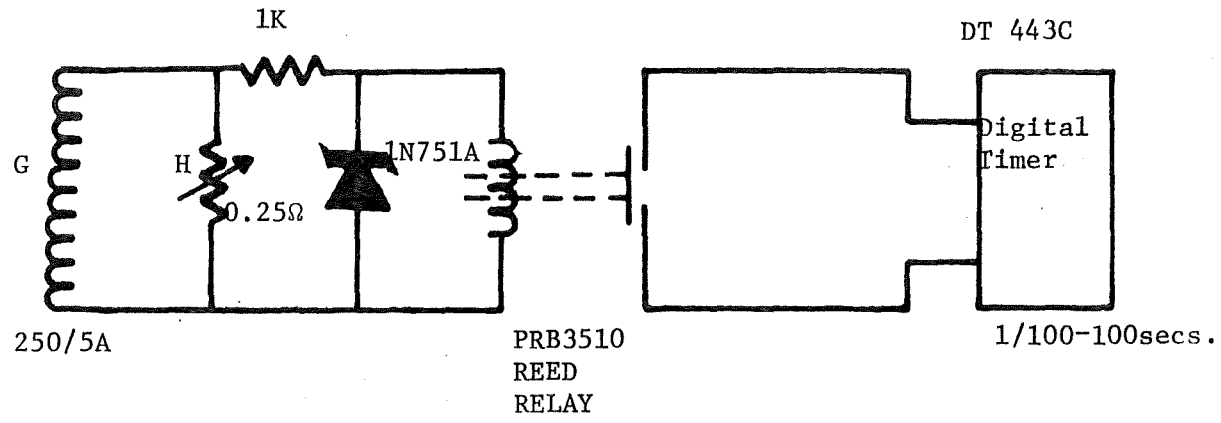

Fig. C.2. Circuit for Actuating Digital Timer.

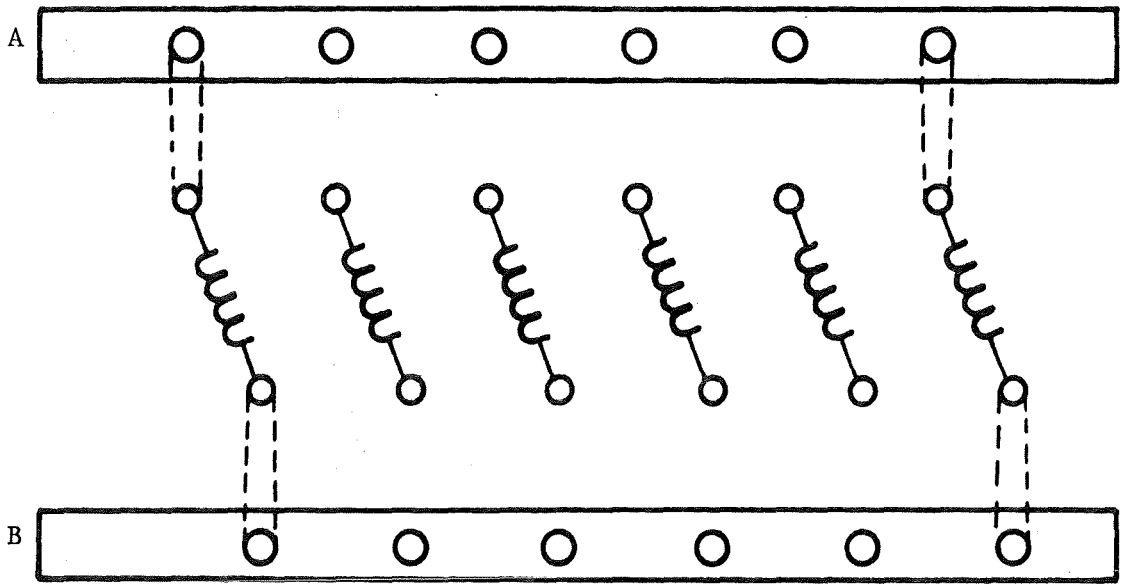

Fig. C.3. Connection Diagram for Inductors.

Thus, for an output voltage of 4 V, the potentiometer setting

will be = $\frac{4 \text{ X}}{0.266}$ = 15.04 Ω

Similiarly for the highest expected value of current the potentiometer setting is 0.60 Ω.

The diagram of connections for the relay and the digital timer is shown in Fig. C.2. The zener diode is used to regulate the voltage across the relay coil.

C.2.8 Main Transformer (H)

This transformer supplies the short circuit current to the breaker under test. It is rated at 480/32 V, 25 kVA. The secondary voltage is chosen to counteract the voltage drop across the arc.

Full load current $(I_{FL}) = \frac{25000}{32} \simeq 800$ A

Assuming the safe value of short circuit current is approximately 6 per unit, the maximum test current is 800 x 6 A or 4800 A.

The base impedance is $\frac{(480)^2 \text{ x } 10^{-3}}{25}$ or 9.216 Ω.

If the transformer impedance is assumed to be around 6 per-cent the transformer inductance comes out to be 1.47 mH. This has to be taken into account when calculating inductance values for limiting the test current.

C.2.9 Inductor Bank (I)

These air-cored inductors are used to limit the level of the test current. Air-cored inductors were preferred over resistors or capacitors because of their smaller size and lower power dissipation.

After careful analysis it was decided to use six inductors each of 12 mH. The conductor chosen is 14 AWG. The specifications are:

Rated current = 20 A
Fusing current = 166 A
Ohms/Lb = 0.2032
Lbs/1000 ft = 12.43

The former chosen for winding the inductors is 3.5" in length and 3" inside diameter. It is found that to get the required value of inductance 500 turns are needed. This amounts to a total weight of 6 lbs. per coil.

Since the test current has to pass for only a few seconds, the conductor is grossly undersized. The ratio of the design current to the rated current is around three.

To achieve the desired values of the test current the inductors have to be connected in various series parallel combinations. The various feasible configurations and the level of the test currents obtained are indicated in Table C.1. The maximum time for which the test current should be allowed to flow is also indicated for each setting. This limitation has been imposed because of under-sizing of the conductor for the coils. The test times indicated have been determined after careful experimentation and should not be exceeded.

To achieve this flexibility in connections the inductors are connected as shown in Fig. C.3.

The terminals of the coils are arranged in a triangular fashion, forming corners of an equilateral triangle. A and B are two metallic busbars which act as terminals for the inductor bank. By connecting metal strips from the coils to the busbars or ends of other coils, all the possible configurations indicated in Table C.1. can be achieved.

C.2.10 TRV Network (K)

This network is used to shape the transient recovery voltage across the breaker. C_1 and C_2 are each rated at 1000 V, 10 μF and 2 μF, respectively. With these values the peak value of the transient recovery voltage is $\frac{480 \times 20}{12}$ or 800 V.

The frequency of the T.R.V. can be controlled by switching appropriate values of inductance L. For designed values of frequencies 1000, 2000, 5000 and 10000 HZ, the respective values of inductances calculated are 30.4, 7.6, 1.22 and 0.30 mH.

The higher the value of the frequency, the greater is the stress on the circuit breaker.

The thyristor T used is rated at a peak reverse voltage (PRV) of 1000 V at 10 A.

C.2.11 Control Enclosure (L)

This houses the electronic circuitry, power supplies, digital timer and associated equipment. It has to be separated from the main enclosure because the high magnetic fields set up might impair the operation of the various electronic components.

Table C.1

Various feasible configurations of current limiting inductors and corresponding test currents

Connection	Transformer Primary Current (A)	Breaker Test Current (A)	Max. Allowed Test Time (secs)
6S	17	255	20
5S	21	315	20
4S	26	390	20
3S	35	525	20
3S-P-3S	65	975	20
4S-P-2S	72	1080	15
3S-P-2S	80	1200	20
2S-P-2S-P-2S	134	2010	10
3S-P-2S-P-1S	159	2385	5
2S-P-2S-P-1S	170	2550	5
2S-P-2S-P-S-P-1S	232	3480	5
3S-P-1S-P-1S-P-1S	254	3810	5
4-P	284	4260	2
5-P	328	4920	2
6-P	366	5490	2

Legend: S means series connection
P means parallel connection
5S means 5 in series
3S-P-3S means three in series in parallel with three in series and so on.

C.2.12 Control Cable (M)

This is a nine conductor control cable used to carry control signals from the main enclosure to the control enclosure. The description of various conductors is as follows:

Conductor #	Description
1 & 2	120 V signal for power supplies
3 & 4	Current signal for trigger control
5 & 6	Breaker contact actuating signal
7 & 8	Triggering pulse for Thyristor T
9	Ground.

REFERENCES

1. "Manual on Electrical Insulation Testing" No. 21-P8 by James G. Biddle Co.

2. "Infra-Red Use for Maintaining Power Cables" by Ivan A. Nichols, Sixteenth Annual IEEE Pulp and Paper Conference, June 17-19, 1970.

3. H. L. Saums and W. W. Pendleton, "Materials for Electrical Insulating and Dielectric Functions", Hayden Book Company, Inc., N.J., 1973.

4. K. A. Macfadyen, "Small Transformers and Inductors", Chapman and Hall, London, 1953.

5. L. F. Blume, "Transformer Engineering", John Wiley & Sons, Inc., London, 1938.

6. Alfred Still and Charles Siskind, "Elements of Electrical Machine Design", McGraw-Hill Book Company, N.Y., 1954.

7. Bernard Ostle, R. W. Mensing, "Statistics in Research", The Iowa State University Press, 1975.

8. Charles Lipson and N. J. Sheth, "Statistical Design and Analysis of Engineering Experiments", McGraw-Hill Book Company, 1976.

9. "Statistical Analysis of Thermal Life Test Data", IEEE Std. 101-1972.

10. W. Yorkowsky, "Accelerated Testing Technology", Hughes Aircraft Company, California, 1967.

CHAPTER II

DIGITAL COMPUTATION AND SUPPRESSION OF ELECTRICAL TRANSIENTS

2.1 INTRODUCTION

This is the second year of effort on USBM grant number G0144137 related to the control of electrical transients on mine power systems. During the first year, the effort was concentrated on digital simulation of electrical transients on mine power systems. The major thrust that year was to analyze the capabilities of various general circuit analysis programs (such as ECAP, CSMP and TESS) and to develop models for the various power system components for use in these programs.

The status of the research at the end of the first year was essentially one of budding capability. Sufficient experience had been gained with the programs so that the model limitations and other problems with the flexibility of ECAP were recognized. Also, the difficulty in putting all of the system equations in a form acceptable to CSMP for transients studies was a problem. The TESS system provided the greatest flexibility and put the fewest restrictions on the system size. Therefore, the decision was made to use TESS for the bulk of the programming during the second year.

At the end of the first year, models of all of the key elements in the power system had been developed but the flexibility of these models and the validity of the assumptions embedded in them (such as linearity) was doubtful. Therefore, a sizable amount of time was devoted to the removal of several deficiencies. Among these deficiencies was the fact that the cable models formerly allowed only length to be varied and not cable size. In a similar manner, former models were for specific size machines and transformers rather than for types of machines with variable ratings. Finally, there were no provisions in some of the models for nonlinear effects due to the saturation characteristics of iron in the devices. The manner in which all of these problems were alleviated will be discussed in detail below. In addition, the first system that will be studied will be presented along with a discussion of elimination techniques that can be used to combat transient problems.

Another improvement in the device models is the recognition that the duration of the transient influences the complexity of the system models. For instance, when one studies transients related to machine start-up, the relative time duration is quite long and the mechanical system's parameters have time to change. Thus, velocities, slips, and kinetic energies can change. Therefore, these quantities must be reflected into the machine models. For other transients, such as cable energization or transformer energization, the duration of the transient is much shorter and the mechanical aspects of the system models need not be represented.

Next, the dc machine models will be examined. In this case the long duration model is relatively simple and is shown in Fig. 2.3. The thing that makes this model so simple is the use of the torque-current analogy. This technique allows one to represent the mechanical parameters of damping and shaft inertia by resistance and capacitance, respectively. The nonlinearity in this machine is represented by varying the parameter k_f according to the slope of the B-H curve at the operating point.

The short duration model for the dc machine is shown in Fig. 2.4. This model is quite simple and consists of a R-L circuit in series with a controlled source. In this case the source e.m.f. is still dependent on the shaft velocity but the velocity is assumed to be a constant in this case. The e.m.f. is a function of the field current which equals the armature current for the series machine. Finally, the saturation level controls the value of k_f which is the third factor controlling the e.m.f. of the armature.

The long and short duration models for synchronous machines are shown in Figs. 2.5 and 2.6, respectively. Once again the simplification in the equivalent circuit is clearly visible for short duration transients. This difference is accentuated by the fact that the long duration model of Fig. 2.5 must be augmented by two equations for the electromechanical systems. These equations are for the electromechanical torque produced by the machine and Newton's equation of motion for the shaft of the machine.

The long and short duration models for a single-phase transformer are shown in Figs. 2.7 and 2.8, respectively. The major difference between the two models is the inclusion of winding-to-ground and winding-to-winding capacitance in the long duration model. These capacitances are responsible for rather high per unit surges on the secondary (low voltage side) of a transformer when a steep front surge appears on the primary. This phenomenon will be described in detail below. The saturation effects in the transformer are included in the model by modifying the mutual impedance, M_{12}, in Fig. 2.7. The equivalent circuit of Fig. 2.8 has saturation included by modifying the inductance L_m which once again arises out of the mutual inductance M_{12}.

The long and short duration single-phase equivalent circuits for cables are shown in Fig. 2.9. The definition of what constitutes a long or short cable is somewhat complicated. Actually three distinct lengths can be identified. The longest cables should be handled as true distributed elements by modeling them as delay lines (lossy) or as ladder networks of RLC elements. Intermediate lengths should be modeled as a single pi section in order to retain the effects of the shunt capacitance. Short cables can be modeled adequately as series impedances.

During the second year's effort a new thrust on the evaluation of suppression devices was started. The results of this investigation will be presented in the second half of this chapter. In essence, commercial suppression devices were analyzed with respect to three parameters: Frequency or rise time, voltage magnitude and energy.

2.2 MODEL IMPROVEMENTS

As mentioned above, a sizable number of improvements have been made in the models developed through the first year's effort. These improvements will be covered in this section and include a representation of nonlinearities, adding flexibility in device ratings or size and modification of models for short duration studies.

2.2.1 Representation of Nonlinearities

The economic design of machines and transformers requires that the iron in these devices be worked as hard as possible. This means that even in the steady state, at rated voltage, the devices will have magneto-motive forces that will produce fluxes in the nonlinear portion of the iron's characteristic. During transients these excursions can be well into the saturated or nonlinear regions of the device's B-H curves. Therefore, it is very important that nonlinearities be represented in all machines and transformers.

A method of representing the effect of saturation is described by Shackshaft.[1] This consists of assuming that only the mutual inductances of a device change with saturation levels. The basic result of increasing the levels of saturation is to reduce the values of mutual inductance. For instance, the e.m.f. generated in a dc machine is generally written as $k_f i_f w_m$. In reality, k_f is a mutual inductance and as the field current builds up, saturation will occur and this reduces the effective value of k_f. Of course, as k_f decreases this also affects the mechanical behaviour of the machine since the torque produced is $k_f i_f i_a$.

All of the machine and transformer models now include this technique to simulate saturation with the exception of the synchronous machine model,where it was not deemed necessary.

2.2.2 Modification of Machine or Transformer Ratings

The previous models developed using the TESS system to represent machines and transformers had a serious weakness. This weakness was due to the fact that the models were for a particular machine or transformer rating, such as a 25 hp induction motor or a 250 kVA transformer. It was decided to make the models more flexible by making use of the fact that almost all devices of the same type have essentially the same parameters when expressed in per unit using the devices' own ratings as base values (see Table 2.1). Once the model is stored

in per unit, one can supply the device's ratings as input data and the program can calculate base quantities. These base quantities are then used to convert per-unit quantities in the general model to specific values for that particular machine or transformer.

This feature has been included in the model of the dc machine, induction motor, synchronous machine and three-phase transformer. A slightly different approach was used to allow the size of cables to be varied. This is explained below.

2.2.3 Modification of Cable Size

The models developed during the first year's effort for various types of cables were not general because they were for a specific size of cable. The cable length could be changed by specifying a value in the input data stream. A peculiarity of cable design was used to overcome this shortcoming. This peculiarity of design is that the ratio of any two dimensions in a given cable type tends to be the same for cables of various sizes. For instance, the ratio of the phase conductor radius to the phase-to-phase spacing is almost the same for a 4/0 or a 2/0 cable of the same type.

Suppose the cable model is stored for a certain base cable which has a conductor diameter D_{old}. Also suppose that one wished to know the resistances, inductances and capacitances of a similar type of cable that has a conductor diameter, D_{new}. Because resistance is inversely proportional to cross-sectional area, it is clear that the ratio of the new to old resistance is

$$\frac{R_{new}}{R_{old}} = \left(\frac{D_{old}}{D_{new}}\right)^2 \tag{2.1}$$

The relationship for cable capacitance and inductance is not nearly as simple. For instance, the inductance matrix for a cable consists of terms of the form

$$L_{ij} = \frac{\mu_o}{2\pi} \ln \frac{1}{D_{ij}} \tag{2.2}$$

where L_{ij} = the mutual inductance between conductors i and j in henries

$$\mu_o = 4\pi \times 10^{-7} \text{ h/m}$$

D_{ij} = distance from conductor i to j in m.

If i equals j in equation 2.2, then Lij is a self inductance and D_{ij} is the geometric-mean radius of the conductor.[2]

If all dimensions of the cable change by the same factor (to

preserve the ratios as described above) then each L_{ij} will become

$$L_{ij}' = \frac{\mu_o}{2\pi} \ln \frac{1}{kD_{old}} \tag{2.3}$$

where k equals D_{new}/D_{old}.

But, the inductance in equation 2.3 can be rewritten as

$$L_{ij}' = \frac{\mu_o}{2\pi}\left[\ln \frac{1}{D_{ij}} + \ln \frac{1}{k}\right] \tag{2.4}$$

Therefore, the effect of changing the conductor size in a cable is to add a correction term, $(\mu_o/2\pi)\ln(1/k)$, to each term of the original inductance matrix. This correction term will be positive when k is less than 1.0 and the term will be negative when k is greater than 1.0.

The only requirement to change the cable model from the base case to some other size is to provide the new cable size as input data. The program computes the correction matrix.

The correction to the capacitance matrix from the base case follows along the same lines as the inductance matrix but is somewhat more complicated because one normally computes the electrostatic coefficients and forms the capacitances by matrix inversion. The correction factors are added to the electrostatic coefficients. This will now be shown.

The electrostatic coefficient matrix for a cable consists of terms of the form

$$P_{ij} = \frac{1}{2\pi\varepsilon} \ln \frac{1}{D_{ij}} \tag{2.5}$$

where P_{ij} = the electrostatic coefficient between conductor i and conductor j

ε = permitivity in f/m

D_{ij} = the distance between conductor i and conductor j in m.

As before, if i and j are equal, P_{ij} is the self-electrostatic coefficient and D_{ij} is the geometric-mean radius.

The capacitance matrix is formed by inverting the matrix of electrostatic coefficients.

$$\underset{\sim}{C} = \underset{\sim}{P}^{-1} \tag{2.6}$$

If the conductor size is changed as before, the new electrostatic coefficients become

$$P_{ij}' = \frac{1}{2\pi\epsilon} \ln \frac{1}{kD_{ij}} = \frac{1}{2\pi\epsilon}[\ln \frac{1}{D_{ij}} - \ln k] \qquad (2.7)$$

Now, one can write the electrostatic coefficient matrix as the difference between the old matrix and a correction matrix that has each term equal to $\frac{1}{2\pi\epsilon} \ln k$. Thus, the new capacitance matrix is

$$\underset{\sim}{C}' = (\underset{\sim}{P} - \Delta\underset{\sim}{P})^{-1} \qquad (2.8)$$

The right hand side of equation 2.8 can be expanded using the binomial theorem (remembering the $\underset{\sim}{P}$ and $\Delta\underset{\sim}{P}$ are matrices). The higher order terms in $(\Delta\underset{\sim}{P})$ $(\underset{\sim}{P}^{-1})$ can be neglected yielding

$$\underset{\sim}{C}' = \underset{\sim}{P}[\underset{\sim}{U} - (\Delta\underset{\sim}{P})\ \underset{\sim}{P}^{-1}] \qquad (2.9)$$

This is the equation used to compute the capacitance matrix for cable sizes that differ from the base size of 4/0 AWG.

The cable types for which models are stored include G-GC, G-GC special, type 2, SHD-GC and dc flat cables.

2.2.4 Review of Present Models and the Effect of the Duration of Transients

The models that were presented in the first annual report were not classified as to the duration of transient for which they could be applied. Basically, the models were all very detailed and were valid for both long and short duration transients. This philosophy of modeling is wasteful in terms of computer time. For instance a very detailed model can require more complex computations to generate a short duration transient solution without adding much to the accuracy of the solution. The specific details that can normally be left out for short duration solutions are any effects related to the shaft or mechanical system. These mechanical systems have such long time constants (compared to the electrical system) that they do not change appreciably during the electrical transient. The only time mechanical systems need be represented is for long duration transients such as when a machine start-up current is required for several cycles of the system voltage.

With these facts in mind the models for all devices in the system will be reviewed and both long and short duration versions will be presented.

The first device to be looked at will be the induction motor. Fig. 2.1 shows the long duration version of the induction machine equivalent circuit or model. Notice that mechanical quantities like angular velocity, etc. are preserved. The short duration version is shown in Fig. 2.2 In this short duration model one assumes that the slip, s, is constant. This is basically the model used to perform steady-state ac analysis of induction motors.

TABLE 2.1

TYPICAL PER UNIT VALUES FOR INDUCTION MOTOR PARAMETERS

Parameter	Range of values
R_s	0.015 to 0.045
n^2R_r	0.015 to 0.045
$X_{\ell s}$	0.06 to 0.11
$n^2X_{\ell r}$	0.08 to 0.11
X_m	1.5 to 4.5

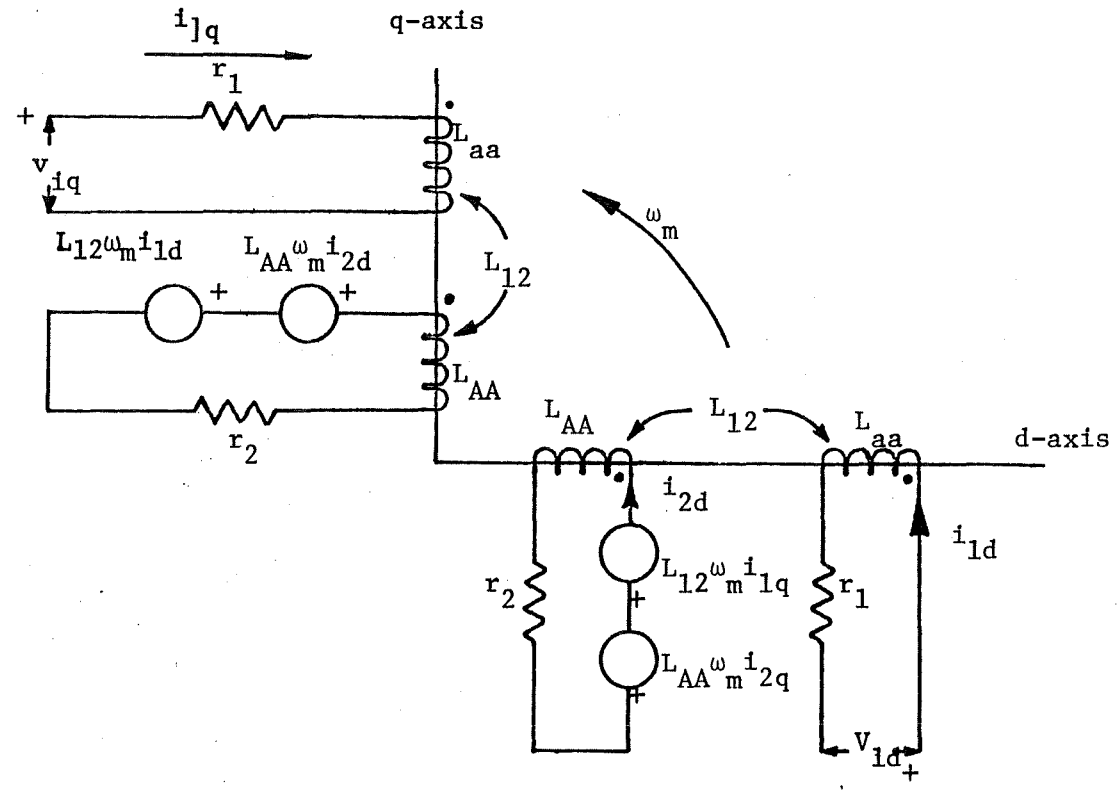

Fig. 2.1. Induction Motor Model for Long Duration Transients in d-q-o Coordinates.

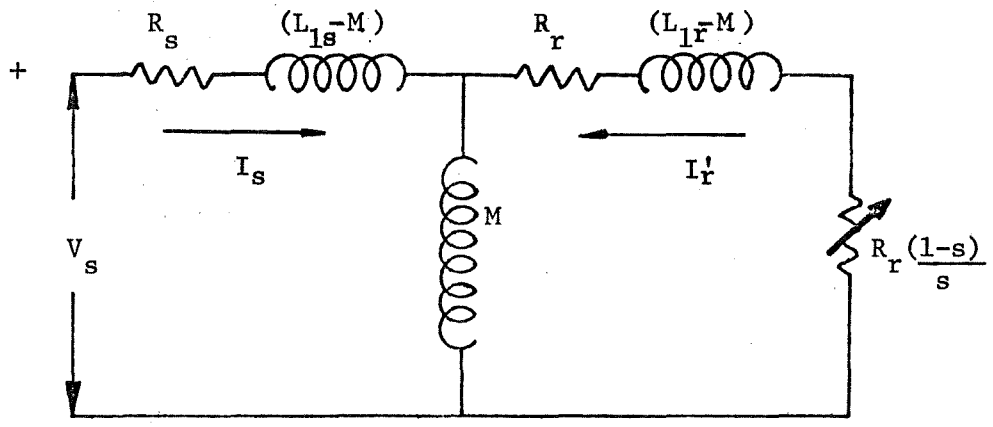

Fig. 2.2. Equivalent Circuit of An Induction Machine For Short Duration Transients.

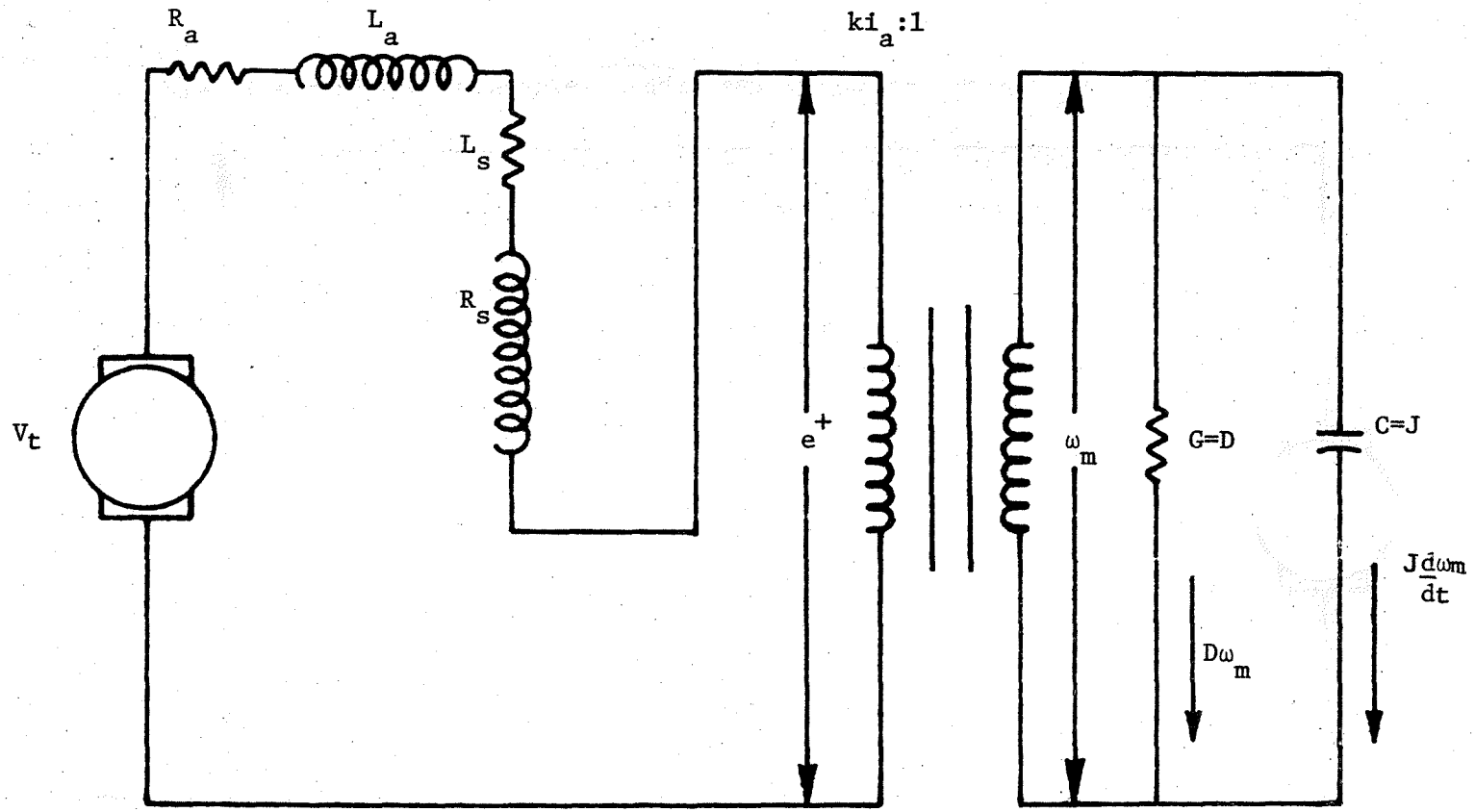

Fig. 2.3. Series DC Machine Model with Torque-Current Transformation Used for Long Duration Transient Studies.

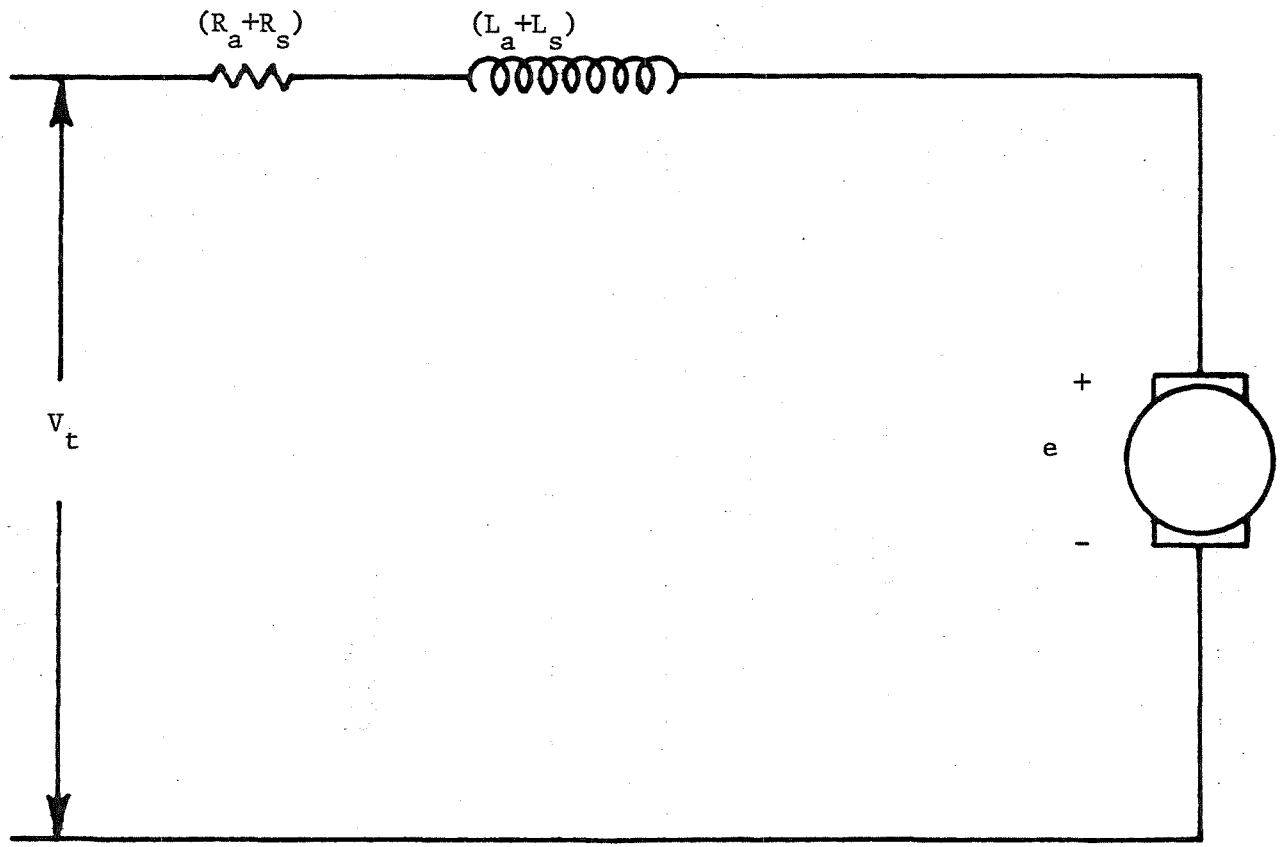

Fig. 2.4. Series DC Machine Model Used for Short Duration Transient Studies.

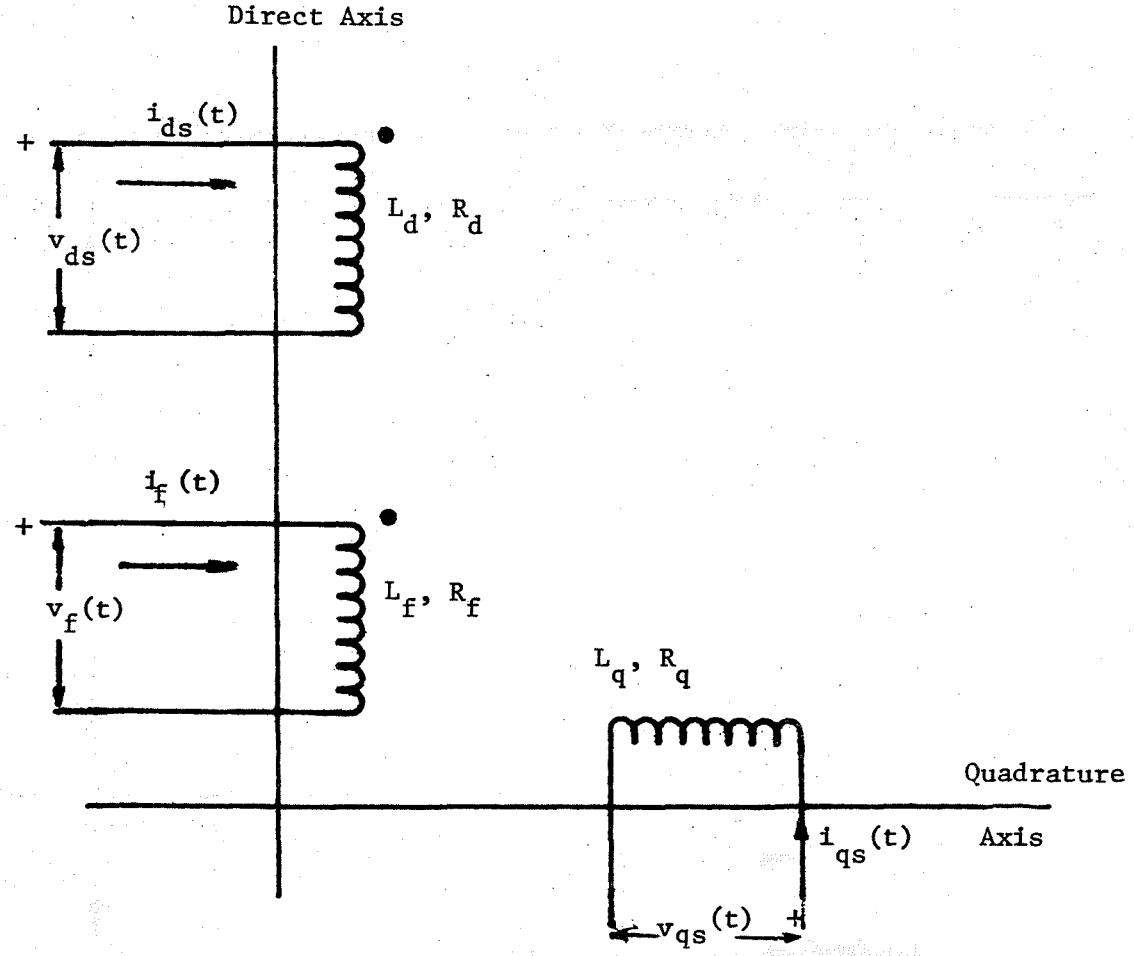

Fig. 2.5. Synchronous Machine Model for Long Duration Transient Studies.

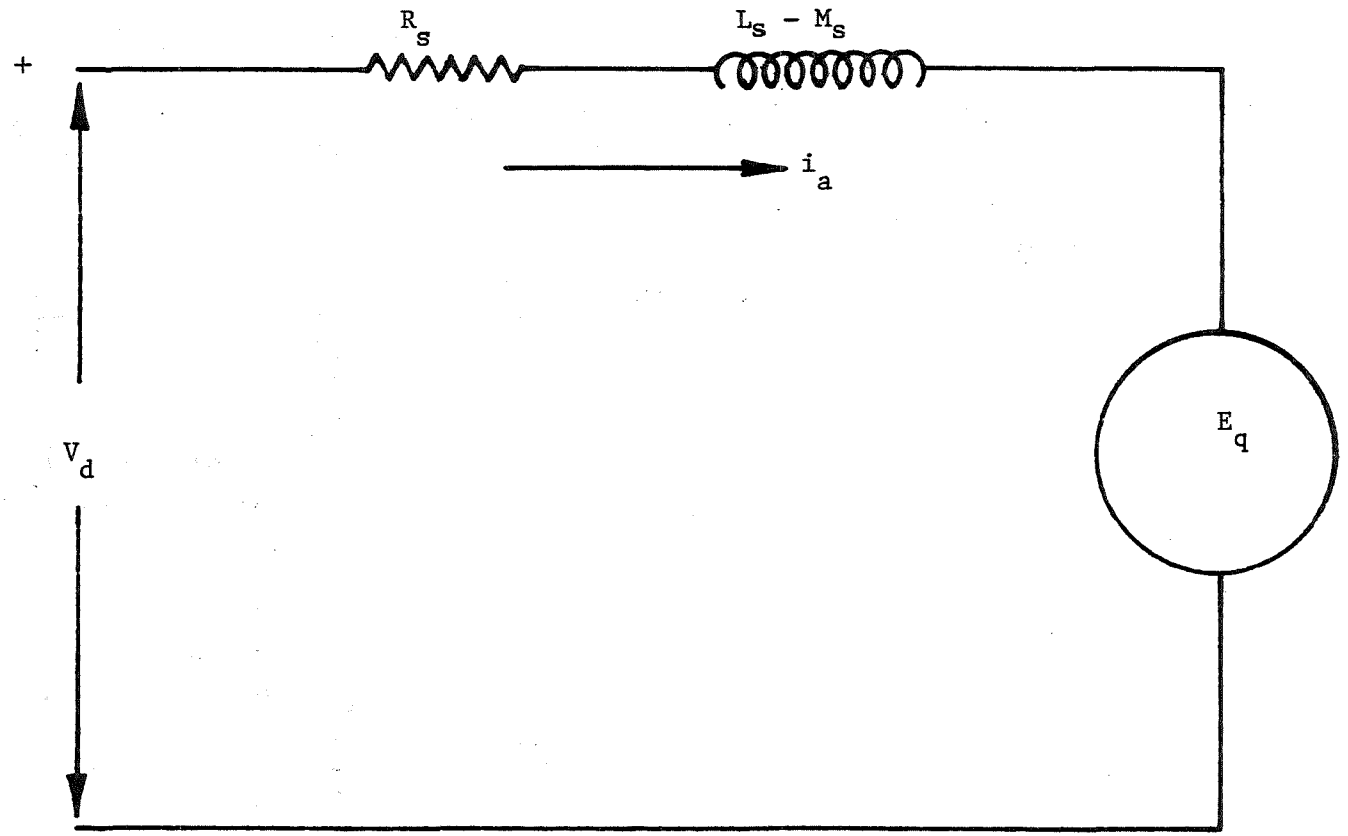

Fig. 2.6. Simplified of Synchronous Machine Model for Short Duration Transients.

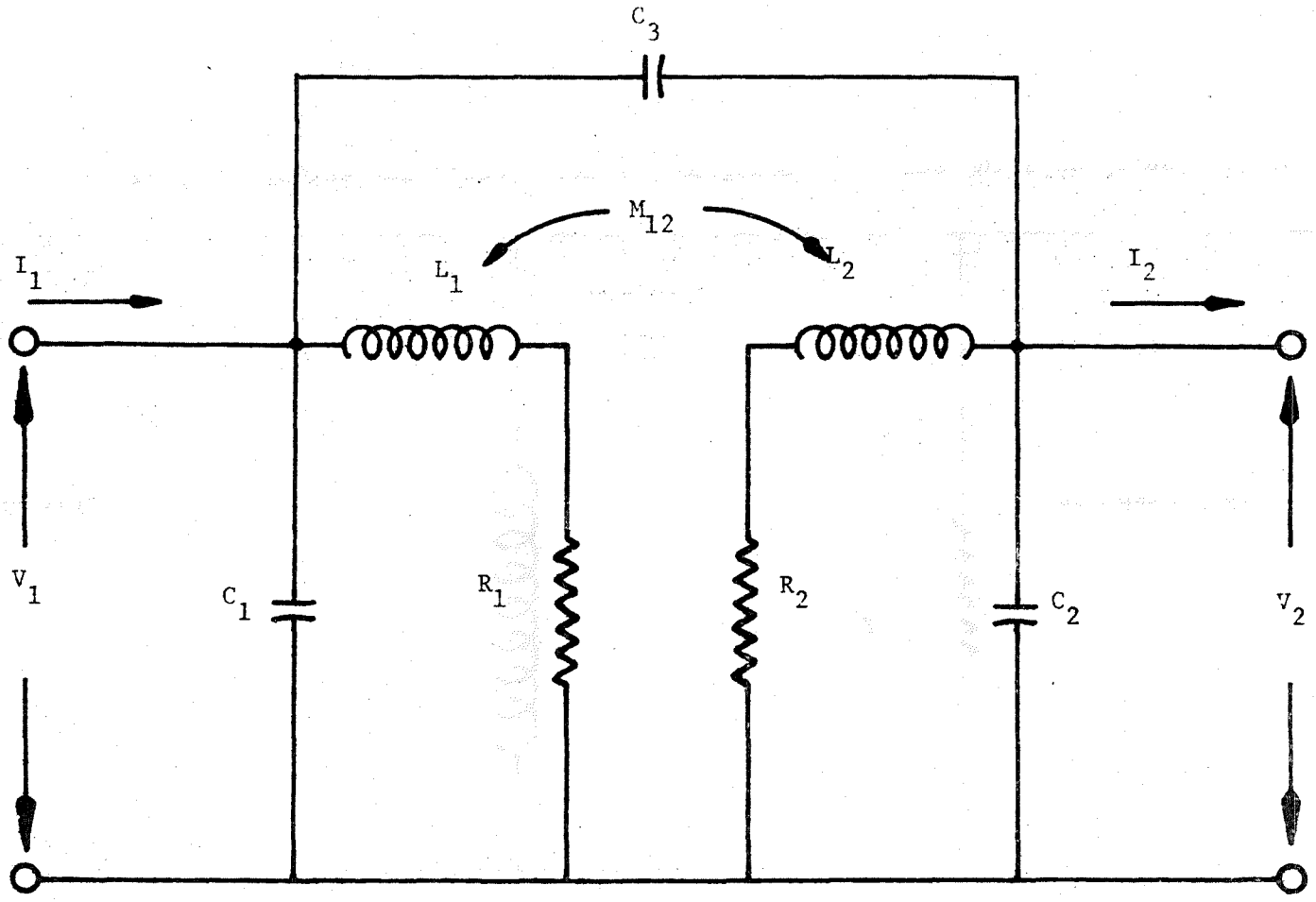

Fig. 2.7. Short Duration Transient Transformer Model.

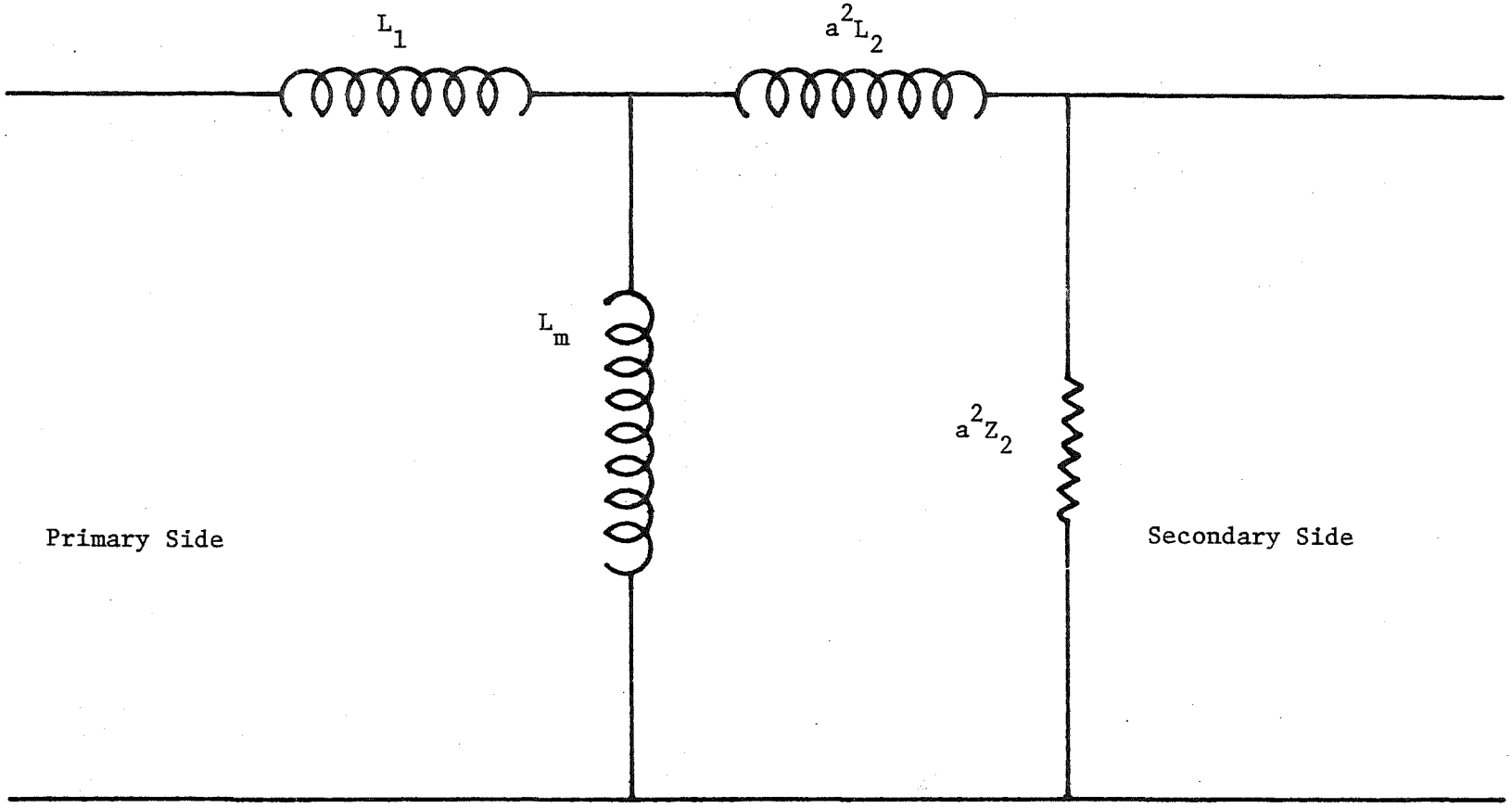

Fig. 2.8. Equivalent Circuit for a Transformer for Long Duration Transient Studies.

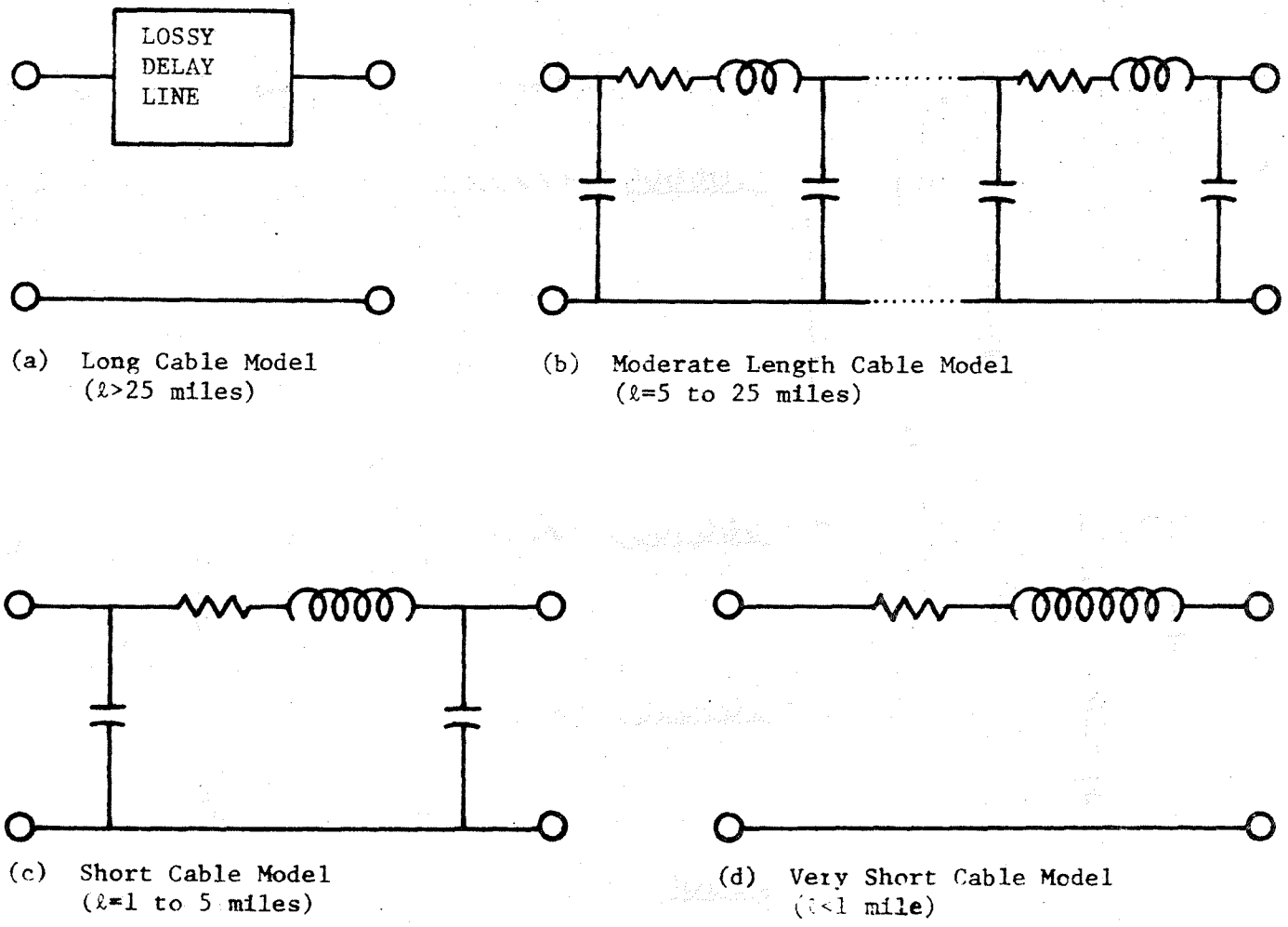

(a) Long Cable Model
(ℓ>25 miles)

(b) Moderate Length Cable Model
(ℓ=5 to 25 miles)

(c) Short Cable Model
(ℓ=1 to 5 miles)

(d) Very Short Cable Model
(ℓ<1 mile)

Fig. 2.9. Single-Phase Cable Models for Various Cable Lengths.

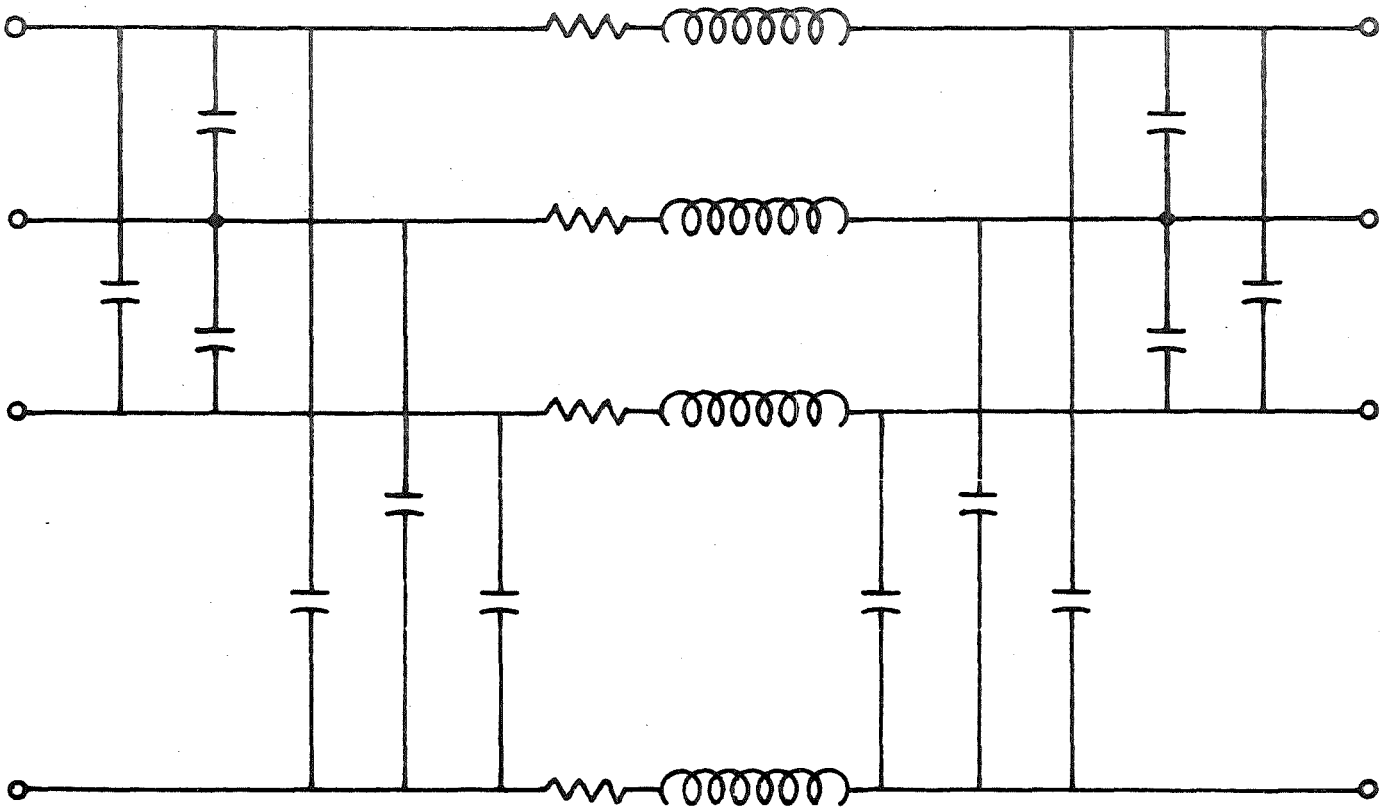

Fig. 2.10. Three-Phase Model of a Short Cable.

The decision as to what is long, intermediate and short can be judged along the lines of propagation times and the steepest front times expected. Generally, a switching surge will have a rise time of 100 μs or greater. The velocity of propagation on a cable is around 500 ft/μs. Thus, the propagation time for a one mile cable is about 10 μs and in 100 μs a wave can be transmitted and reflected five times on a one mile cable. Thus, it should resemble a lumped element.

Based on the above argument, cables substantially longer than one mile (about 5-10 miles long) should be modeled as distributed elements. Cables 1 to 5 miles long should be modeled as pi-sections and cables less than 1 mile long can be adequately modeled as series impedances. Since cables over five miles long are rare in mining, only short and very short cable models are needed. These two models are shown for a single-phase cable in Fig. 2.9, c and d. It can be seen that the only difference between the models is the absence of shunt capacitance in the very short cable model. Fig. 2.10 shows a three-phase cable model for a type G-GC cable.

2.2.5 Other Models

The models of other elements are rather simple. Rectifier models are relatively simple because all general purpose circuit analysis programs have built-in diode models. Surge or power factor capacitors are modeled simply as capacitors. Breakers are modeled either as ideal switches or a resistor can be included to represent arc or contact resistance. None of these will be discussed in detail here.

2.3 SWITCHING TRANSIENTS, NORMAL AND ABNORMAL

2.3.1 Normal Transients

A survey of the literature [3,4,5,6] on the causes of severe electrical transients in power systems is quite interesting for a mine electrical engineer because almost all of the causes of severe transients are present to a degree in mine electrical systems. For this reason it is not surprising that reports of transient oriented problems from mine operators are numerous. Perhaps one of the devices most prone to transient errors is the ground check monitor. These devices are frequently fooled into interpreting transient conditions as open ground conductors. This has been the subject of another USBM grant and will not be discussed in detail here.

Any switching operation creates a transient on a power system. This switching operation can be an energization or de-energization of cables, machine start-up, interruption of transformer excitation current, etc. Generally, a switching operation produces a transient overvoltage that is less than or equal to twice the steady-state peak line-to-

neutral system voltage. These are generally termed "normal switching transients."[3] The currents associated with these surges are generally limited to the surge voltage divided by the effective surge impedance at that point in the system. Surge current is not normally a problem for insulation systems since its duration is too short to cause appreciable heating. However, surge current (especially if it has a high rate of change) can be a serious problem for solid-state devices.

These so-called "normal" transients are not a severe problem on low-voltage power systems because of the safety margin built into the insulation systems of low-voltage power systems. Only in extra-high voltage power systems (345 kV and above) do normal switching transients lead to voltages approaching the breakdown level of the system insulation. In these cases, it is necessary to use opening and closing resistors to limit the surges to acceptable levels.[7]

While normal switching transients may not be a critical problem they may represent a subtle nuisance. Transient voltages in the range of twice normal system peak voltage on 4.16 to 13 kV systems may very well erode insulation strength over a period of time, leading to hazardous faults and loss of production due to down-time. This is a difficult theory to prove.

2.3.2 Abnormal Switching Transients

Coal mine electrical power systems represents a classical system as far as the generation of excessive transient voltages and currents are concerned. Frequently mentioned sources of abnormal switching transients (transients greater than twice the system peak voltage) include those in Table 2.2.

TABLE 2.2

SOURCES OF ABNORMAL TRANSIENTS

a) current chopping
b) capacitance switching-circuit breaker restriking
c) transformer magnetizing in-rush currents
d) ferroresonance
e) arcing ground faults
f) starting large machines on a relatively weak system
g) rectifiers
h) wave propagation through transformer winding capacitance

All these phenomena are possible in coal mine power systems. For instance, the use of vacuum interrupters leads to current chopping. Switching unloaded cables or power factor capacitors can lead to

circuit breaker restrikes. Energizing power centers or surface transformers can produce large transformer inrush currents. The conditions for ferroresonance can be obtained when a power center transformer is supplied through a long cable (a common condition). Arcing ground faults can occur on any system that is not solidly grounded. Many continuous miners have a rating that is a large percentage of the system capability. Some mines have rectifiers for haulage supplies and some mines have transformers without electrostatic shields.

An important phenomenon occurs in power transformers. The equivalent circuit for this device for short durations is shown in Fig. 2.7. Long duration models would not normally include the winding-to-ground and winding-to-winding capacitance shown (Fig. 2.8). These capacitances are quite important for short duration or steep-front surges. For instance, suppose a step of voltage is applied to the transformer of Fig. 2.7. The initial voltage on the secondary of the transformer is independent of the turns ratio and is given by

$$V_2 = \frac{C_3}{C_1 + C_3} V_1 \qquad (2.10)$$

If the device in Fig. 2.7. is a 4160 to 480 V transformer and the values of C_1 and C_3 are such as to allow 60% of the surge through to the secondary, a 2 per unit surge on the primary can create a surge of more than ten times normal in the secondary. This example demonstrates the need to represent the transformer in sufficient detail to reproduce all of the physical phenomena present in the actual device.

With all of these sources of transients present it is not surprising that transient voltages and currents are a problem in mine power systems. A starting point for the elimination or suppression of transients on mine power systems is to determine which of the items listed above are the most serious sources of transients. This will be accomplished by a series of computer simulations using models developed for electrical elements found in mine electrical power systems. Once the primary sources of transients are identified one can establish guidelines for the elimination of transients.

2.4 ELIMINATION OF TRANSIENTS

While all of the simulation has not been carried out to pinpoint the causes of transients, it is possible to discuss elimination of the sources of these transients. It is necessary to distinguish between suppression of transients and elimination of transients. The classical suppression technique is the use of a surge protection device such as a lightning

arrester. Usually the surge suppression device is made using a non-linear circuit element. On the other hand elimination of surges consists of removing the source of the problem. A good example of this is the replacement of old circuit breakers by new, non-restriking circuit breakers. Most power systems have relied on surge suppression devices rather than design to eliminate the source of electrical transients.

Each of the sources of electrical transients listed above should be studied and the possibility of its being eliminated from the mine electrical power system evaluated. For instance, current chopping is largely a phenomenon of vacuum interrupters. The main advantage of a vacuum interrupter is its smaller size compared to a device using an air or oil interruption medium. However, because of the transients introduced by vacuum interrupters (and other sources) it is necessary to install surge suppression devices and stronger thicker insulation. Perhaps an analysis will reveal that this is a poor trade-off in space.

Table 2.3 presents a list of elimination techniques that could be used to alleviate problems from various causes. This listing of techniques does not answer questions with respect to effectiveness, economy, reliability, availability and practicality of the elimination techniques. The computer modeling and study of transients by the authors has verified the effectiveness of the techniques while the assessment of the other qualities is in progress.

TABLE 2.3

ELIMINATION TECHNIQUES FOR SOURCES
OF ABNORMAL TRANSIENTS

Source of transient	Elimination technique
current chopping	replace vacuum interrupters by air or oil interrupters
breaker restriking	use non-restriking breakers
inrush current	avoid excessive transformer switching
ferroresonance	avoid circuit configurations prone to this phenomenon
arcing ground faults	avoid ungrounded systems
large machines-weak system	reduce machine size or increase system capacity
rectifiers	use filters on ac side
wave propagation through transformers	use transformers with electrostatic shields

Clearly, it is not possible to eliminate all of the sources of transients through either system design or modification of operational procedures. Thus, it is necessary to be able to assess the severity of transients and the effectivenss of surge suppression devices. Therefore, the evaluation of surge suppression techniques, is quite important. This is presented below.

2.5 EXAMPLES OF TRANSIENT STUDIES

2.5.1 Comparison of Analytical and Computer Results

As a means of verifying some of the models developed and the general accuracy of the TESS programming the system of Fig. 2.11 will be analyzed in two separate ways. The first is a direct analytical solution and the second is by digital computation using the TESS system. The results will then be compared to see if the frequencies of oscillation and peak values of transients are the same.

The system in Fig. 2.11 that was used for program verification was kept relatively simple to facilitate the analytical solution. The TESS system is capable of solving much more complex networks. The system studied consists of a source, a circuit breaker and a static load. The source is modeled with an internal voltage, winding resistance and leakage inductance as well as winding capacitance. The static load is actually leakage inductance for a motor shunted by winding capacitance. The initial conditions for the circuit are shown in Fig. 2.12. It will be assumed that the circuit breaker is closed when the capacitor has a voltage of $-V_m$.

The system is simple enough to solve by direct analytical means. The results of the analysis shows that the worst case of transient voltage across capacitor C_1 is three times peak line-to-neutral system voltage when the initial voltage on C_1 is $-V_m$.

The frequency of oscillation is

$$\omega = \left(\frac{L_1 + L_2}{L_1 L_2 (C_1 + C_2)} \right)^{1/2} \tag{2.11}$$

but $L_2 >> L_1$ and $C_2 >> C_1$, so

$$\omega = \frac{1}{\sqrt{L_1 C_2}} \tag{2.13}$$

or f = 3183 Hz.

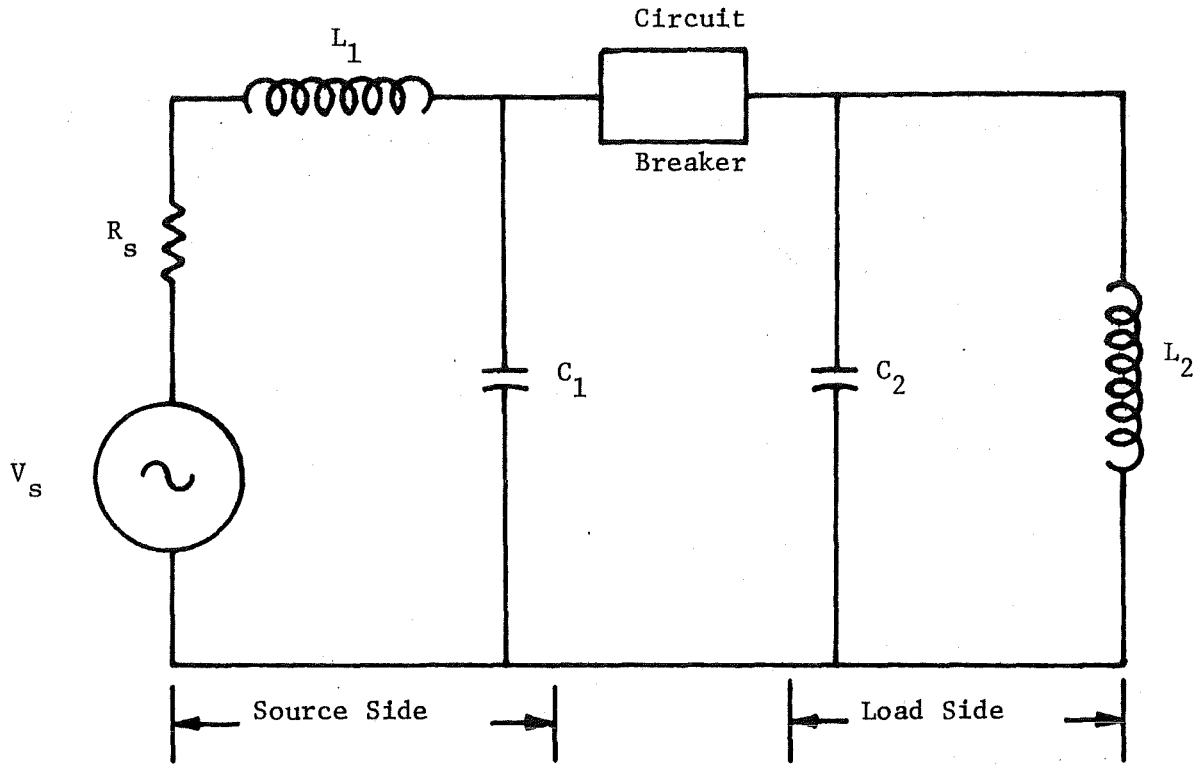

Fig. 2.11. Example Circuit.

$V_s = V_m \cos 377t$

$V_m = 11267.65$ volts

$C_1 = 4 \times 10^{-8}$ farads

$L_1 = 1 \times 10^{-3}$ henry

$C_2 = 1.0 \times 10^{-6}$ farads

$L_2 = 13.2 \times 10^{-3}$ henry

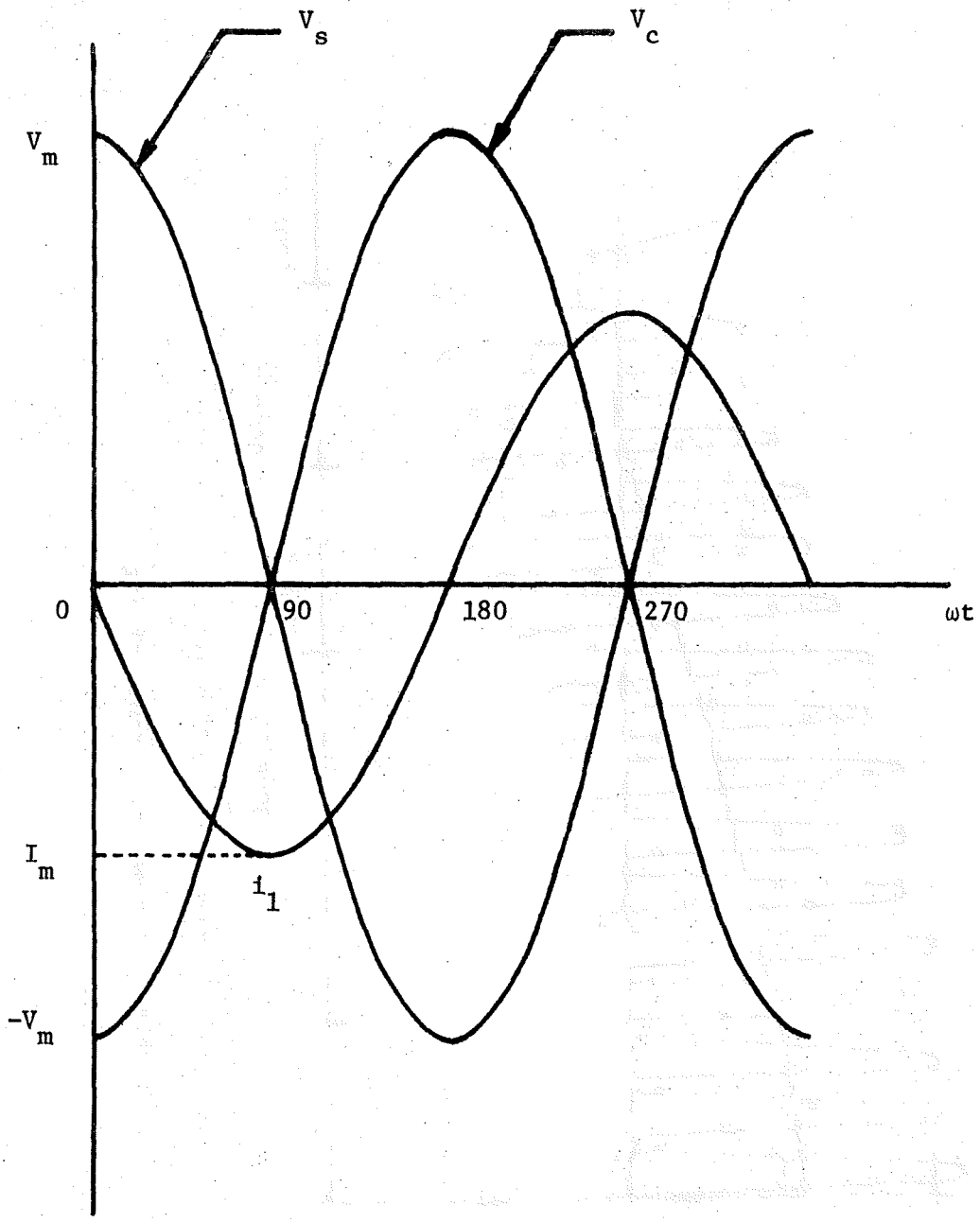

Fig. 2.12. Curves of Initial Conditions of Fig. 2.14.

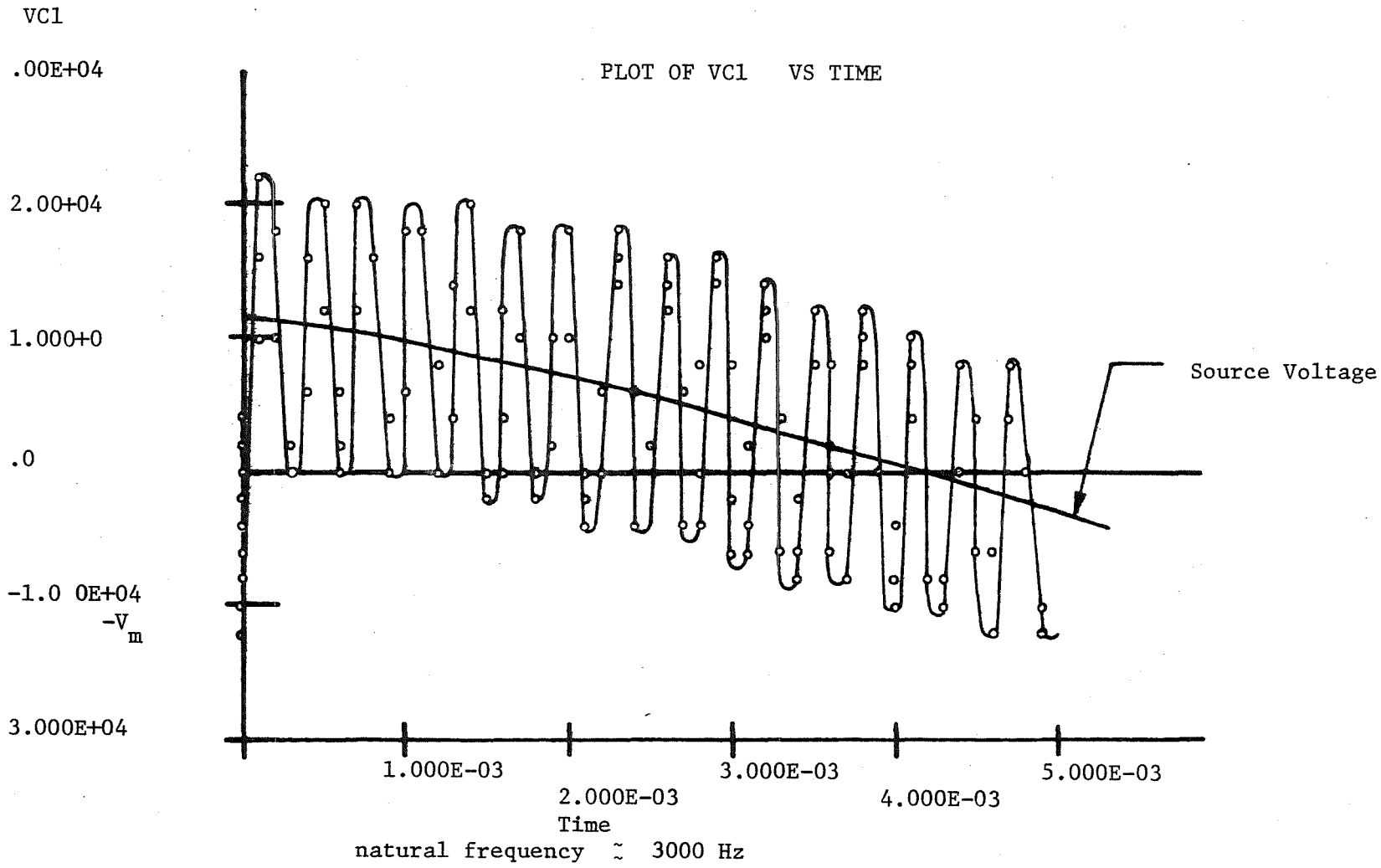

Fig. 2.13. Transient Voltage for Circuit of Fig. 2.11.

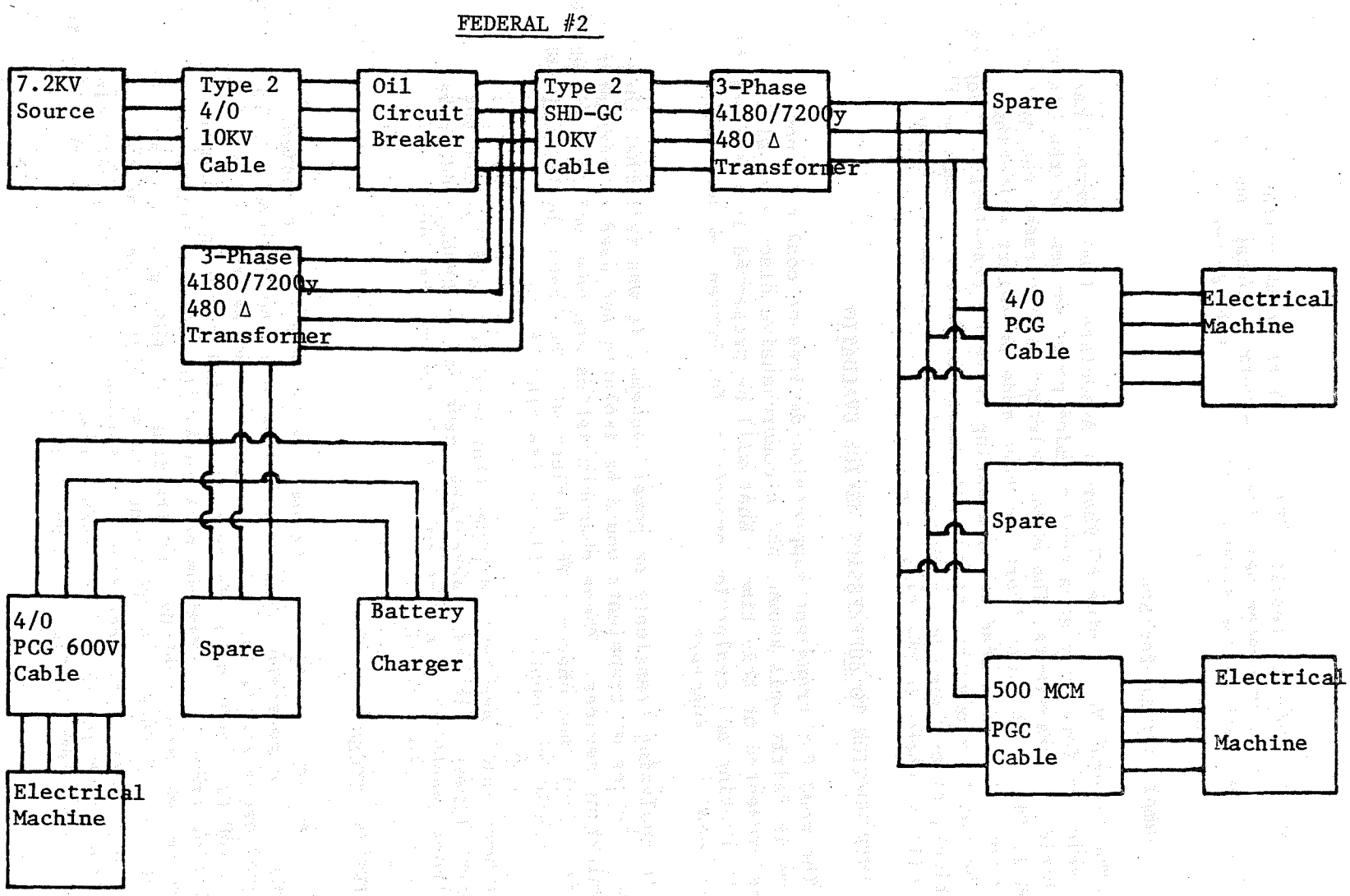

Fig. 2.14. Block Diagram of Federal #2 Power System I Section.

From the computer results (Fig. 2.13) the peak voltage across C_1 is also 3 times the system peak line-to-neutral voltage and the frequency of oscillation is about 3000 Hz. This demonstrates the accuracy of the digital simulation.

2.5.2 Sample System for Study

The Federal No. 2 mine of Eastern Associated Coal Company has been selected for study as a typical mine power system for the digital simulation of transients. The model selected to represent the system is shown in Fig. 2.14. An effort has been made to select switching operations that will lead to interesting (severe) transients. Programs will be run to study the various parameters of interest such as the durations, rise-times, and peak values of the transients. These data will be shown in the final report.

2.6 INTRODUCTION TO SUPPRESSION DEVICE EVALUATION

The need for transient suppression devices on coal mine power systems is fairly well known, and a comprehensive discussion will not be presented at this time. What will be presented is a description of the testing and evaluation procedures for current methods and devices used for suppression.

In analyzing transients on power systems, it was felt that three characteristics of transients would be isolated and used as parameters in evaluating devices. These characteristics are peak voltage, frequency (or rise time), and energy. The devices will be tested by holding two of the parameters constant, while varying the third.

Commercially available devices that were tested fall into three different types - lightning arresters, zener diode types, and surge capacitors (snubbers). A list and description of the devices considered is given in Table 2.4.

2.7 TESTING TECHNIQUES

Preliminary testing was done using a bread-boarded transient generator. The generator consisted of a single-shot trigger circuit that produced a single half-wave pulse. This pulse was fed into a 1:10 400 VA, 100 Hz - 5000 Hz audio-transformer that produced a damped oscillating transient. Maximum peak output is 3.6 kV. Frequency of oscillation was around 60 Hz. Limitations of this generator are its inability to change the frequency of oscillation and its minute energy capability. The generator did, however, illustrate quite clearly the voltage clamping ability of each device. The test set-up and typical waveforms are shown in Fig. 2.15 and Fig. 2.16.

TABLE 2.4

TRANSIENT SUPPRESSION DEVICES

Trade Name	Manu-facturer	Model Number	Number Ordered	(RMS) Normal Line Voltage	(Pk) Clamp Volt.	(Single Pulse) Diap. Cap.	Frequency Response	3Ø 1Ø	Suppressor Action	Cost/ Unit
Mov-Varistor	G.E.	V480PA80	4	480VAC	1350V	80J	N.A.	1Ø	Zener	$10.94
Thyrector	IRC	KSA19DBF	3	475V	1300V	2A	N.A.	1Ø	Zener	$13.24
AC Transient Suppressor[2]	MCG	LPTSA-480-3-8	2	480VAC	±800	8J.	N.A.	3Ø	Zener	$98.85
Voltrap	(W)	S04CA48AC	3	480VAC	1200V	10A	N.A.	1Ø	Zener	$35.68
Secondary Power Arrestor[3]	DALE	SPA-400	1	400VAC	1500V	60KA	10KV/μsec.	1Ø	SPARK OVER	$49.50
Snubber Ckt.		15μf, 1500V		480VAC	-		N.A.	1Ø	Snubber Ckt.	$30.00

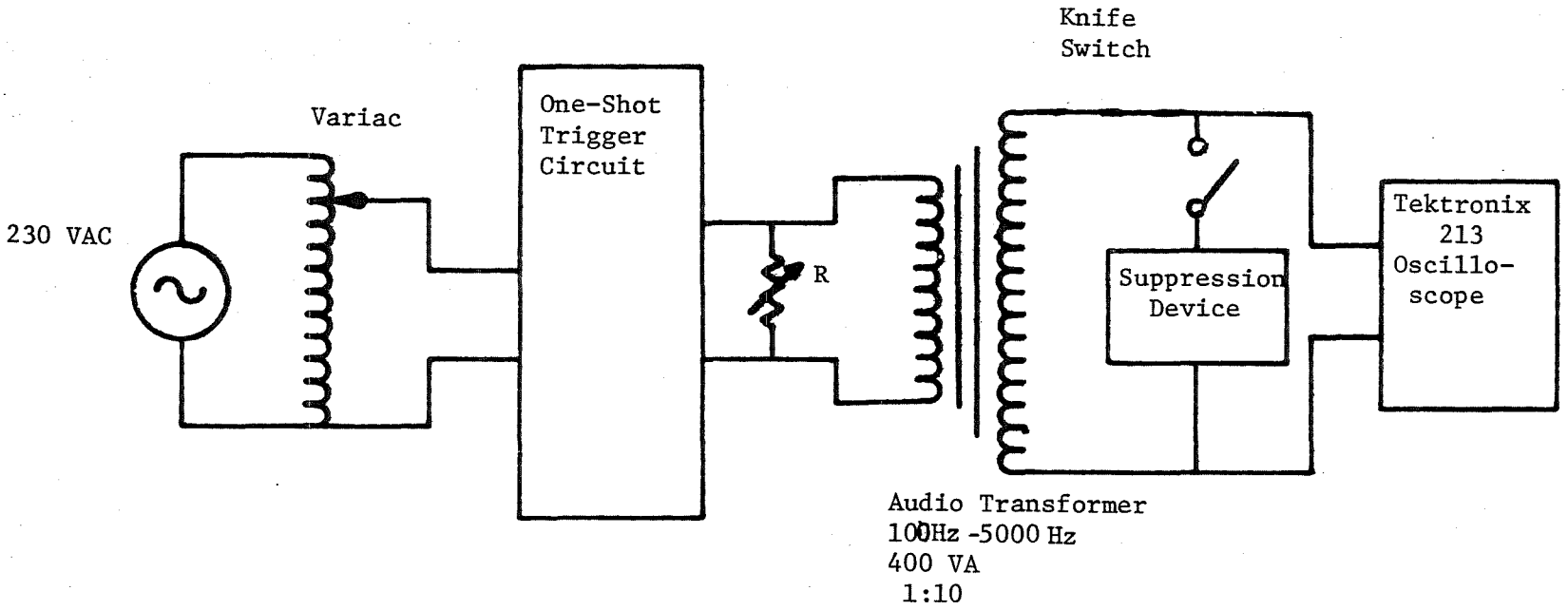

Fig. 2.15. Preliminary Transient Suppression Testing Circuit.

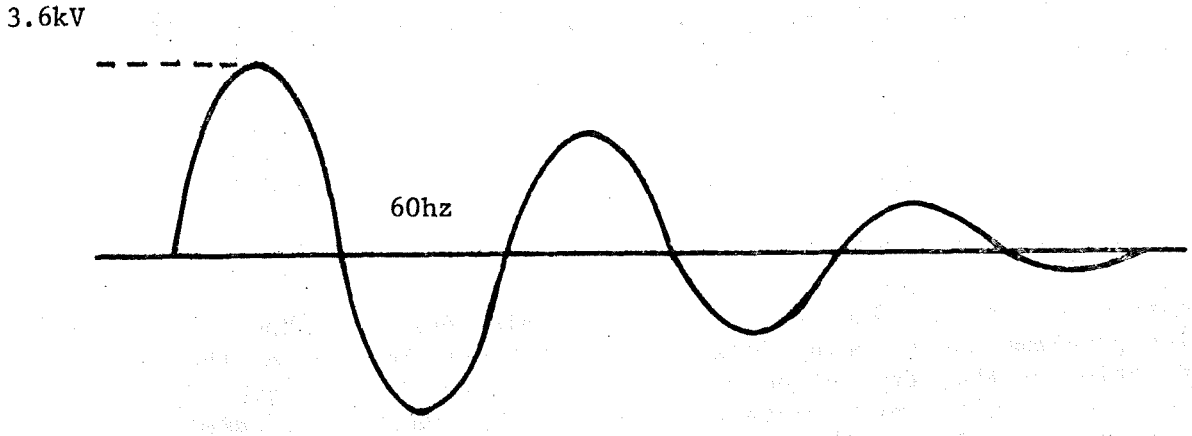

Unsuppressed Output of Preliminary Generator.

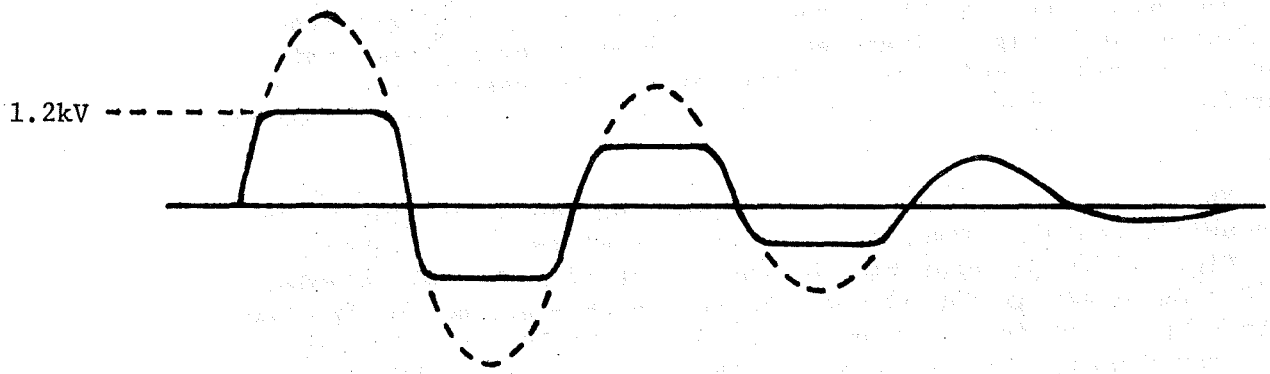

Typical Suppressed Output of Preliminary Generator.

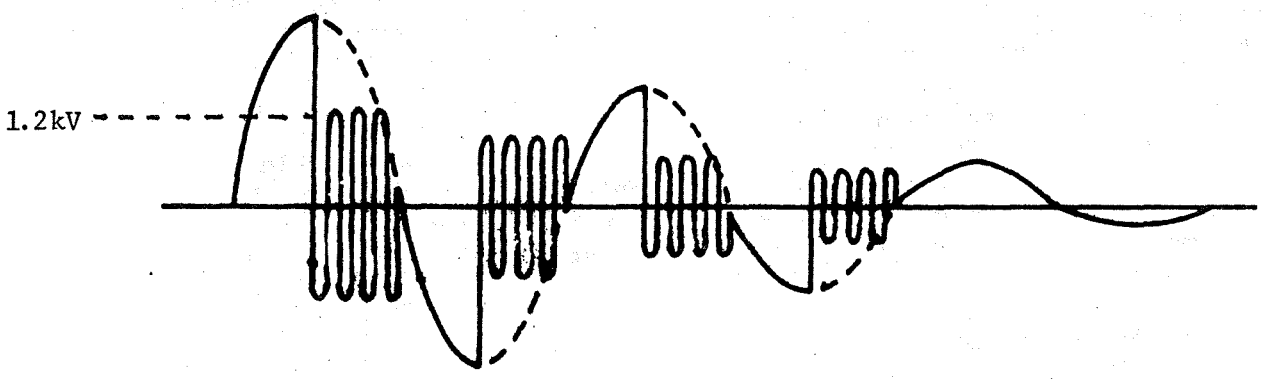

Dale Lightning Arrestor Suppressed Output.

Fig. 2.16.

Criteria for a more flexible transient generator were established as follows:

Maximum Voltage Peak: 5000 V

Frequency Selectability: 100 Hz - 10kHz

Energy Output: 200 J

An output waveform of damped oscillation is also desired. However, design problems and shipping delays forced the postponement of the fabrication of this type of generator. In its place a generator that gives a double exponential output was built. The waveform is similar to a lightning pulse. (See Fig. 2.19) and involves charging and discharging two capacitors.

The manufacture of this transient generator necessitated the development of a high-voltage switch. A search for a commercially made, inexpensive, safe, high-voltage switch was unsuccessful. Therefore, a punematic switch was developed and which proved electrically satisfactory.

Material used in switch construction included plexiglas tubing, an aluminim contact disk, and an inch of a miniature "Slinky". (See Fig. 2.17.) The operation of the switch is relatively simple. 50-60 psig of air is forced into the switch chamber, moving the lower contact up and striking the upper contact. The "Slinky" acts as a conductor from the base terminal to the lower contact. When the air pressure is released, the "Slinky" also acts as a spring and pulls the lower contact back to its resting position. Although pre-strike is present during switch operation, it does not adversely affect the transient generation. A layer of GE-7600 silicon conductive rubber was added to the upper contact, however, to reduce contact bouncing.

The transient generator set-up used in testing the devices is shown in Fig. 2.18. The testing procedure is initiated by charging up capacitor C_1, using the high voltage supply. Once C_1 reaches the desired voltage, the high-voltage supply is removed from the circuit. The pneumatic switch is then closed, developing a double exponential output voltage.

In order to operate the test set-up correctly, the following assumptions are made:

$$C_1 \geq 10\ C_2$$

$$R_2 \geq 10\ R_1$$

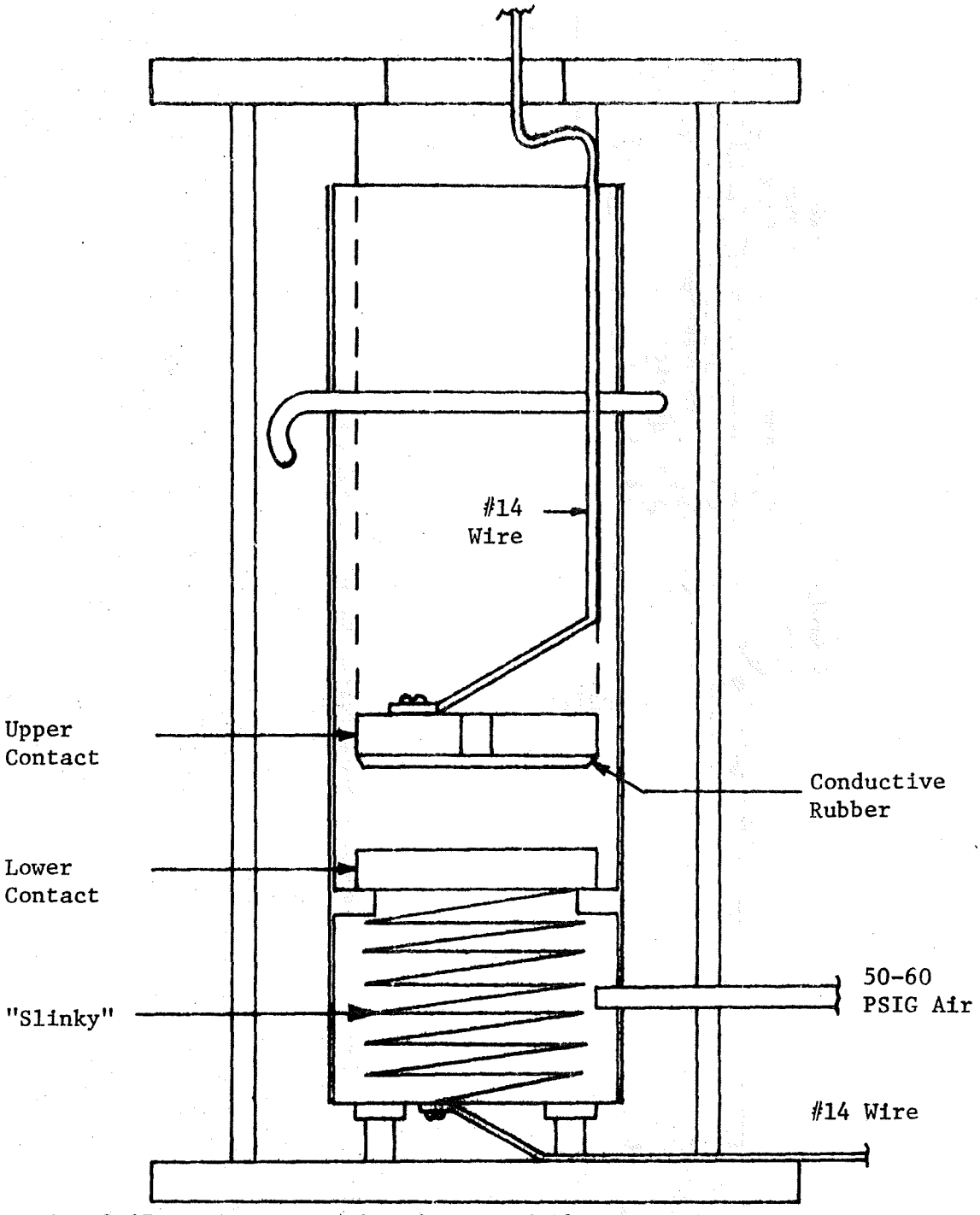

Fig. 2.17. Pneumatic High Voltage Switch.

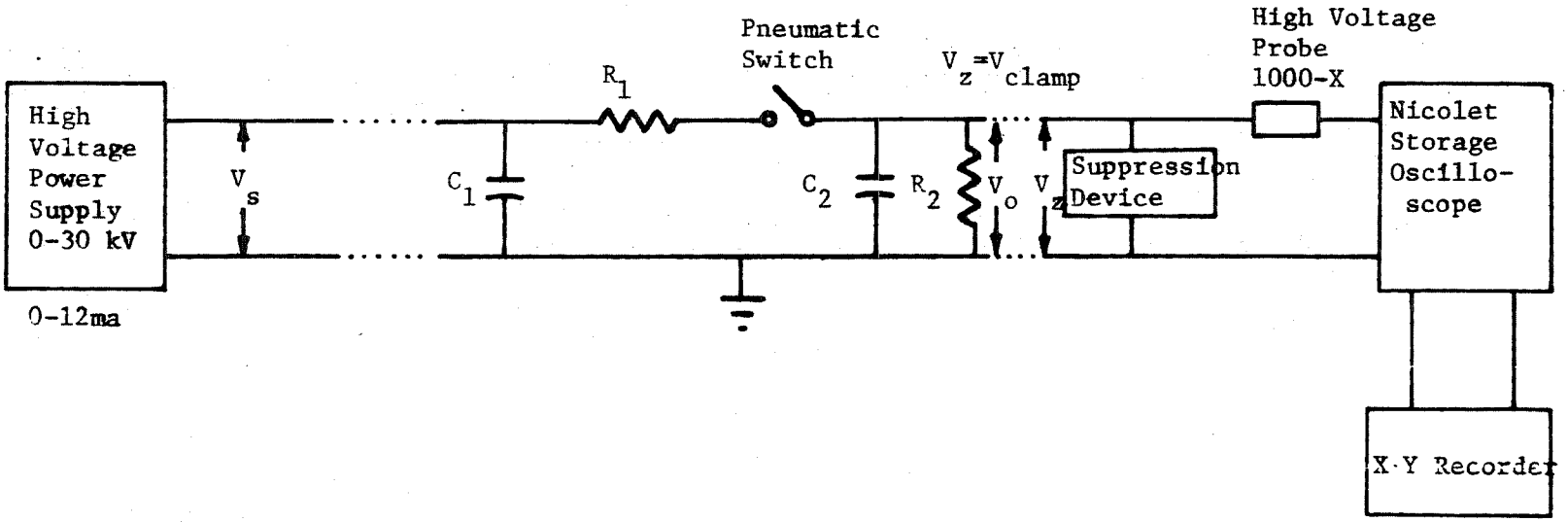

Fig. 2.18. Transient Suppression Device Testing Circuit.

The 10% to 90% rise time of the pulse is found to be $3R_1C_2$, while the fall time is governed by time constant, R_2C_1. The amount of energy in the transient is mainly a function of C_1 and its initial voltage, V_1.

2.8 TESTING PHILOSOPHY

Each device was subject to three different tests: voltage test, frequency test, and energy test. The Dale Lightning Arrester was not tested because of its poor performance on the preliminary test.

The voltage test was to illustrate the relative clamping ability of each device. The rise time of the pulse was kept in the middle of the frequency range and energy absorbed low so as to look solely at the effect of a high-voltage transient.

Likewise, the frequency test was used to show each device's ability to handle high (8.3kHz) and low (110 Hz) frequency transients. The energy is kept low to avoid its interference in the testing.

For the energy test, two test points were used (high and low energy.) The amount of energy absorbed was calculated by picking-off points from the device's current and voltage curves. These points were then entered into a modified HP-65 numerical integration program. It should be noted that the limitation of the storage oscilloscope prevented simultaneous recording of both current and voltage. Therefore, the current graph for the MCG failure test is that of a short circuit current after the failure occurred.

The transient generator used for these tests was designed for loads of high input impedance. Since these devices have low input impedance, they will "load" the generator down. To realize a comparison of device performance, the open-circuit voltage is kept fairly constant and the devices are compared on what relative effect they have on that open-circuit voltage. A significant amount of work has been started on a transient generator that would handle these lower impedances.

2.9 SUPPRESSION DEVICE EVALUATION

In performing the various evaluation tests, the components' values and results were as shown in Tables 2.5, 2.6 and 2.7.

2.10 DISCUSSION OF RESULTS

All suppressors tested in the voltage test clamped the transient well below the devices rated value (1200 to 1350 V). The MCG suppressor showed the most high frequency leakage, but was still below 1200 V. The 15 μf-capacitor clamped at the lowest value of 350 V.

TABLE 2.5

VOLTAGE TEST

$C_1 = 1.0\ \mu f,\ R_1 = 3.3\ k\Omega,\ C_2 = .10\ \mu f,\ R_2 = 30\Omega,\quad 1\ KV \leq V_o \geq 5.5\ kV$

Device	V_o (Fig. 2.19)	V_{clamp} (Fig. 2.20)
GE MOV-Varistor	5400 V	1000 V
IR Thyrector	5400 V	1000 V
MCG Transient Suppressor	5400 V	600 V
(W)- Voltrap	5400 V	1050 V
15 μf - surge capacitor	5400 V	350 V

TABLE 2.6

FREQUENCY TEST

case a

$C_1 = 1.0\ \mu f,\ R_1 = 400\ \Omega,\ C_2 = .10\ \mu f,\ R_2 = 30\ k\Omega,\ V_o = 5.6\ kV$

Rise time = $3R_1C_2$ = .12 ms (8.3 kHz)

Device	V_o (Fig. 2.21)	V_{clamp} (Fig. 2.22)
GE MOV-Varistor	5500 V	1300 V
IR Thyrector	5500 V	1600 V
MCG Transient Suppressor	5500 V	1000 V
(W)- Voltrap	5500 V	1300 V
15 μf - surge capacitor	5500 V	300 V

case b

$C_1 = 1.0\ \mu f,\ R_1 = 3.3\ k\Omega,\ C_2 = .1\ \mu f,\ R_2 = 30\ k\Omega,\ V_o = 5.6\ kV$

Rise time = $3R_1C_2$ = 1ms (1KHz). Note: V_o and V_{clamp} for case b are the same as Fig. 2.19 and Fig. 2.20.

Device	V_o	V_{clamp}
GE MOV-Varistor	5500	1000 V
IR Thyrector	5500	1000 V
MCG Transient Suppressor	5500	600 V
(W)- Voltrap	5500	1050 V
15 μf - surge capacitor	5500	350 V

case c

C_1 = 1.0 μf, R_1 = 30 kΩ, C_2 = .10 μf, R_2 = 80Ω, V_o = 5.6 kV

Rise time = $3R_1C_2$ = 9 ms (110 Hz)

Device	V_o (Fig. 2.23)	V_{clamp} (Fig. 2.24)
GE MOV-Varistor	5700 V	800 V
IR Thyrector	5700 V	600 V
MCG Transient Suppressor	5700 V	1300 V
(W)- Voltrap	5700 V	900 V
15 μf - Surge capacitor	5700 V	350 V

TABLE 2.6

ENERGY TEST

case a

C_1 = 16.7 μf, R_1 = 100 Ω, C_2 = 1 μf, R_2 = 1000 Ω, V_o = 2000 V

Device	V_o	J_z (energy absorbed Fig 2.25)
GE MOV-Varistor	2000 V	25.3 J
MCG Transient Suppressor	2000 V	16 J - Failure (Fig. 2.26)
IR Thyrector	2000 V	28.8 J
(W)- Voltrap	2000 V	21.5 J
15 μf - Surge capacitor	2000 V	13.0 J

case b

C_1 = 16.7 μf, R_1 = 100 Ω, C_2 = 1 μf, R_2 = 1000 Ω, V_o = 6000 V

Device	V_o	J_z
GE MOV-Varistor	6000 V	129.6 J
IR Thyrector	6000 V	139.0 J
(W)- Voltrap	6000 V	127.0 J
15 μf Surge capacitor	6000 V	100.6 J

Once again the 15-μf surge capacitor performed the best in the frequency test. The GE MOV-Varistor, IR Thyrector, and Westinghouse Voltrap all showed leakage (1600 V worst case) in the 8.3 kHz frequency test, while the MCG gave a 1300 V initial ringing on the 110 Hz frequency test.

TYPICAL OPEN-CIRCUIT OUTPUT VOLTAGE USED

IN VOLTAGE TEST

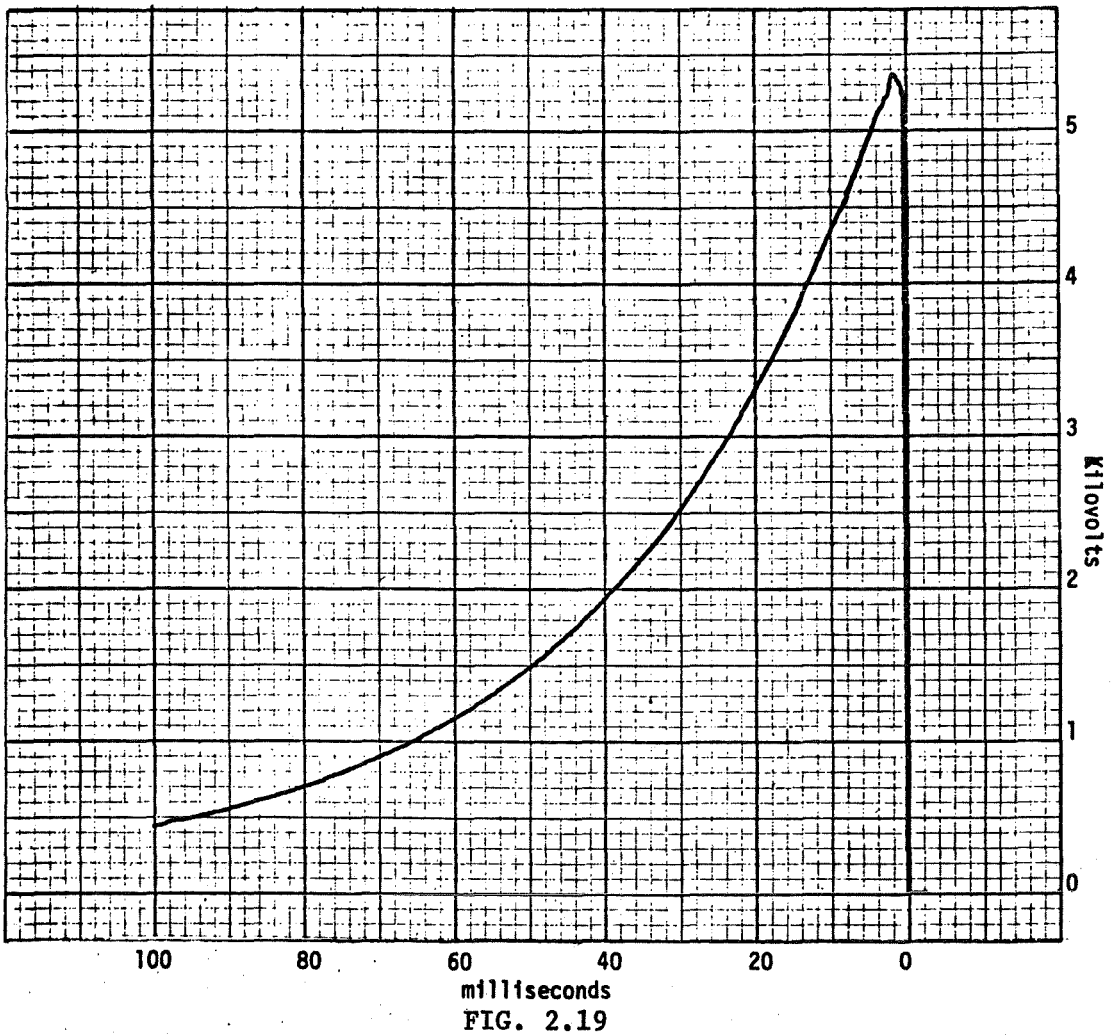

FIG. 2.19

COMPARISON OF DEVICE CLAMPING VOLTAGE (V_{CLAMP}) WHEN SUBJECTED TO VOLTAGE TEST

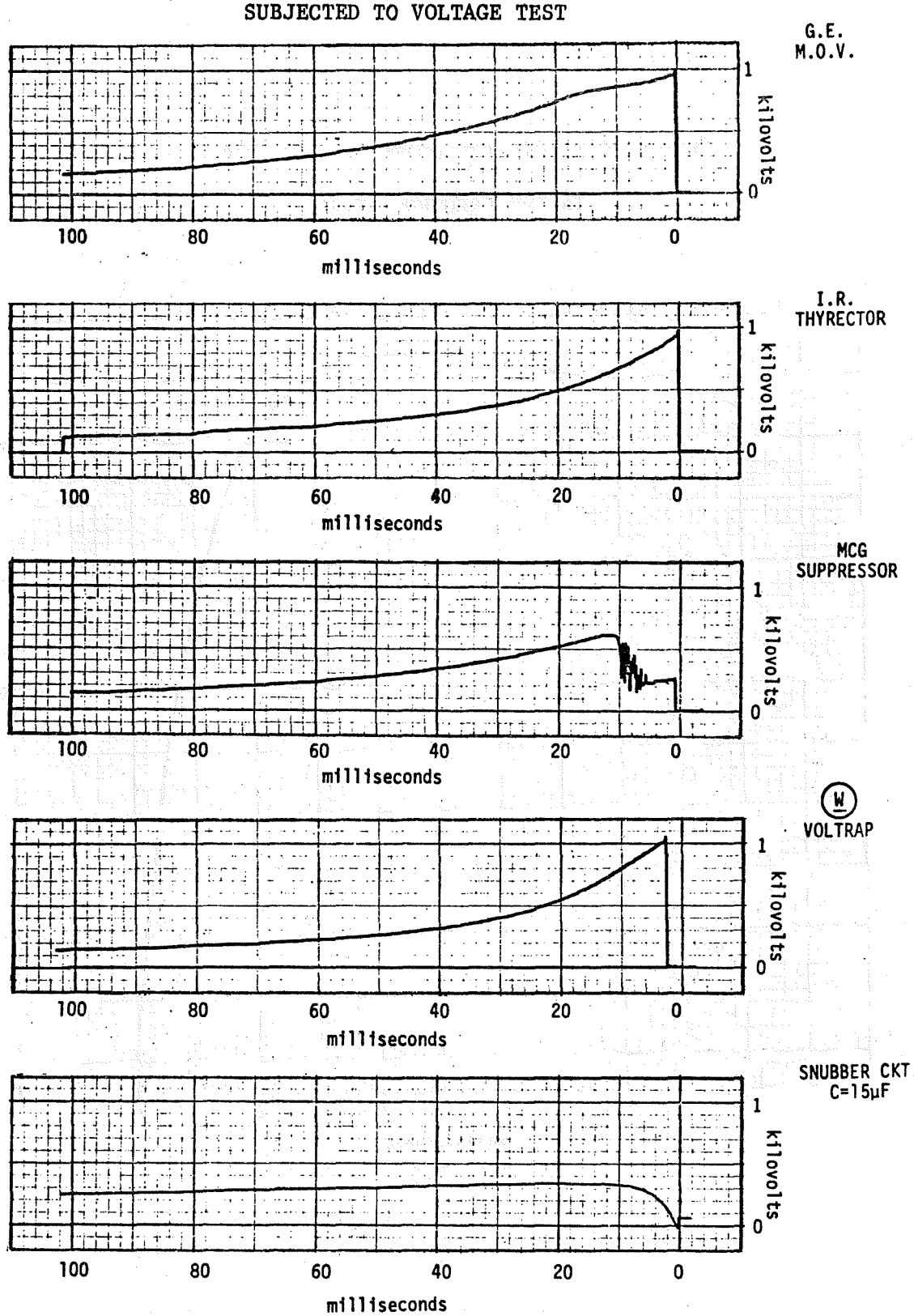

FIG. 2.20

TYPICAL OPEN-CIRCUIT OUTPUT VOLTAGE USED

IN LOW FREQUENCY TEST

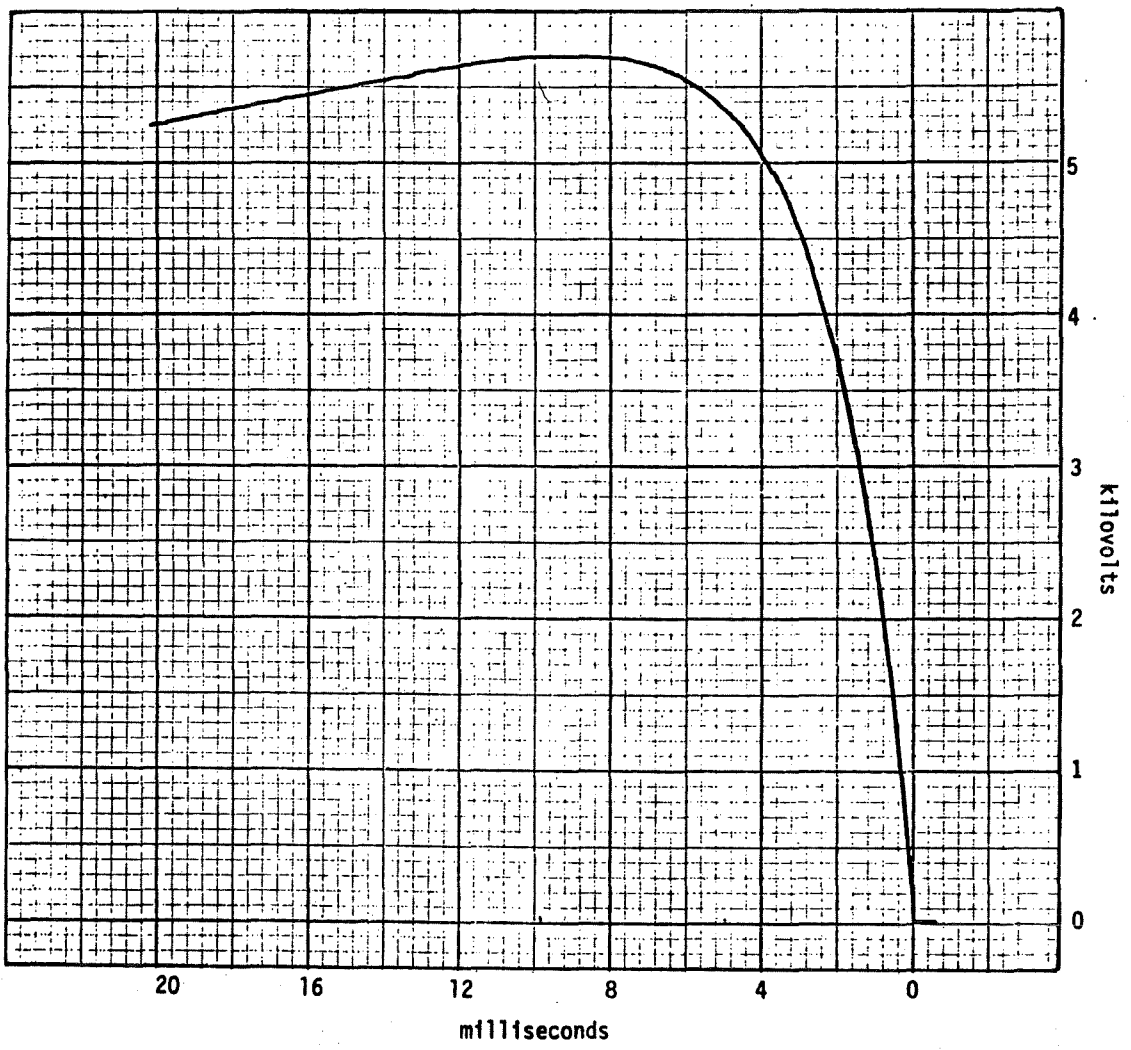

FIG. 2.21

COMPARISON OF DEVICE CLAMPING VOLTAGE (V_{CLAMP}) WHEN SUBJECTED TO LOW FREQUENCY TEST

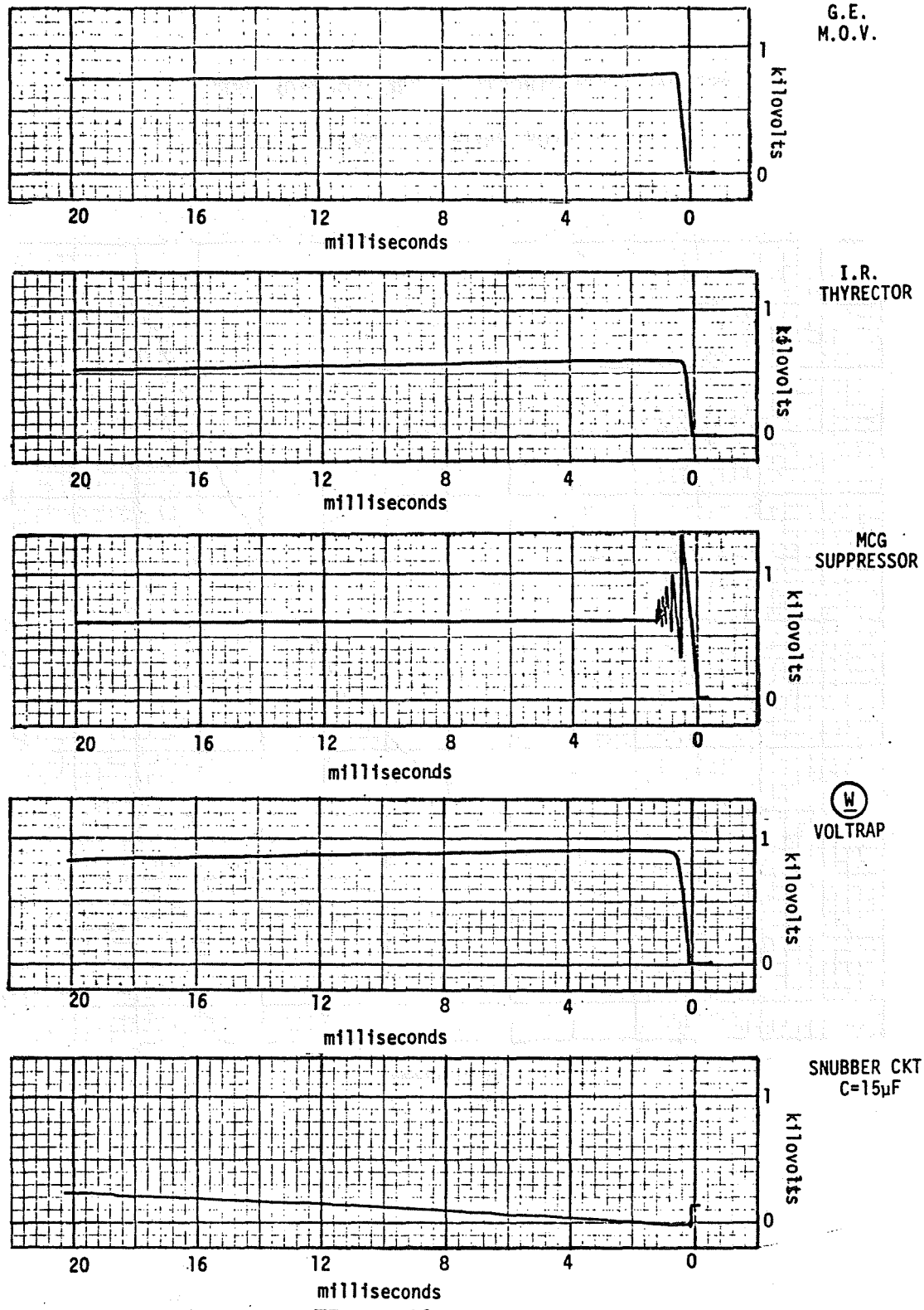

FIG. 2.22

TYPICAL OPEN-CIRCUIT OUTPUT VOLTAGE USED

IN HIGH FREQUENCY TEST

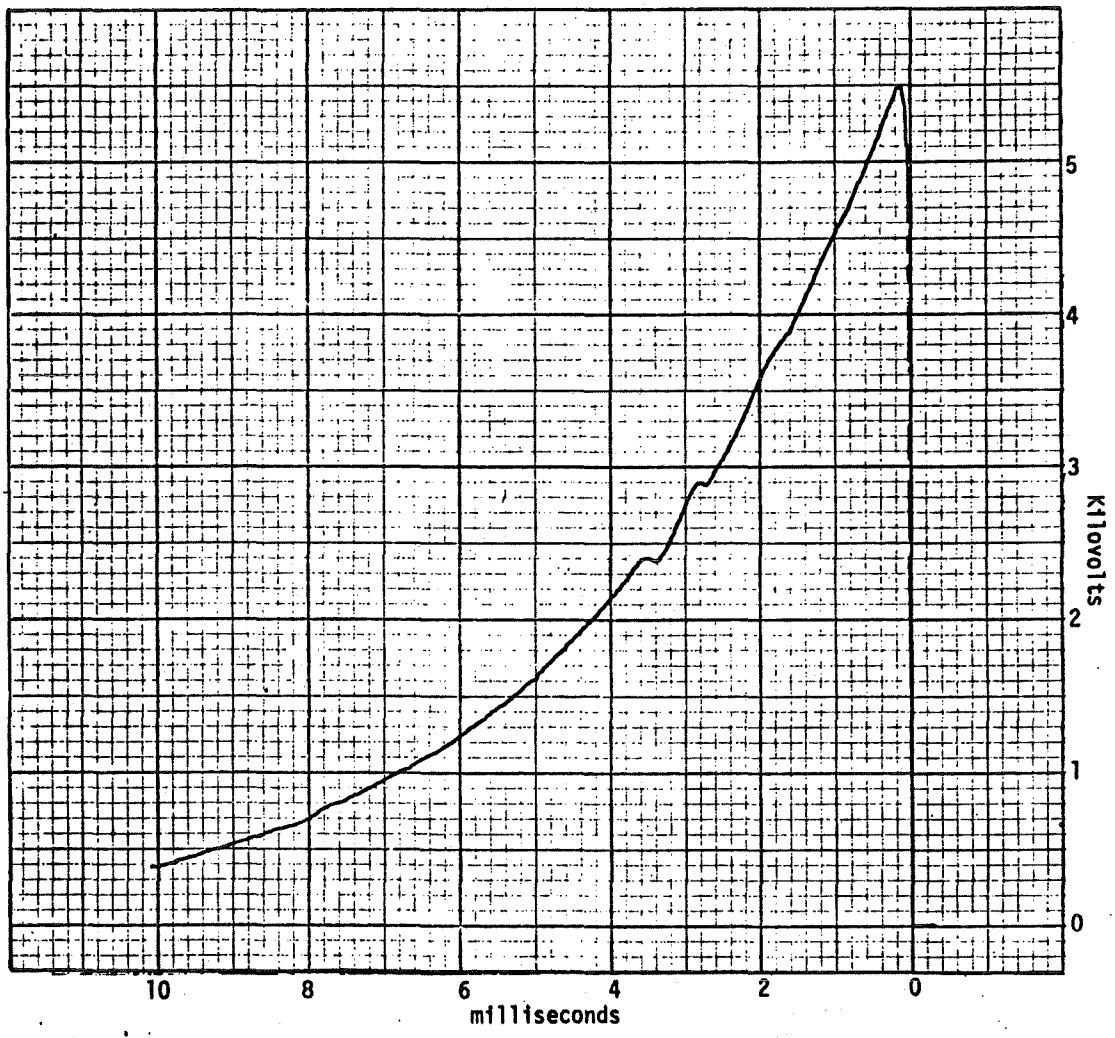

FIG. 2.23

COMPARISON OF DEVICE CLAMPING VOLTAGE (V_{CLAMP}) WHEN SUBJECTED TO HIGH FREQUENCY TEST

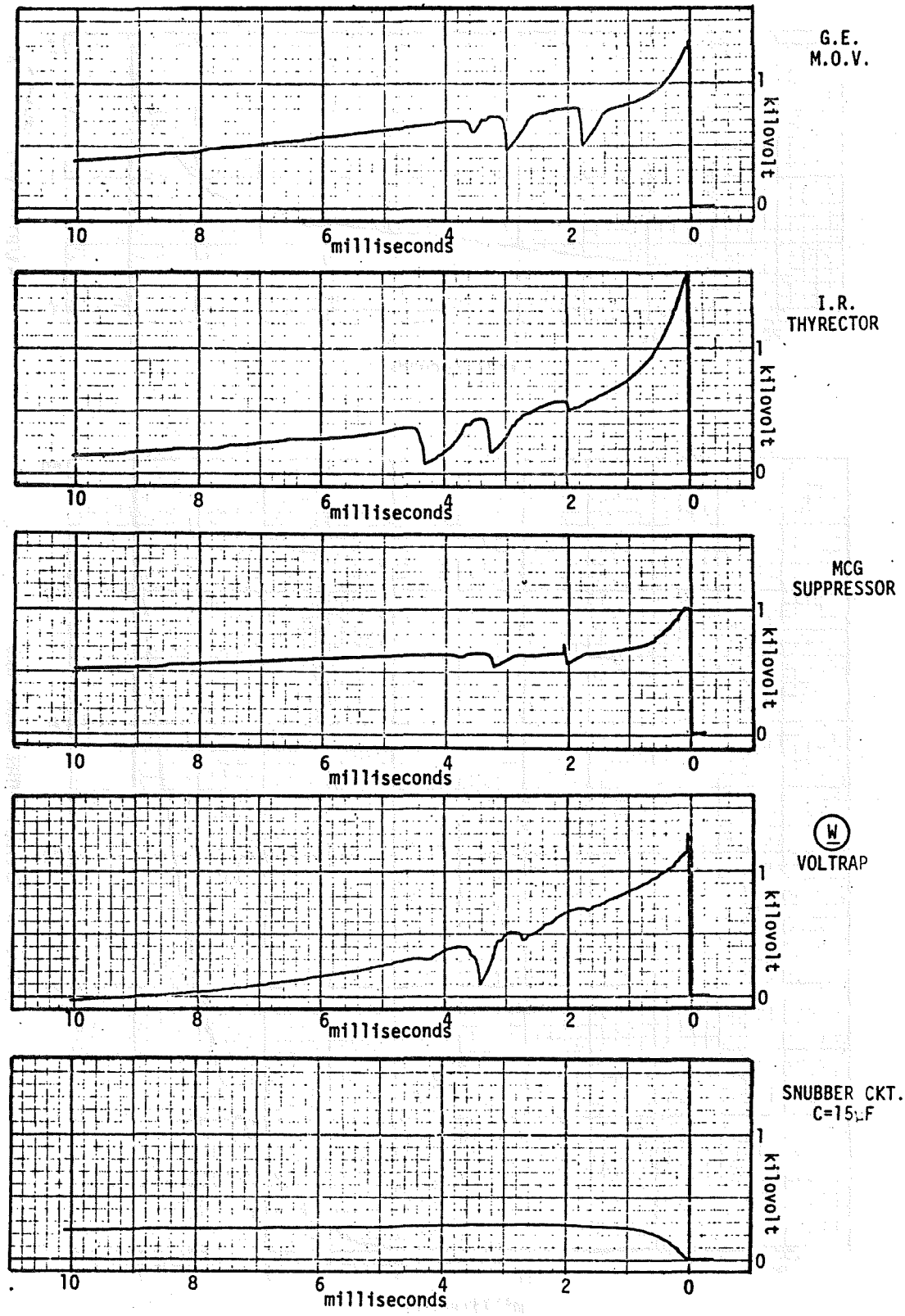

FIG. 2.24

TYPICAL ENERGY DISSIPATED BY DEVICE-CALCULATION

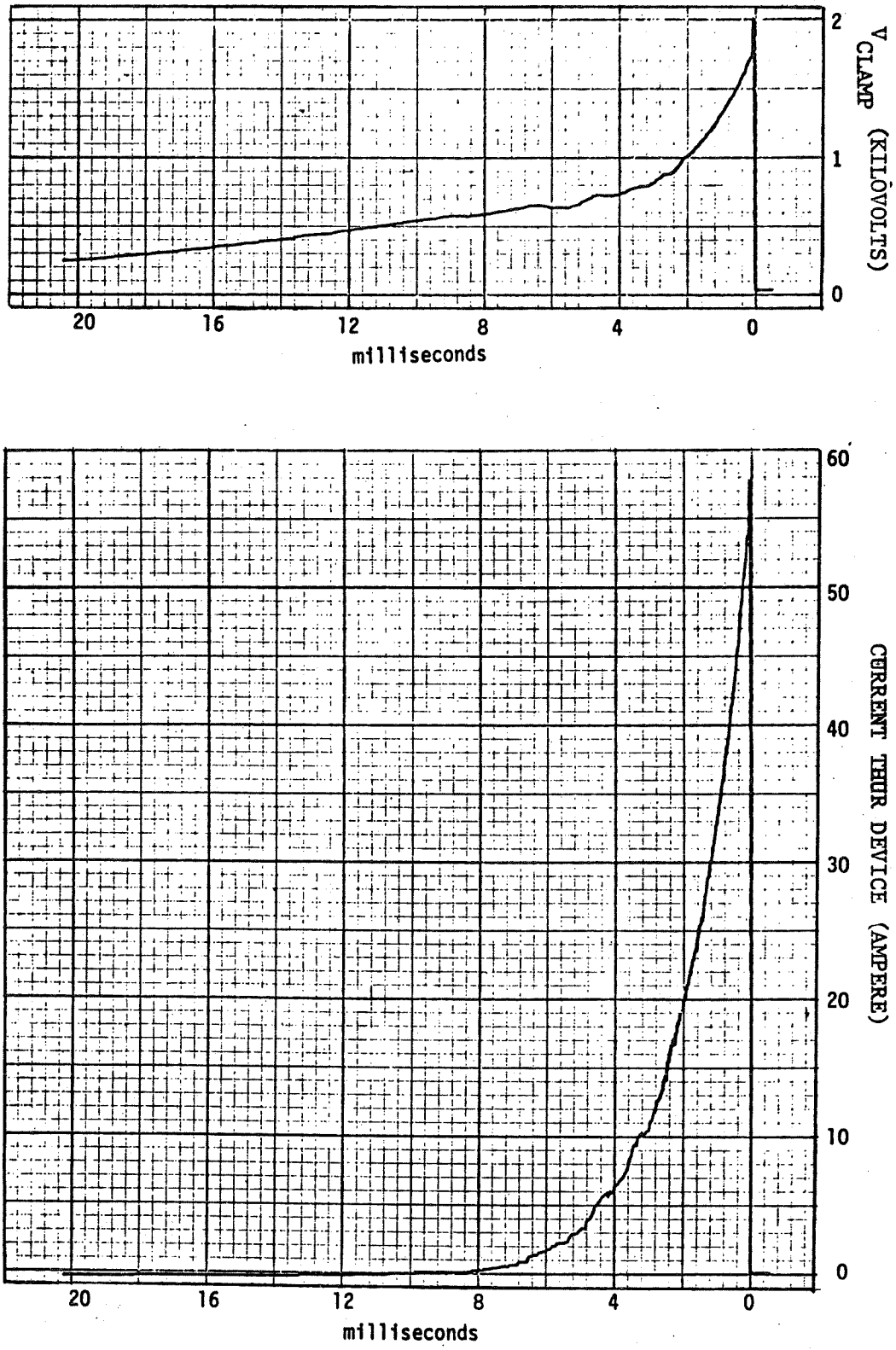

FIG. 2.25

ENERGY TEST - MCG FAILURE

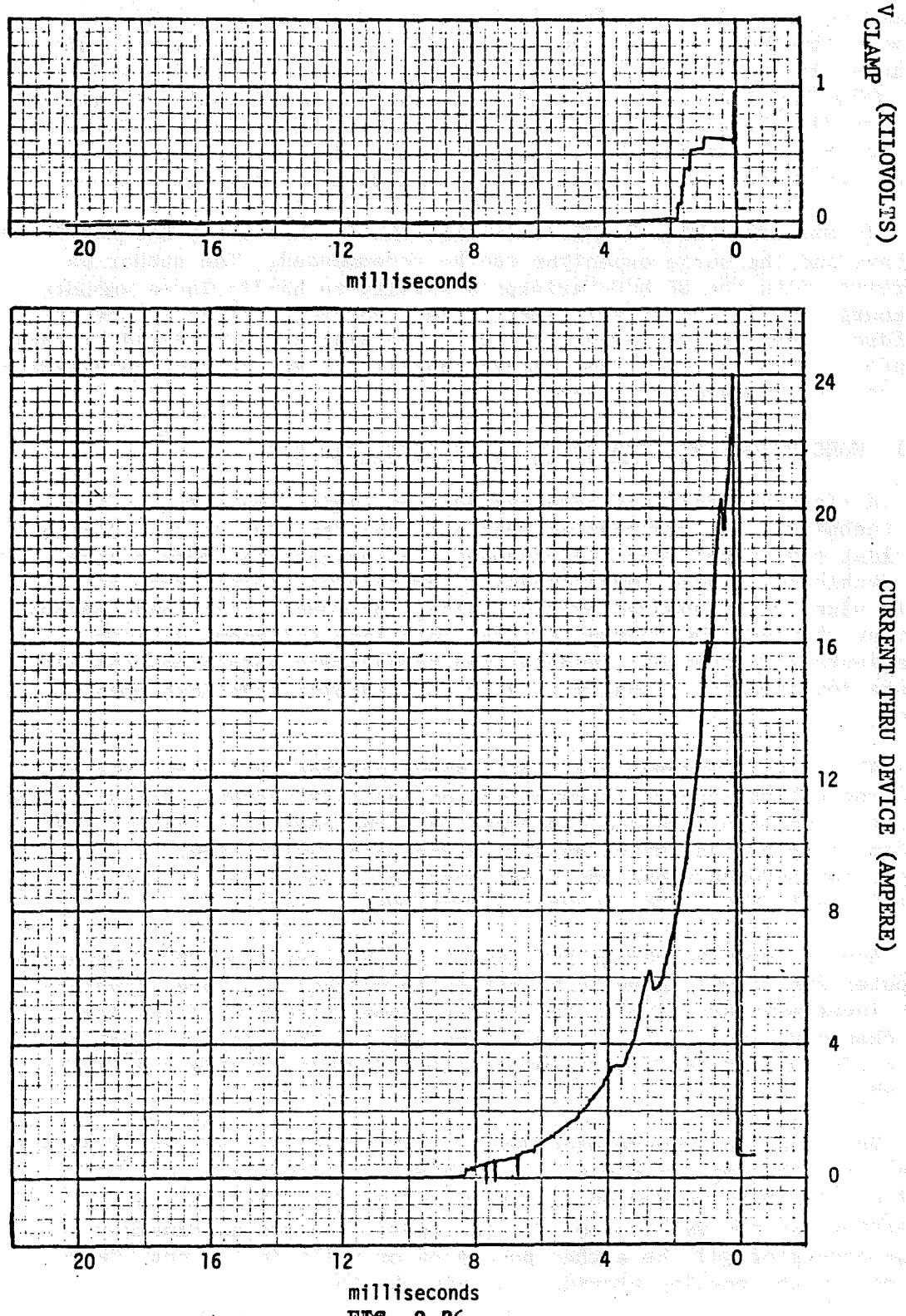

FIG. 2.26

Although only one device was tested to failure, the transient generator was able to deliver at least rated energy to all devices. Because the MCG transient suppressor did fail (internal zener diode failure) at 16 J (rated at 8J) it can not be recommended for 480 V use. (See Fig. 2.26). All other devices showed considerable leakage (as high as 3100 V) at the high energy test point (Fig. 2.27). This may not be as alarming as it appears because in most cases, the amount of energy absorbed greatly exceeded the device's energy rating.

In summary, the G.E. MOV-Varistor, the IR Thyrector, the Westinghouse Voltrap and the surge capacitor can be recommended. The author was impressed with the GE MOV-Varistor's ability to handle large amounts of energy for its relatively small size. However, the other devices performed just as well electrically. Depending on such considerations as price, physical size, and energy capability, any of four suppression devices could prove satisfactory.

2.11 CONCLUSIONS RELATED TO THE TRANSIENTS PROGRAM

A sizable effort has been expanded on digital modeling of transients and techniques for suppressing them over the last two years. During the last year significant improvements in the computer models have been achieved. These improvements allow machine, transformer and cable sizes to be changed easily. Also, the models have been improved so that they are now appropriate for both long and short duration transients. Furthermore, machine and transformer models now contain saturation effects. Finally, a series dc machine model has been added.

All of the improvements listed above provide the capability of studying a large variety of problems on the TESS system. One unfortunate aspect of the study is the discovery that the cost of using the TESS system for practical sized systems seems to be quite high. A comparison between these costs and costs on other computer systems (specifically WVU's IBM computer system) will be made.

Any decision to change the thrust of the work from CDC to another computer system will have to be carefully weighed. A large development investment has already been made. Some of this would be lost in the changeover and would subtract from any possible gain. Finally, the study is near its finish, with only a few mine system studies to be made.

The transient suppression device evaluation has gone quite smoothly except for the impedance matching problem. A couple of commercial devices have been weeded out in spite of the fact that the surge generator was not well suited for the tests. A more appropriate surge generator will be either purchased or built in the near future to confirm the results provided in this chapter.

COMPARISON OF DEVICE CLAMPING VOLTAGE (V_{CLAMP}) WHEN SUBJECTED TO ENERGY TEST

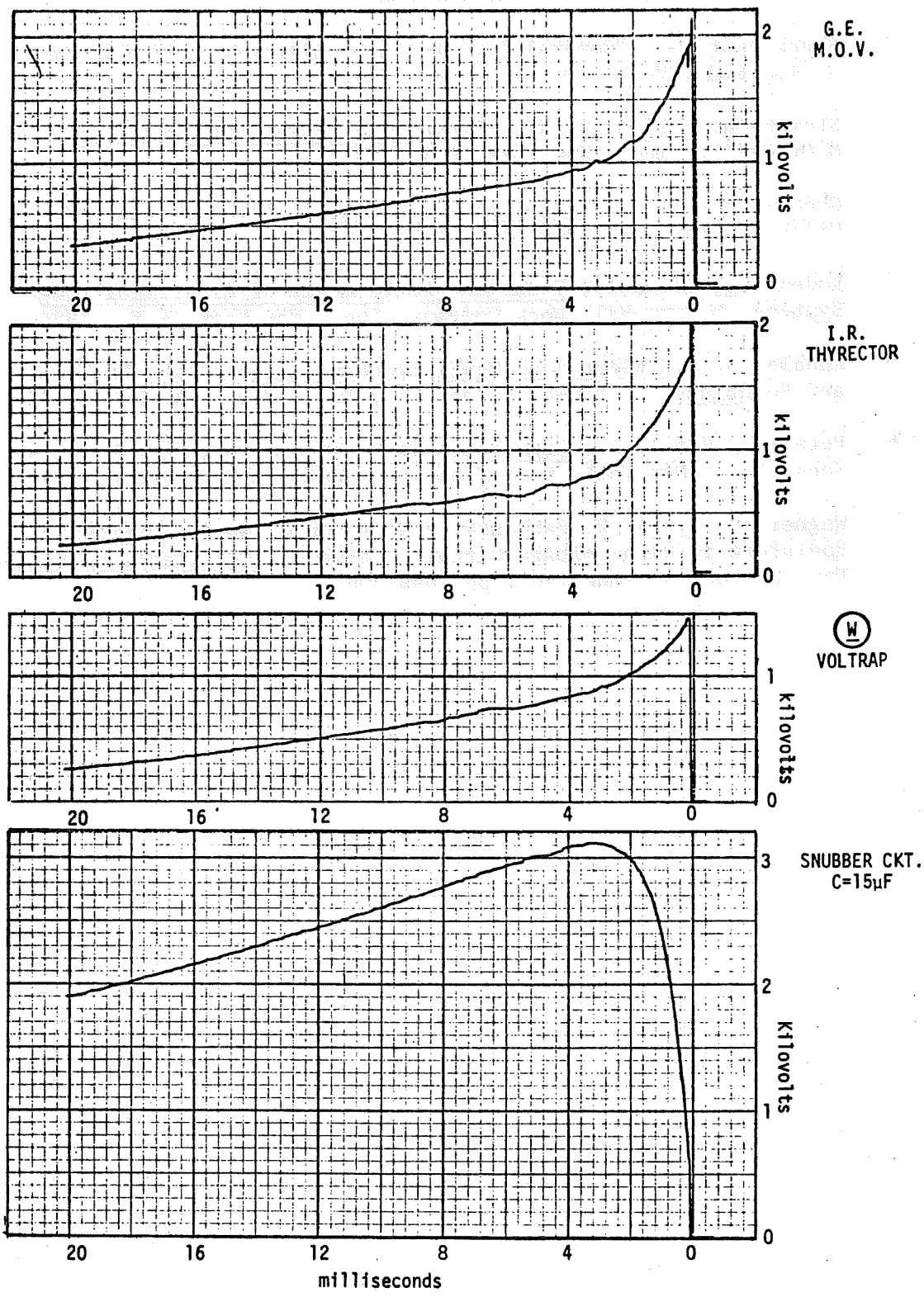

FIG. 2.27

REFERENCES

1. Shackshaft, G., "General Purpose Turbo-Alternator Model," Proc. of I.E.E.E., Vol. 110, No. 4, p. 703.

2. Stevenson, William D. Jr., Elements of Power System Analysis, McGraw-Hill, Inc., New York, N.Y. 1962.

3. Greenwood, Allen, Electrical Transients in Power Systems, John Wiley & Sons, Inc., New York, N.Y., 1971.

4. Rudenburg, Reinhold, Transient Performance of Electrical Power Systems, McGraw-Hill Book Company, Inc., New York, N.Y., 1950.

5. Knable, A. H., Electrical Power Systems Engineering: Problems and Solutions, McGraw-Hill Book Co., Inc., New York, N.Y., 1967.

6. Peterson, Harold A., Transients in Power Systems, John Wiley & Sons, Inc., New York, N.Y., Campman & Hall, Ltd., London, 1951.

7. Wagner, C. L., J. W. Bankoske, Evaluation of Surge Suppression Resistors in High-Voltage Circuit Breakers, IEEE Trans. on P.A. & S., Vol. 86, No. 6, June 1967, pp. 698-706.

BIBIOGRAPHY

1. Fich, Sylvan, Transient Analysis in Electrical Engineering, Prentice-Hall, Inc., New York, New York, 1951.

2. Gourishankar and Kelly, Donald H, Electromechanical Energy Conversion, John Wiley and Sons, Inc. New York, New York, 1959.

3. IEEE Committee Report, "Computer Representation of Excitation System", IEEE Transactions on Power Apparatus and Systems, June 1968.

4. Knable, A. H. "Lightning Protection of Equipment with Remotely Mounted Lightning Arresters," IEEE Transactions on Power Apparatus and Systems, June 1968.

5. Lee, C. H., "Saturation Harmonics of Polyphase Induction Machines," IEEE Transactions on Power Apparatus and Systems, October 1961.

6. Majmudar, Herit, Electromechanical Energy Converters, Allyne and Bacon, Inc. Boston, Boston, 1965.

7. Rorden, H. L., Dils, J. M., Griscom, S. B., Skooglund, J. W., Edward, Beck, "Investigation of Switching Surges Caused by 345 Kv Disconnecting Switch Operation," IEEE Transactions on Power Apparatus and Systems, October 1958.

8. Venikov, V. A., Adkins, Bernard, Rutenburg, Daniel Trans., Transient Phenomena in Electrical Power Systems, The Macmillan Company, New York, New York, 1964.

9. White, David C., Woodson, Herbert, H., Electromechanical Energy Conversion, John Wiley and Sons, Inc. New York, New York, 1959.

10. Fitzgerald, A. E., Kinsley, Jr., and Kusko, Alexander, Electrical Machinery, McGraw-Hill, Inc. New York, New York, 1971.

11. Powell, Gary L. The Safety Grounded System, West Virginia University, Morgantown, West Virginia 1972.

12. The Electrification Council, New York, Industrial and Commercial Power Distribution New York, New York, 1969.

CHAPTER III

RELIABILITY ASSESSMENT OF PROTECTIVE DEVICES

3.1 INTRODUCTION

This chapter is concerned with the reliability assessment of protective devices used in coal mine power systems. During the 1975-76 project year, the analysis was performed on 1) molded-case circuit breakers, 2) electromechanical undervoltage releases (UVR) and 3) solid-state undervoltage relays (UVR). The research work related to these devices was proposed to proceed in three different directions, namely, field tests, laboratory tests, and theoretical analysis. The results of these tests will be beneficial to verify and correlate the theoretical results. Section 3.2 is devoted to the reliability assessment of circuit breakers and the following section deals with the design and the development of threshold counting devices required for field testing of the circuit breakers. Section 3.4 entails the work on UVR's, which represents the continuation of the 1974-75 effort.

3.2 RELIABILITY ANALYSIS OF AC MOLDED CASE CIRCUIT BREAKERS

3.2.1 Selection of Mine and Circuit Breaker

The work in this area did not proceed at as fast a rate as anticipated since considerable time was spent in selecting a suitable mine for performing the necessary field tests on the circuit breakers. On December 5, 1975, the Consolidation Coal Company suggested that their Blacksville No. 2 mine located in Blacksville, West Virginia could be used to perform the field tests on the breakers. Two visits were made to this mine to select the type of molded-case circuit breaker to be used for the reliability investigation. Based on these visits, the following type of breaker was selected: Westinghouse LA-Frame, 3-phase, 3-pole, 600-Vac and 400-A ac continuous current rating. This type of breaker, which is being used in the mine for supplying power to loaders and bolters, is expected to draw a full load current of only 130 amperes. Therefore, this type of breaker also requires a special thermal tripping level of 225 amperes and the magnetic tripping range is 350-850 amperes. An order was placed for the purchase of twenty of this type of breaker during the first week of March 1976. It is hoped to receive the breakers by the end of July 1976.

3.2.2 Field Testing of Molded Case Circuit Breakers

Once the breakers are received, ten of them will be exchanged with a similar number already in service in the mine. Before the ten new ones are placed at several different locations in the mine for field testing, each of these breakers will be equipped with a threshold counting device to record the following:

1. Number of no-load operations.
2. Number of operations between no-load and thermal tripping level
3. Number of operations between thermal tripping level and the lower magnetic tripping range.
4. Number of operations in the magnetic tripping range.
5. Number of operations beyond the magnetic tripping range.
6. The number of times the device failed to operate when it was supposed to do so.

It is planned to collect the data mentioned above as indicated by six counters in the device over a given period of time (at least one year, but preferably two to three years). These data will be useful in the reliability evaluation of the breakers. This device has already been designed and the details of it are given in Section 3.3.

3.2.3 Laboratory Tests

The remaining ten new breakers and the ten used breakers obtained from the mine will be subjected to several laboratory tests to obtain the necessary data for reliability evaluation. It was desirable to come up with a comprehensive scheme for the laboratory tests. As a result, it was decided to visit the companies that manufacture molded case circuit breakers, the purposes being

1. To study the procedures used in testing the breakers, and
2. To obtain data on the reliability aspects of the circuit breakers.

Since the circuit breakers ordered were manufactured by Westinghouse two trips were made to the Westinghouse Low-voltage Circuit Breaker Division in Beaver, Pennsylvania. It is in this plant that molded-case circuit breakers of the type ordered are manufactured.

During these two trips, the test facilities inspected were those used for quality control. There were no testing procedures that would provide failure rate data of the circuit breakers. Also, based on these trips two comprehensive schemes for laboratory tests have been worked out. Both the schemes entail the following:

1. A regulated power supply capable of providing various voltage levels.
2. A voltage regulator supplying the UVR coils in the breakers.
3. A fault detector.
4. A mechanism to switch on and reset the breakers, and
5. Counters and accompanying electronic circuits.

It has been decided to perform the tests in the WVU electrical engineering laboratory, where certain environmental aspects of the mine will be simulated. It is planned to make the tests run automatically with provision for manual interruption. The block diagrams of the

testing schemes are given in Figs. 3.1 and 3.2. The difference between the two schemes is that the scheme of Fig. 3.1 has motorized devices for closing and resetting the breakers, while the scheme in Fig. 3.2 has pneumatic devices to perform the same functions. Other parts of the schemes are basically identical. At the time of writing this report, the two devices, motor operated device and the pneumatic device are under very close scrutiny. The decision as to which device should be used will be made in the near future. The necessary controls for the device chosen, will be designed. Subsystems common to both schemes are described below.

A. Voltage Regulator

Fig. 3.3 is the diagram of the voltage regulator. The timer operates on a 120-Vac supply and the fact that it is a recycle type facilitates performing the tests automatically.

It controls the relay S through the contacts T. The relay S also requires a 120-Vac input supply. When the supply is impressed on the timer its "off" period begins and the contact T is open. By this time the normally closed contact, S_1, of relay S stays closed. Consequently 120-Vac is impressed on the UVR coils. At the end of the "off" period which will be about 3 minutes, the contact T will switch to the "on" position and S opens its contacts, S_1, the "on" period will be for 2 minutes. During the "off" period the breakers remain closed, when the contacts S_1 are opened the voltage impressed on the UVR coils is reduced by the resistor R_1 to 60% of its maximum value, which is the drop-out level for the UVR's. Thus, during the "on" period the breakers trip and remain open to the end of this period. The entire cycle of five minutes duration repeats until a fault occurs. When a fault occurs in any of the circuit breakers on test, the normally closed contact P_1, of the relay P of the fault detector circuit (shown in Fig. 3.4) opens. Consequently, the timer is disabled and the entire test stops until it is started again manually.

B. Fault Detector

The fault detector shown in Fig. 3.4 is made up of three subsystems B, C, and D. B detects faults from the circuit breaker and actuates the relay P. C senses the voltage level from the regulator at which the fault in the breaker occurs. The signals from both B and C are fed into D to actuate one of the two light sources, LED_1 and LED_2. LED_1 lights up if the fault occurs when the breakers are closed, while LED_2 lights up if the fault occurs when the breakers are open.

C. Counter Circuit

Fig. 3.5 is the schematic of the counter circuit. The actuating signal comes from the subsystem B of the fault detector circuit and it enters this circuit at A_1. An electromechancial counter is attached to each circuit breaker on test as shown in Figs. 3.1 and 3.2. The

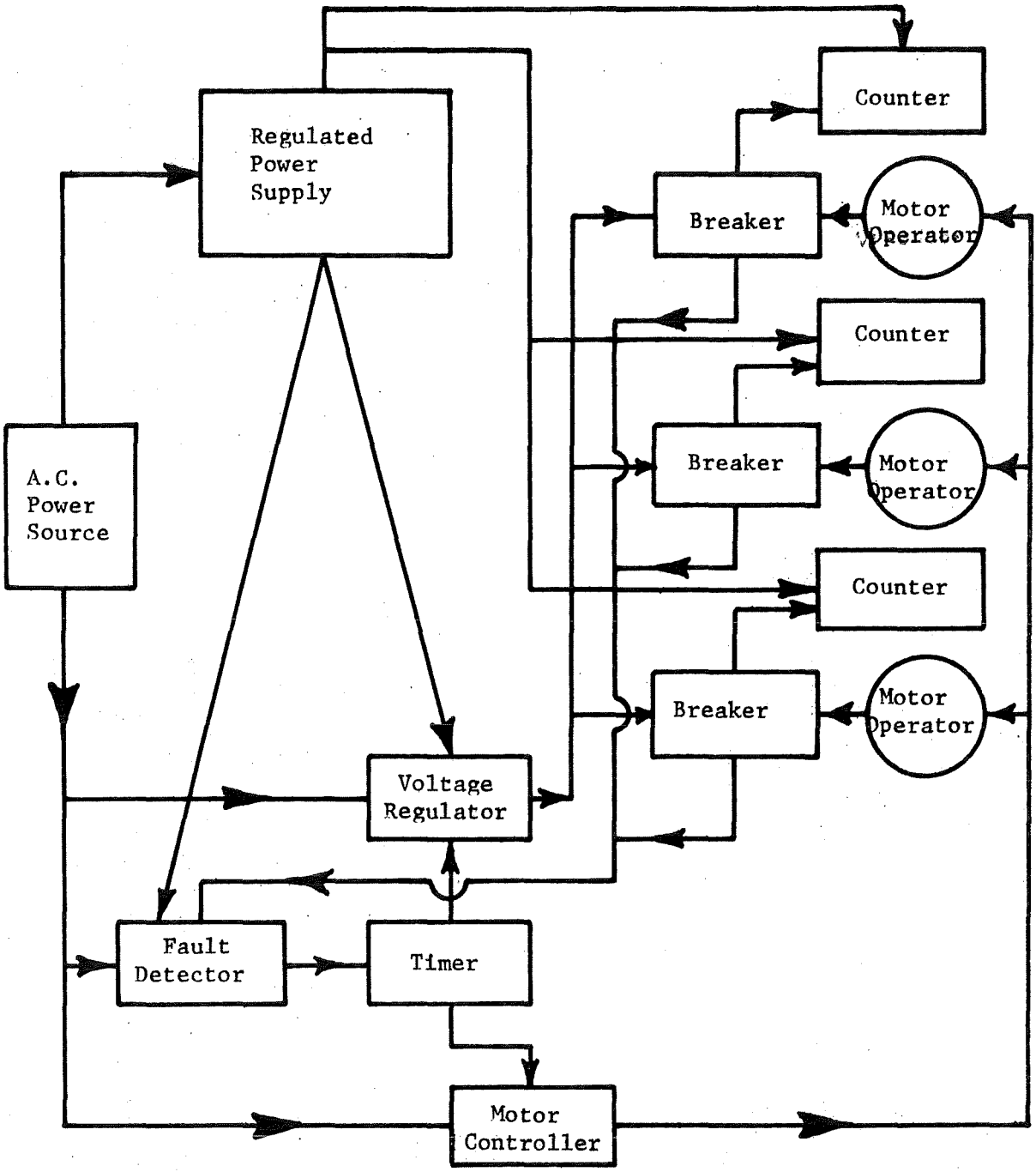

Fig. 3.1 Block Diagram of the Test Set-up for Molded Case Circuit Breakers Using Motor Operators

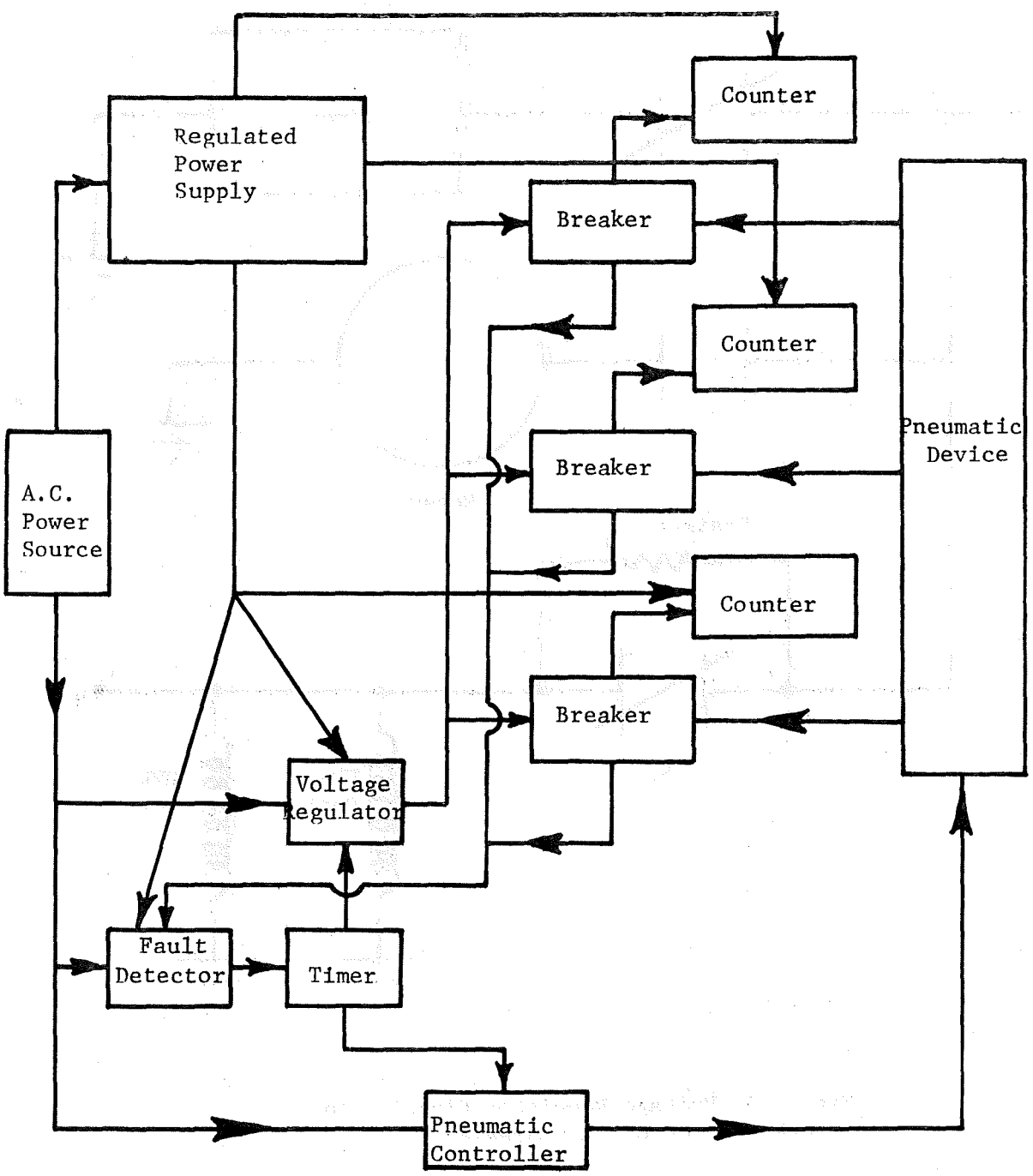

Fig. 3.2 Block Diagram of the Test Set-up for Molded Case Circuit Breaker Using Pneumatic Device.

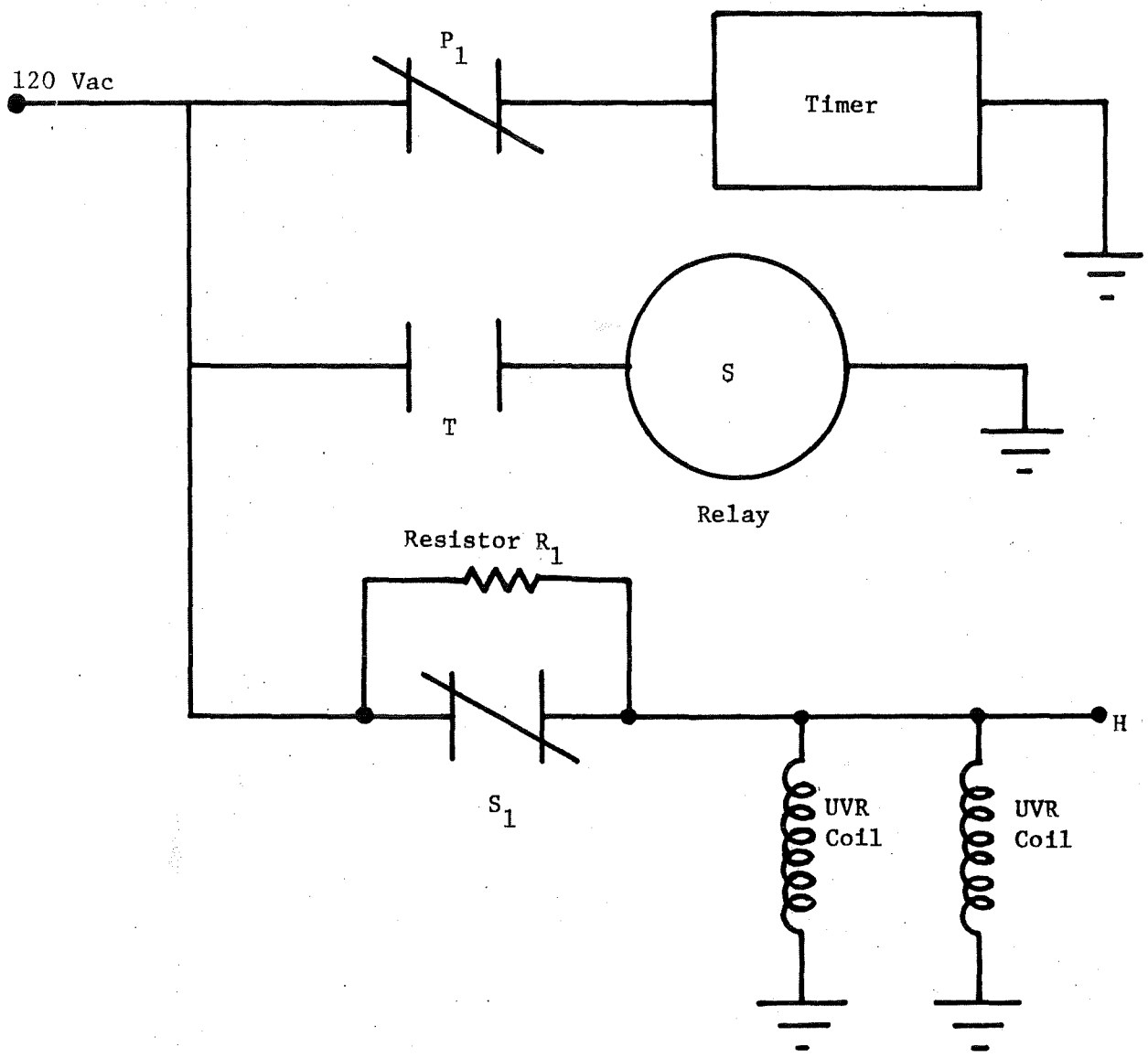

Fig. 3.3 Voltage Regulator Circuit for UVR Coil of Circuit Breaker.

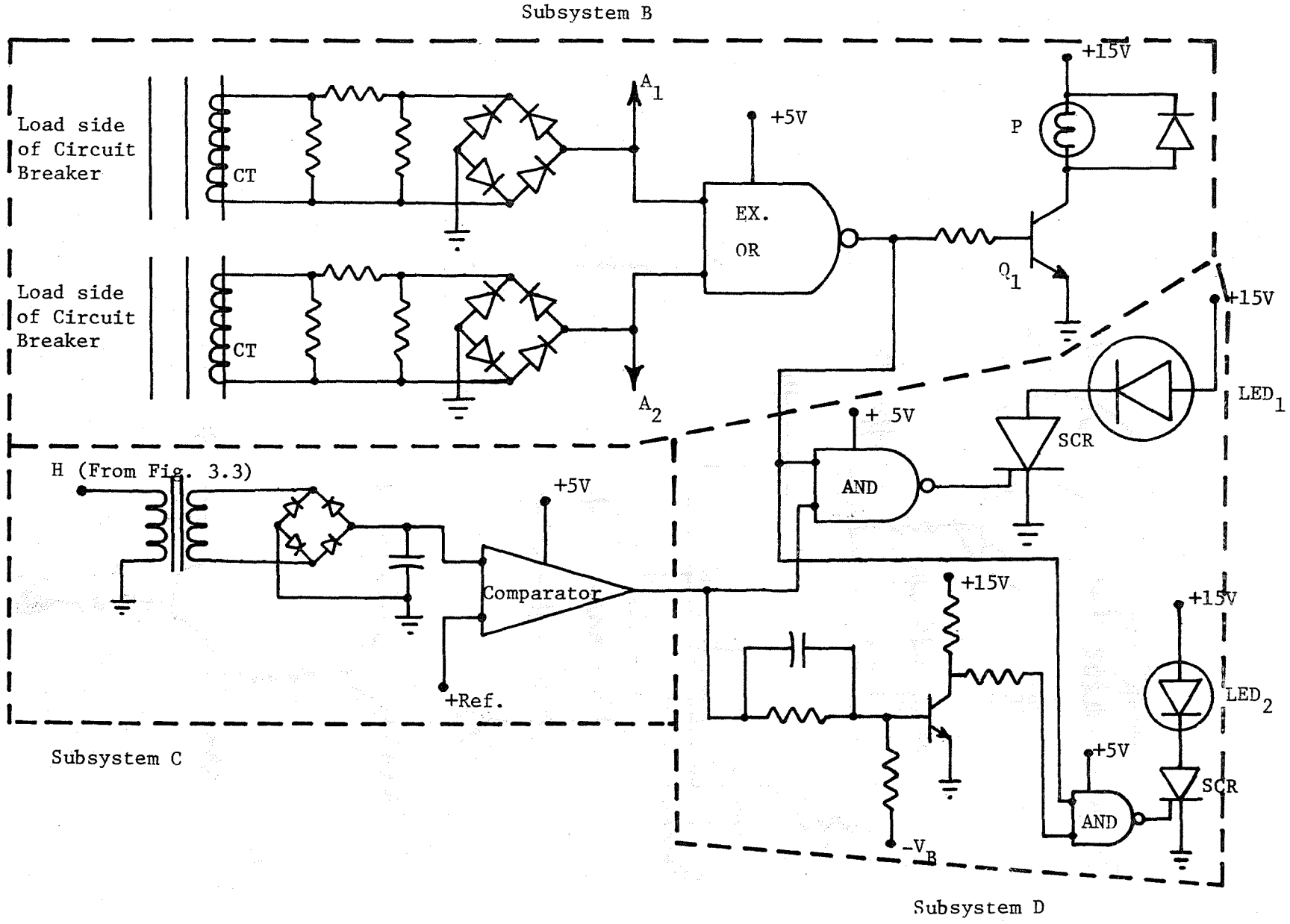

Fig. 3.4 Circuit for Fault Detector

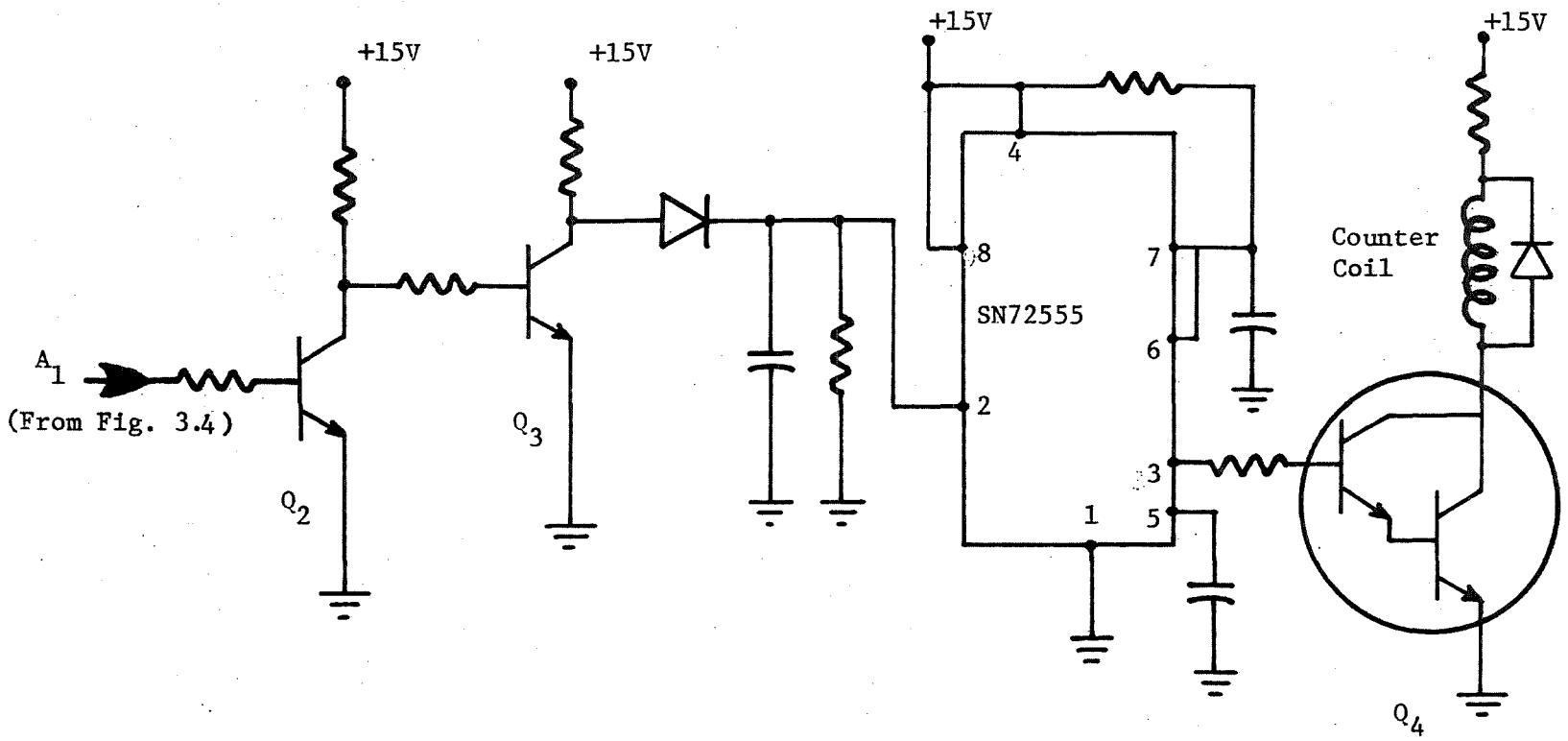

Fig. 3.5 Counter Circuit

most important components in this circuit are the transistors Q_2 and Q_3 the Darlington pair Q_4, and the integrated circuit precision timer, SN72555.

The counter is required to register the number of times the circuit breaker opens. It will then be possible to know the number of times the circuit breaker operates before failure occurs.

D. Regulated Power Supply

Fig. 3.6 is the schematic diagram of the regulated power supply subsystem. There are two regulator chips. One gives out 15-Vdc and the other 5-Vdc. These two levels of voltage are used at different points in other circuits.

3.2.4 Theoretical Reliability Analysis

The theoretical reliability analysis of the breaker will be conducted using the minimal cut-set method. The necessary tools for this are: the reliability block diagram, reliability graph of the breaker, and mathematical model, which are discussed below.

A. Reliability Block Diagram

The reliability block diagram of a typical molded case circuit breaker is as shown in Fig. 3.7. The components numbered in this figure are:

1, 2, 3	Input terminals of phases a, b, and c, respectively.
4	UVR
5, 7, 9	Bimetallic strips (thermal trips) of phases a, b, and c, respectively.
6, 8, 10	Magnetic elements (Magnetic trips) of phases a, b, and c, respectively
11	Trip bar
12	Latch
13, 14	Springs
15	Contact Lever
16, 17, 18	Moving contacts of phases a, b, and c, respectively.
19, 20, 21	Arc chutes of phases a, b, and c, respectively.
22, 23, 24	Output terminals of phases a, b, and c, respectively.

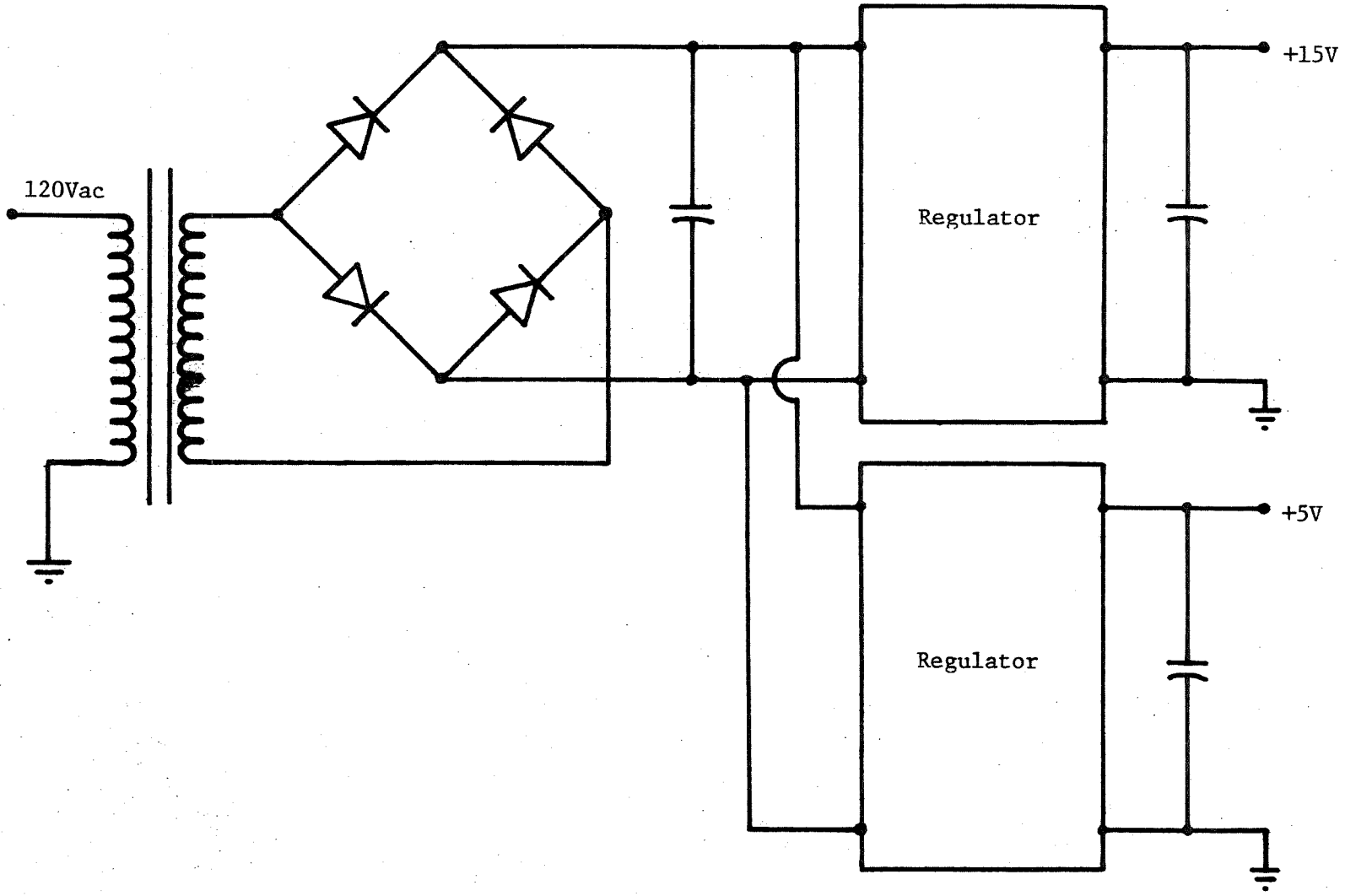

Fig. 3.6 Regulated Power Supply

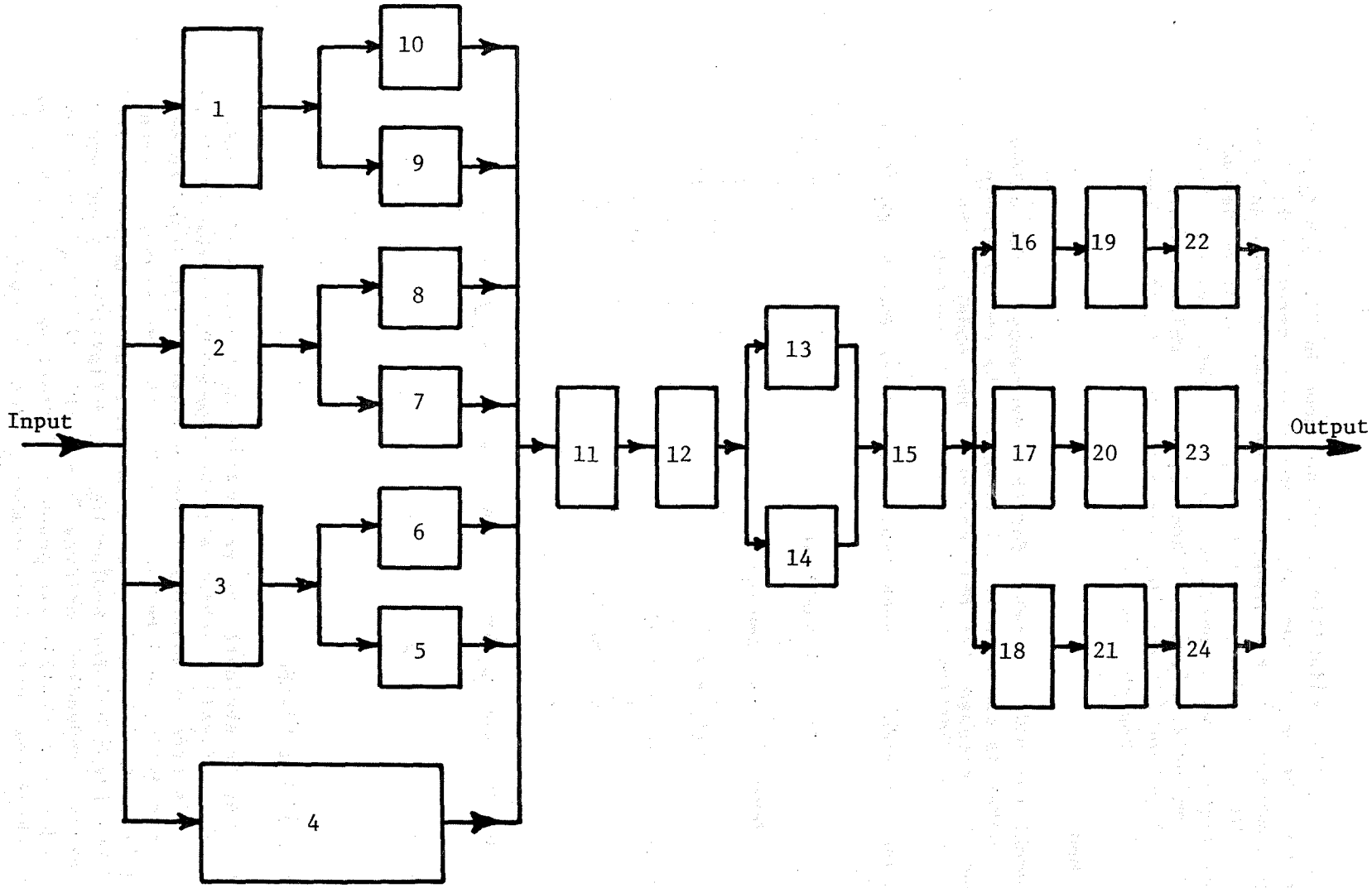

Fig. 3.7 Reliability Block Diagram of Circuit Breaker

From Fig. 3.7, the reliability graph as shown in Fig. 3.8 is drawn. This graph gives a better picture of the operational sequence in the breaker. The components of the breaker are replaced by lines and are numbered as in Fig. 3.7. The components 16, 19, 22 are in series and can be grouped together as a subsystem 16a. The same procedure could be applied to the components 17, 20, 23 and 18, 21, 24 which could be designated as subsystems 17b and 18c, respectively. Similarly components 11 and 12 are together called 11d.

Mathematical Model

The mathematical model suitable for the components of the molded case circuit breaker is the exponential (constant hazard rate) distribution model. The reason for this choice of the model is that their hazard rates Z(t) are constant over their useful life period.[1]

The exponential model for each component is described by the following equations[1]:

$$Z(t) = \lambda(\text{constant}) \tag{3.1}$$

The reliability index of the component

$$\gamma(t) = e^{-\lambda t} \tag{3.2}$$

The failure index $q(t) = 1-\gamma(t)$

$$= 1-e^{-\lambda t} \tag{3.3}$$

where $0 \leq t < \infty$

The Mean-Time-To-Failure, MTTF of the component is given by

$$MTTF = \int_0^\infty \gamma(t)\, dt = \int_0^\infty (1-q(t))\, dt \tag{3.4}$$

C. The Minimal Cut-set Method[2]

The easiest way to evaluate the reliability of a system is to conduct the worst-case analysis in which all the components of the device are put in series. This type of analysis is not realistic. In order to make the reliability evaluation more realistic where the importance of each component or subsystem is brought out, the minimal cut-set method is used. It is an efficient technique for evaluating the reliability of any system that does not contain dependent failures from a reliability graph of the system[1]. A cut-set of a reliability graph is defined as a set of branches (components or subsystems) which when removed, makes the system fail. The system failure is, thus, given by the probability that at least one

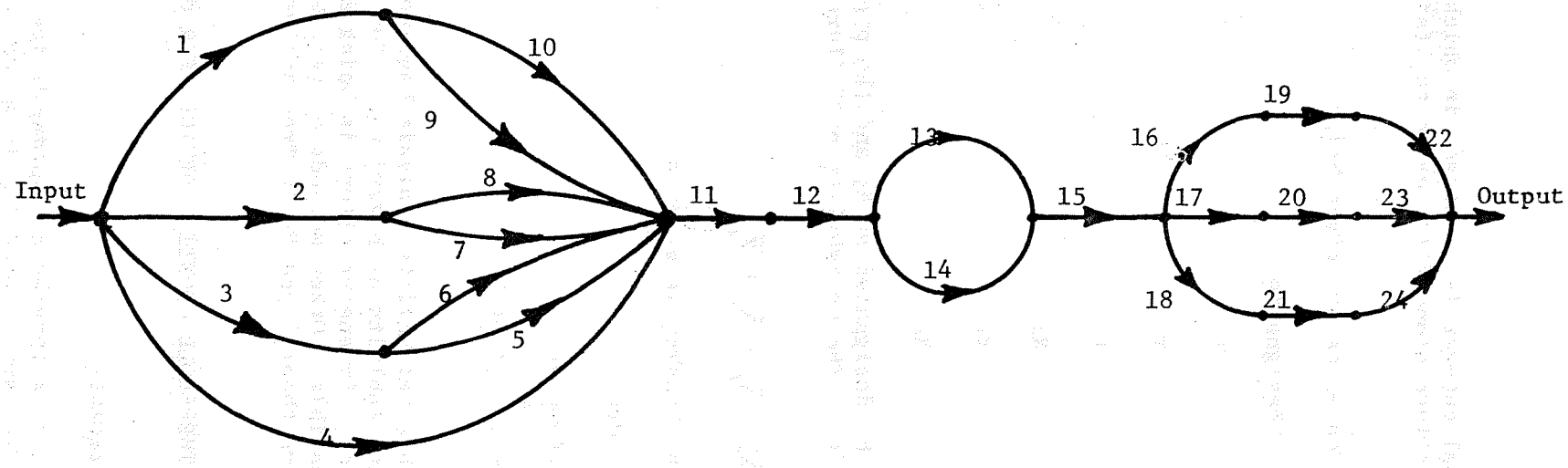

Fig. 3.8. Reliability Graph of Circuit Breaker

minimal cut-set fails. A minimal cut-set is a cut-set in which there is no subset of components whose failure alone will cause the failure of the system[2].

From Fig. 3.8, the minimal cut-sets are given below:

Cut-set	Designation
1, 2, 3, 4	X_1
4, 5, 6, 7, 8, 9, 10	X_2
11d	X_3
13, 14	X_4
15	X_5
16a, 17b, 18c	X_6

Let the failure of a cut-set X_i be designated as $\overline{X}_i$ and the probability of failure of the cut-set be $q_i(t)$. The probability of failure Q(t) of the entire breaker is given as

$$Q(t) = P(\overline{X}_1 \cup \overline{X}_2 \cup \overline{X}_3 \cup \overline{X}_4 \cup \overline{X}_5 \cup \overline{X}_6) \tag{3.5}$$

The reliability index R(t) of the breaker is given as

$$R(t) = 1-Q(t) \tag{3.6}$$

and the MTTF of the breaker is given as

$$MTTF = \int_0^\infty R(t)\, dt = \int_0^\infty (1-Q(t))\, dt \tag{3.7}$$

Specific numerical results of this reliability analysis have not been obtained yet because of the unavailablilty of hazard rates for the components of the circuit breaker. Extensive effort is being made to obtain these data as soon as possible. Other methods of reliability analysis using Coherent Structure theory[3] and Fault Tree Analysis[4] are being investigated.

3.3 DESIGN AND DEVELOPMENT OF THRESHOLD COUNTING DEVICES FOR CIRCUIT BREAKERS

3.3.1 Purpose and Design Requirements

The design and construction of a threshold counting device to register the magnitude of tripping current occuring in molded-case

circuit breakers, used in the mines, has two main purposes. First, to provide the data to study the reliability of the circuit breakers in the mines. Secondly, the device will provide information as to the type and severity of faults which cause the circuit breaker to trip, as well as the frequency of occurence of each type fault.

In designing the device, several criteria have been set as requirements:

1. There are to be five discrete current ranges, the current magnitude at the time the breaker trips being categorized into one of these ranges.

2. The unit is to be reliable. A counter is to register the range of current only when the breaker trips, thus keeping a running total of the number of trips per range.

3. There is to be one display for each of these five ranges.

4. The minimum display size shall be four places, allowing it to count up to 9999 trips for each of the five specified trip ranges.

5. The display is to be non-destructible, that is, it must retain the data during a system power failure.

6. The final unit should be compact. The physical size of the counter should be such that it can be attached directly to the circuit breaker. As mentioned in Section 3.2.1, the breaker under study is an LA-Frame,[5] 400-A, 600-V ac, 3-pole breaker with a 24-V dc undervoltage release and special thermal and magnetic trip settings of 225 and 350-A, respectively. Its dimensions are 10-1/2 x 8-1/2 x 4 inches, and its present mounting position in the load center has a front clearance of 6 inches and bottom clearance of 2-1/2 inches.

3.3.2 Overall Design Outline

A basic block diagram of the device is presented in Fig. 3.9 which shows a building block for each subsystem of the device. The design aspects of each of the subsystems is described in detail in the following sections.

The five discrete ranges chosen for the device are as follows:

Range 1: 0-20A. This represents the case of no-load and undervoltage conditional operation of the circuit breaker. The 20A upper limit was determined according to the acceptable tolerance associated with the type of breaker chosen.

Range 2: 20—225A. This range takes care of fault currents involving the neutral ground resistor.

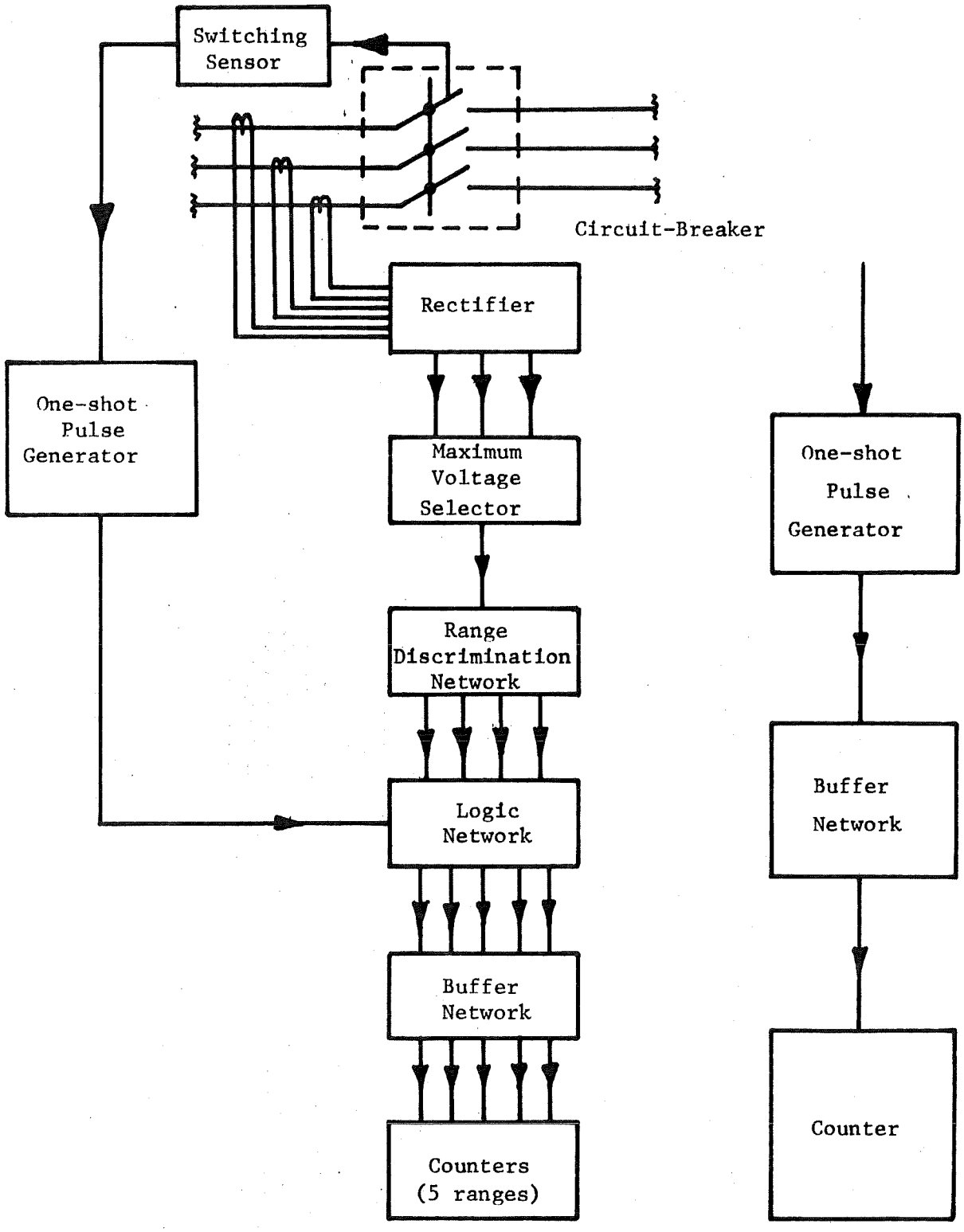

Fig. 3.9 Basic Block Diagram of Circuit Breaker Counters

Range 3: 225-350A. This range is chosen to categorize currents which fall into the thermal trip range of the circuit breaker.

Range 4: 350-800A. This range is chosen to categorize currents which fall into the magnetic trip range of the circuit breaker, and

Range 5: Larger than 800A. This range is chosen to register cases of extremely high tripping current in the circuit breaker. These ranges, however, may easily be changed to conform to circuit breakers with different ratings, or for any other reason desired.

The device basically works in the following manner. The current in each phase is sensed first and rectified. Then the maximum of the three currents is selected and fed into the range discriminating network which in turn operates the appropriate counter depending upon the fault current level. However, the device operates only when the circuit breaker trips. The decision to select the maximum of the three phase currents is based on the following criteria:

1. The faults which are most likely to occur are single line-to-ground faults. These are cleared by sensing current in the grounding resistor rather than sensing overcurrent in the phase conductors.

2. Data as to the severity of fault currents which the circuit breaker must interrupt are desirable.

3. In the event of the occurence of a fault other than a single line-to-ground type, more than one of the lines may be carrying the maximum current.

3.3.3 Current Sensing Technique

The current transformers [6-7] shown in Fig. 3.9, serve the purpose of sensing the ac current in each of the three lines which pass through the circuit breaker. They transform current in the range of 0 to 800-A down to a range at 0 to 5-A. The current transformers used in the design are 800-A, 600-V Westinghouse current transformers. Three current transformers are used, one placed in each of the three lines which pass through the circuit breaker.

The current transformers used in the design after testing are found to have very nearly linear output characteristics. The characteristics are also found to be identical for each of the three current transformers tested, eliminating the need to compensate for differences in the current transformer characteristics.

3.3.4 Rectifier

The block labeled "RECTIFIER" in Fig. 3.9, represents the transformation of the 0-5 A ac output from the current transformers into a corresponding dc value which is compatible with TTL circuitry. The current dropping resistors R_1 and R_2 and a voltage divider network, comprised of R_3 and R_4 shown in Fig. 3.10, are used to reduce the signal to one compatible with TTL circuitry.

The parallel combination of R_1 = 2 ohms and R_2 = 3 ohms is 1.2 ohms. Both resistors are rated at 25 watts allowing for dissipation of power due to the significant amount of current flowing through them. This 1.2 ohm equivalent resistance is essentially in parallel with the series equivalent of R_3 = 680 ohms and R_4 = 680 ohms, or an equivalent resistance of 1360 ohms.

In the limiting case of 800 A in the lines, 5 A will be present at the output of the current transformers. The current in the 1.2 ohm equivalent resistance will then be

$$(5) \quad \frac{(1360)}{(1361.2)} = 4.9956 \text{ A}$$

The current flowing into R_3 will then be

$$5 - 4.9956 = 4.4 \text{ milliamperes}$$

This value is acceptable to the TTL logic circuitry.

The voltage appearing across the 1.2 ohm equivalent resistance will then be $(1.2) \cdot (4.9956) = 5.995$ V or approximately 6 V.

The resistors R_3 and R_4 decrease the voltage across the 1.2 ohm equivalent resistance to a value of about 3 V. This 3 V ac signal is then passed through a bridge rectifier obtaining a dc voltage of 1.414(3)= 4.24 V. Therefore, the values of line current ranging from 0-800 A ac will correspond to dc voltages ranging from 0-4.24 V, which is acceptable to the TTL circuitry.

The rectified signal is integrated with high gain to obtain a square wave pulse beginning when the signal is at its maximum value. This pulse is then passed into a one-shot monostable multivibrator which will produce a short pulse which occurs at the instant the rectified signal reaches its maximum peak. This pulse from the monostable is used to trigger a sample-and-hold circuit[8] whose output will be equal to the peak value of the rectified signal. This arrangement allows for very fast response time to a change in line current, as well as eliminating a high degree of ripple in the dc signal obtained as an output.

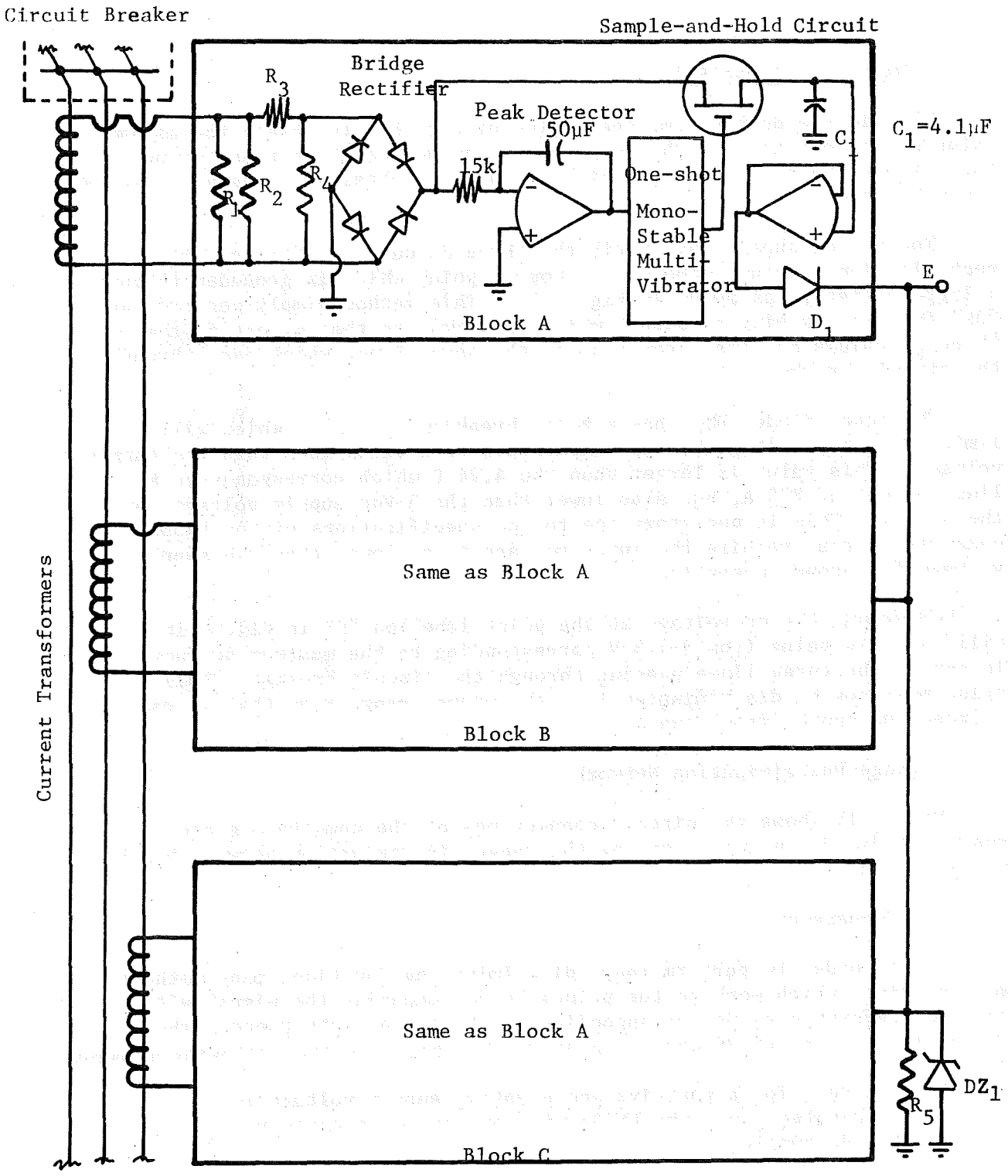

R_1=2Ω, R_2=3Ω, R_3=R_4=680Ω, R_5=100k

Fig. 3.10 Details of Rectifier and Maximum Voltage Selector Parts of the Counting Device.

3.3.5 Maximum Voltage Selector

Next in the design came the choice of a method to obtain the maximum value of the currents in the three phase conductors which pass through the circuit breaker. Only the highest value is obtained since many faults are unbalanced.

The method chosen was to tie the three dc outputs obtained after rectification, through diodes to a common point which is grounded through a large resistor, as shown in Fig. 3.10. This method simply performs an "OR" function, giving an output which is equal to the largest of the three dc values obtained from each of the three lines which pass through the circuit breaker.

The zener diode, DZ_1, has a zener breakdown of 4.5 V which will limit the input voltage to the comparators to a value less than the supply voltage. This value is larger than the 4.24 V which corresponds to a line current of 800 A, but also lower than the 5-Vdc supply voltage for the system. This is necessary due to the specifications of the LM339 comparators that require the input voltage to be lower than the supply voltage for proper operation.

In summary, the dc voltage at the point labelled "E" in Fig. 3.10 will range in value from 0-4.5 V corresponding to the maximum ac current in any of the three lines passing through the circuit breaker. This value must now be discriminated into the proper range such that it can trigger the appropriate counter.

3.3.6 Range Descrimination Network

Fig. 3.11 shows the circuit connections of the comparators and resistive divider network forming the range discrimination network block in Fig. 3.10.

A. Comparator

In order to perform range discriminating function, many methods were examined which work on the principle of comparing the signal with some set reference value corresponding to the appropriate range. The choice in using an LM339 quad. comparator[9] is based on the following reasons:

1. The need for a positive and negative supply voltage is eliminated since the LM339 will operate on a positive 5-V dc supply.

2. The reference voltages are easily obtainable with a voltage divider network.

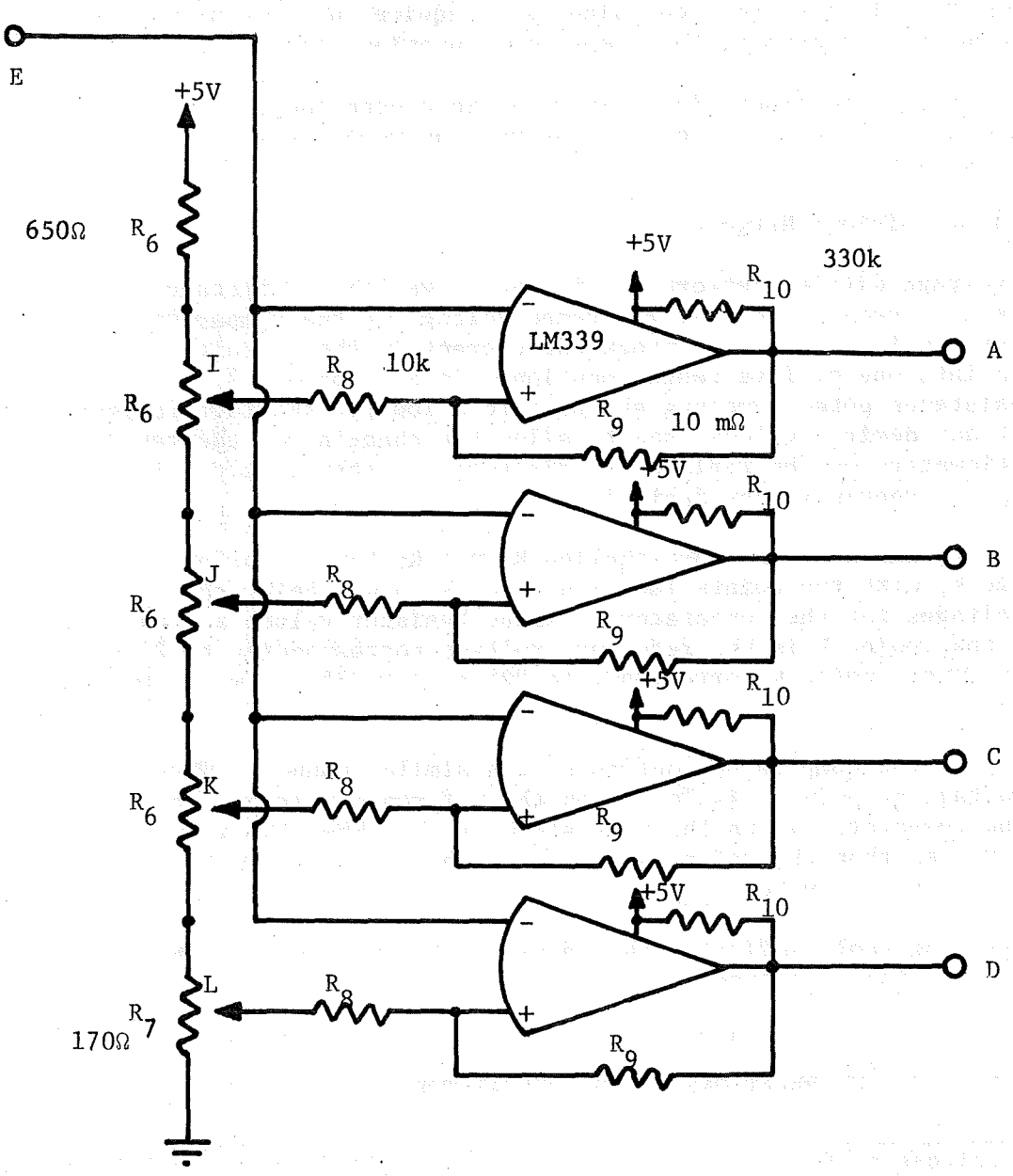

Fig. 3.11 Range Discrimination Network

3. The LM339 contains four comparators on a single 14-pin package, therefore, it is possible to reduce the number of circuit components used.

4. The LM339 is also self contained and requires no external components to perform the comparison function, and

5. The ease of incorporating hysteresis into each comparator to avoid problems of loading was instrumental in the choice.

B. Voltage Divider Network

A voltage divider network consisting of variable resistance potentiometers is used to set the reference voltage of the comparators. The entire system is designed to break the current in the circuit breaker down into one of five ranges mentioned in Section 3.3.2. Variable resistance potentiometers are used to allow for the five ranges to be set at any desired values, and to allow the changing of the ranges. These potentiometers may be replaced by discrete resistance values if variation in the ranges is not desired.

The five variable resistances labelled R_6 and R_7 form a voltage divider network, with the points labelled I, J, K, and L being the reference voltages for the comparators. These resistor values are adjusted such that point L is the reference voltage corresponding to 20 A in the power lines, point K corresponds to 225 A, J to 350 A, and point I to 800 A.

Each one of the comparators operates in a similar manner. When the input voltage at point E is less than the reference voltage, the output of the comparator is in the high state, +5 V. When the input voltage is greater than the reference voltage, the output is in the low state, or at ground potential.

The following table indicates the value of the outputs at A, B, C, and D for a given input voltage.

TABLE 3.1

INPUT-OUTPUT RELATIONSHIP FOR COMPARATORS

Input voltage at E which corresponds to the following values of line current		Output States at A	B	C	D
0-20 A	E less than L	1	1	1	1
20-225 A	$L \leqslant E \leqslant K$	0	1	1	1
225-350 A	$K \leqslant E \leqslant J$	0	0	1	1
350-800 A	$J \leqslant E \leqslant I$	0	0	0	1
over 800 A	$E > I$	0	0	0	0

where a "1" state corresponds to a +5 V, and a "0" state corresponds to ground potential

Resistors R_8, R_9 and R_{10} provide hysteresis for the comparator detection level. Their values are obtained from "Archer" technical data sheet[9].

3.3.7 One - shot Pulse Generators

The specifications of the counters used in the design require that the input to the counters be a pulse of duration less than 60 milliseconds. Therefore, one-shot pulse generators are set up such that the signal applied to the counters lasts approximately 50 milliseconds.

The one-shot pulse generator in Figs. 3.9 and 3.12 which is connected between the switch and the logic network, supplies a pulse to the logic network whenever the circuit breaker trips. The combined presence of this pulse and a signal in the logic network corresponding to the appropriate range is required to advance the appropriate counter by one count. The monostable multivibrator[10] is connected such that when the input to it goes through a transition from a high state, +5 V, to a low state of 0 V, an output pulse of 50 millisecond duration is generated. From Reference 6, the width of this output pulse is obtained by the following equation:

$$t_w = 0.7\ R_T\ C_T \qquad (3.8)$$

From the above equation choosing C_T, the external timing capacitor, = 5 microfarads, and requiring t_w = 50 milliseconds, R_T, the external timing resistor, is calculated to be 14,286 ohms. A value of R_T = 15k ohms is used, thus giving t_w = 52.5 milliseconds, which is less than the 60 millisecond maximum pulse width acceptable for the counters.

The input into the monostable multivibrator is obtained from the switch which is at a value of +5 V when the breaker is closed, and goes to 0 V (ground) when the breaker is opened (tripped). Therefore, the monostable multivibrator normally has a low output, and provides a 5 V, 52.5 millisecond pulse whenever the breaker trips.

3.3.8 Logic Network

The block labeled "Logic Network" in Fig. 3.9 depicts the step in which the signals obtained from the range descrimination network are conformed to a signal which is applied to the appropriate counter. The use of TTL logic gates[11-14] is justified by their simplicity and compatability with a positive 5-Vdc supply. The choice of the logic gates with open collector outputs was made to obtain an output signal which was as close to 5 V as possible due to the requirement of the counters. The open-collector output gates are essentially one step in the buffering of the output signal to a value which is compatible with the counters used.

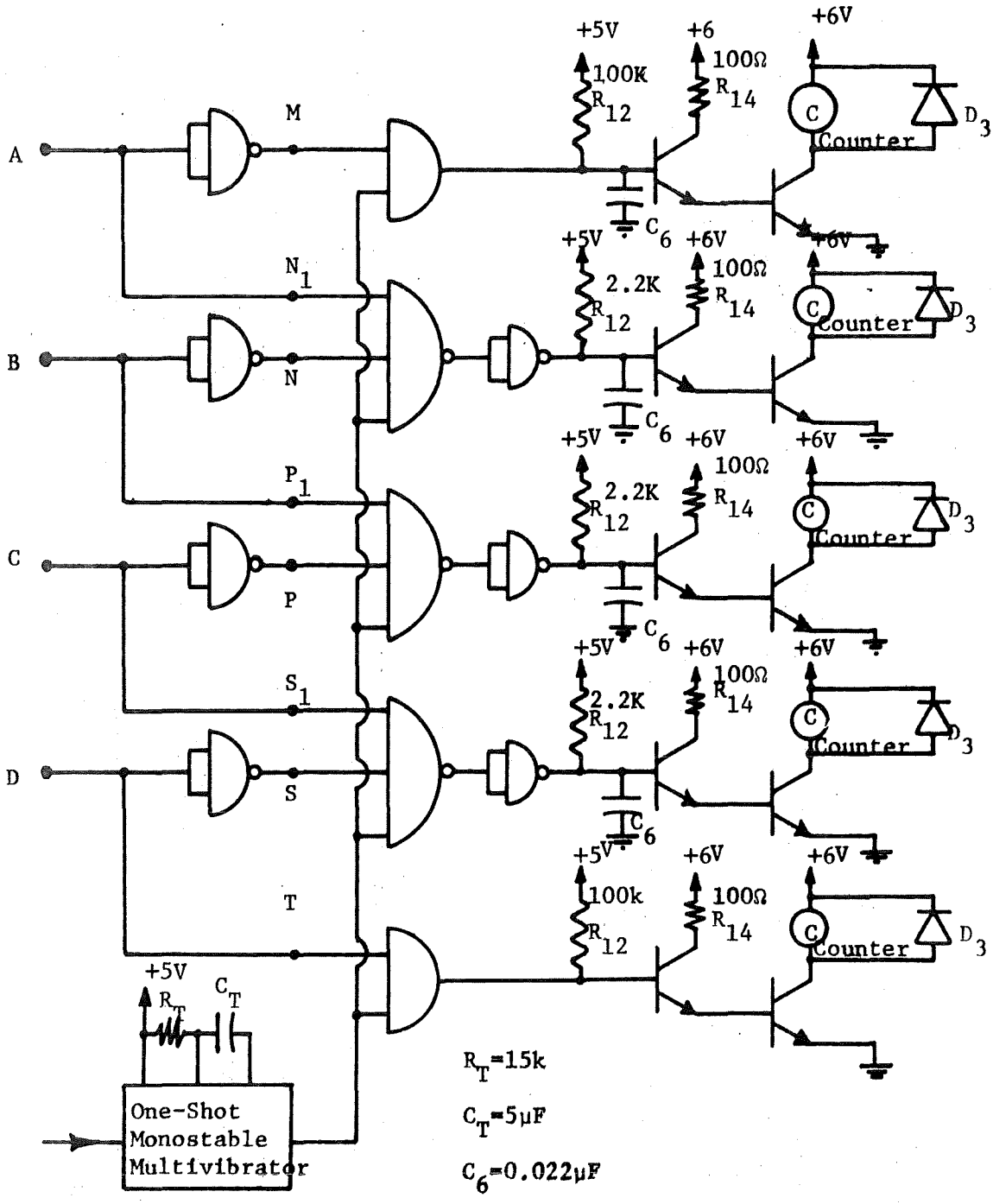

Fig. 3.12 Connection Diagram for Logic Network, Buffer Network, and counters.

The inputs shown in Fig. 3.12 are A, B, C, and D (the outputs of Fig. 3.11). The four 2-input NAND gates(SN7400) of Fig. 3.12 convert the outputs of the comparators to a form such that only one line is in the high state at any one time. The following table shows this relationship.

TABLE 3.2

INPUT-OUTPUT RELATIONSHIP OF LOGIC NETWORK

Line Current Range	A	B	C	D	M	NN'	PP'	SS'	T
0-20 A	1	1	1	1	0	0	0	0	1
20-225 A	0	1	1	1	0	0	0	1	0
225-350 A	0	0	1	1	0	0	1	0	0
350-800 A	0	0	0	1	0	1	0	0	0
over 800 A	0	0	0	0	1	0	0	0	0

In Table 3.2 a "1" represents a high state (+5 V) and a zero, "0", represents ground potential. The combinations, NN', PP', SS' represent the "NAND" function of the respective labeled points.

3.3.9 Counters

Electromechanical counters are chosen since they have non-destructibe display characteristic as required, though their physical size is larger than LED displays. These are well suited for mine applications because of their rugged nature. Each of these five counters is rated 5 watts and 6-Vdc[15-16]. The 6 V regulated dc supply is obtained separately off the power supply depicted in Fig. 3.13. Each of the counters can register up to 5 digits and is therefore, well suited for circuit breaker application.

3.3.10 Buffer Network

The output of the TTL circuitry is not sufficient to activate the counters, therefore, the transistor buffering, as well as the use of the TTL gates with open-collector outputs and pull-up resistors is used which is depicted in Fig. 3.12. This arrangement provides adequate current to activate the counters as desired.

3.3.11 Power Supply

Fig. 3.13 shows the circuit connections for a +5-Vdc and +6-Vdc regulated power supply. The power supply converts available 110-Vac into 5-Vdc and 6-Vdc by the use of a transformer, full-wave bridge rectifier, capacitive filter, and a 5 and 6-V regulators. The output of the power supply is rated at 1 A which is required by the counters as they draw approximately 0.8 A dc.

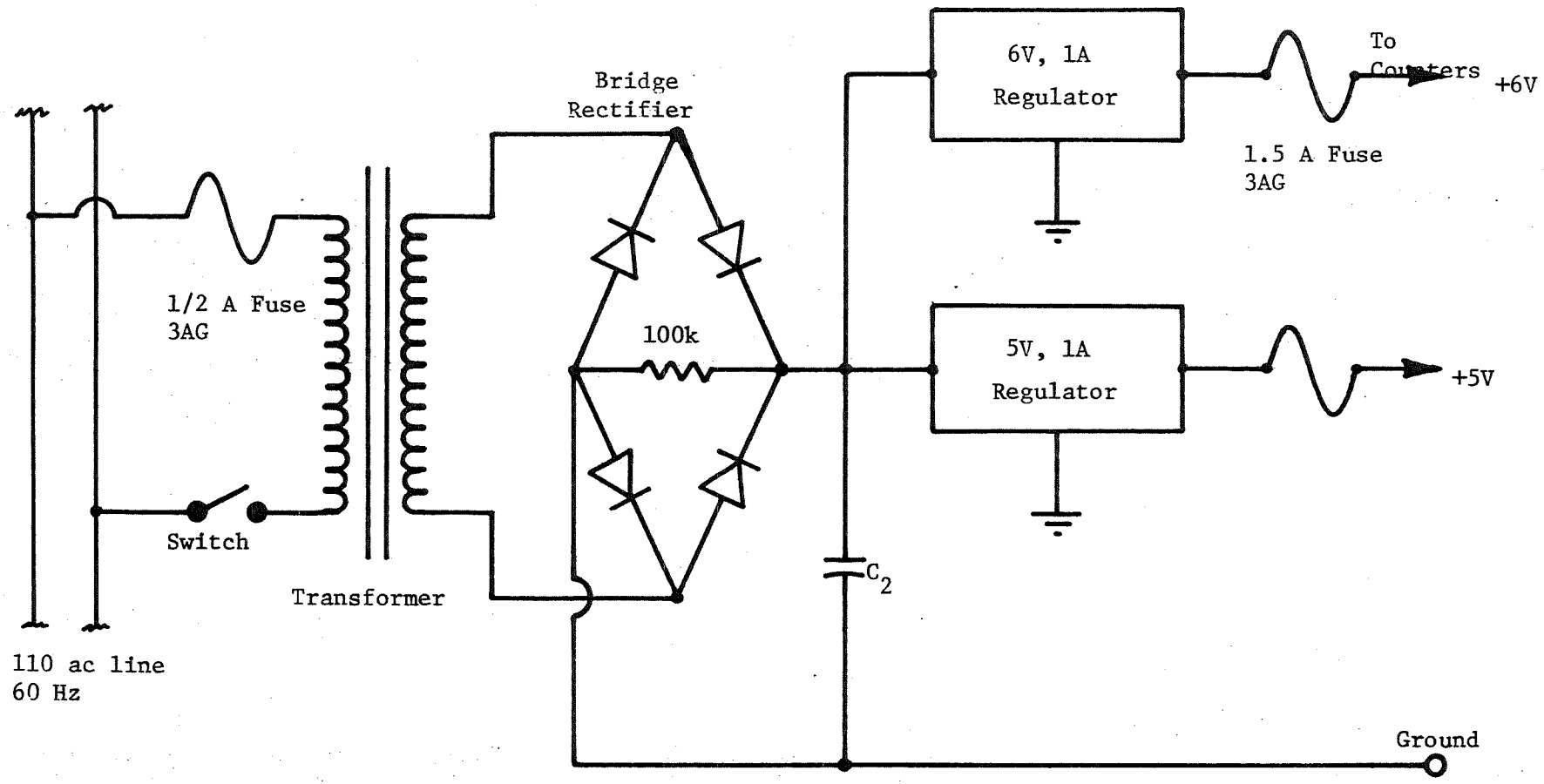

Fig. 3.13 Schematic for Power Supply.

3.3.12 Results and Conclusions on Circuit Breaker Counters

The threshold counting device has been tested and found to perform the desired function to the extent which tests could be performed. Final assembly and testing of the device requires the following additional items:

1) A switch which will indicate when the mechanical contacts of the breaker have tripped, and

2) A sixth counter to study the reliability of the tripping mechanism at the circuit breaker. This counter will be triggered directly from the signal in the circuit breaker which triggers the breaker contacts.

These two items will be included after obtaining the circuit breakers and examining their physical characteristics. The circuitry of the device will be put on a printed circuit board and the device itself will be totally enclosed in the final form. Ten units of the device will then be assembled and incorporated with the ten circuit breakers to be field tested in the mines.

3.4 RELIABILITY ANALYSIS OF UNDERVOLTAGE RELEASES/RELAYS (UVR's)

During the 1974-75 project year, the theoretical reliability analysis of both electromechanical and solid-state UVR's was presented. In this work which was reported in the annual report[17] of Grant #G1022088, a simplified analysis was presented. This approach also represents the worst-case situation.

The work reported in this section represents the continuation of the previous year's research effort. In the following section, a more realistic theoretical reliability analysis of the solid-state UVR is presented. This is followed by the work performed in the laboratory and field testing aspects of both electromechancial and solid-state UVR's.

3.4.1 Theoretical Reliability Analysis of UVR's

The theoretical reliability analysis of the solid-state UVR was carried out using the minimal cut-set method. This UVR is one of the earlier versions manufactured by Westinghouse Electric Corporation. The circuit diagram of the UVR is shown in Fig. 3.14 and its function has been explained in detail in Section 4.5.1 of the last year's annual report[17].

Before outlining the detailed analysis, it is necessary to draw the reliability block diagram as was done for circuit breakers in Section 3.2. The diagram is shown in Fig. 3.15. In this diagram, A_1 represents

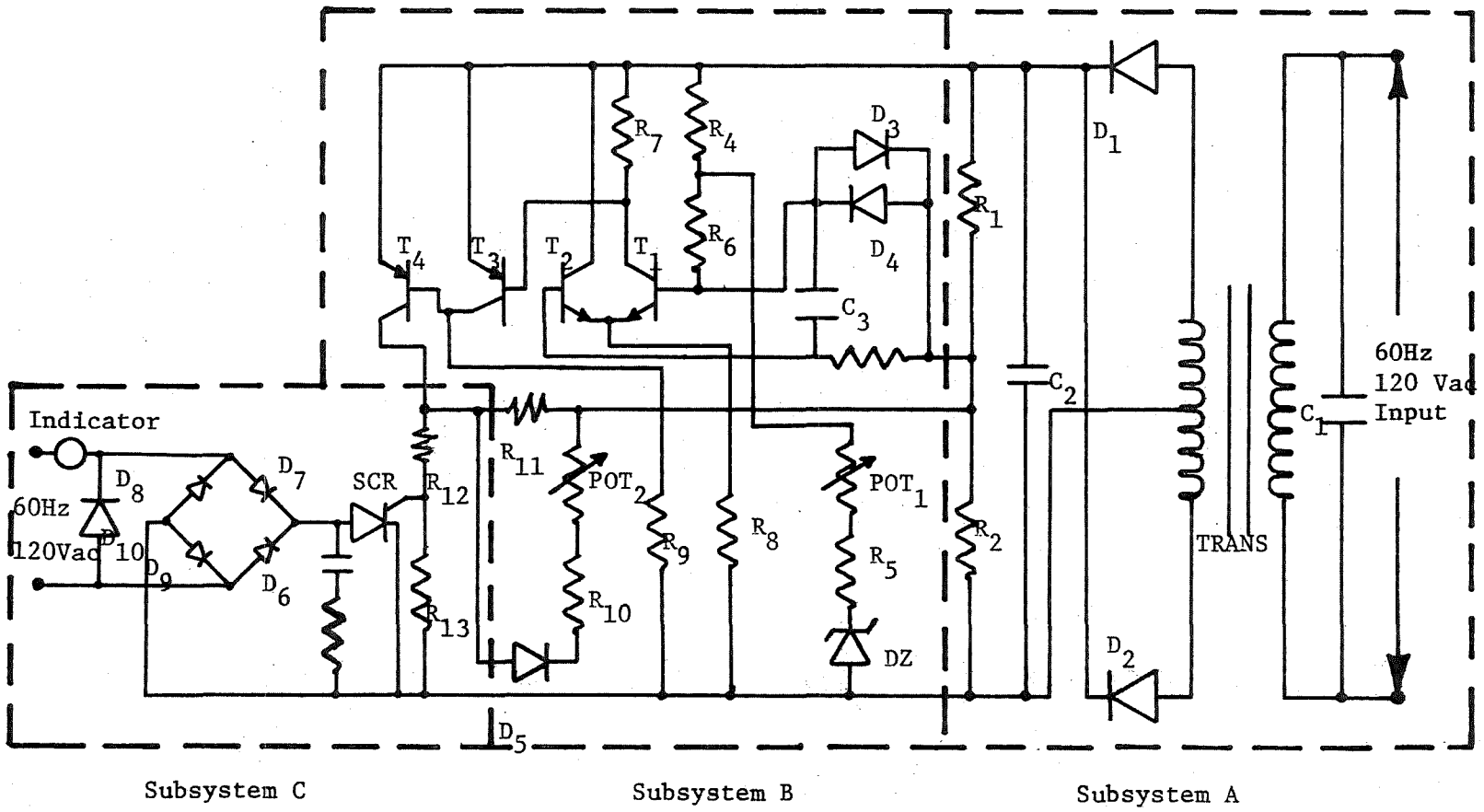

Fig. 3.14 Schematic Diagram of Solid State Undervoltage Relay.

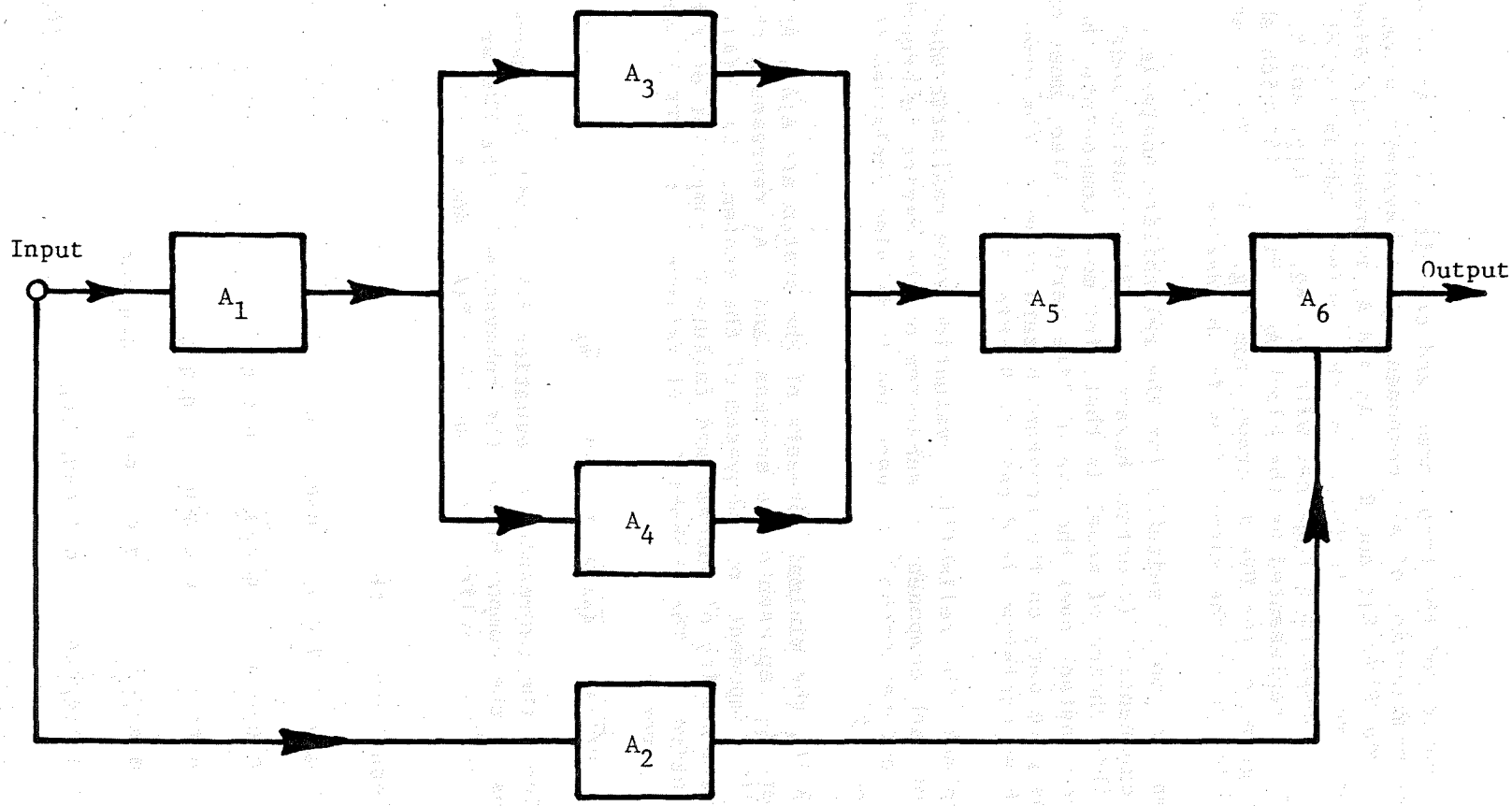

Fig. 3.15 Reliability Block-Diagram of UVR.

the series combination of the transformer and capacitor C_1. A_2 is made up of the series combination of all components in subsystem C shown in Fig. 3.14 except the SCR, R_{12} and R_{13}. A_3 and A_4 represent the diodes D_1 and D_2, respectively. A_5 is formed of the series combination of all the components in subsystem B together with R_1, R_2, C_2, R_{12}, and R_{13} in series. The SCR is represented by the block A_6. Fig. 3.16 which shows the reliability graph of the UVR is drawn from Fig. 3.15. This graph gives a better picture of the signal flow in the device.

The mathematical model suitable for the reliability analysis of the UVR is the exponential (constant hazard rate distribution model). The reason for this choice of model is that, for most components the hazard rates are constant over the useful life period. Also, most of the publications give data on the constant hazard rates of the components. This model has been explained in detail in Section 3.2.4.

In order to make the reliability evaluation more realistic where the importance of each component or subsystem of the device is brought out, the minimal cut-set method[1] is used and it is also explained in detail in Section 3.2.4.

From Fig. 3.16, the minimal cut-sets of the system are A_1A_2, $A_2A_3A_4$, A_2A_5, and A_6 where A_j represents the success and $\bar{A}_j$ represents the failure of the j^{th} component, or subsystem of the system. Let $P(A_j)$ and $P(\bar{A}_j)$ mean the probability of success and failure of component or subsystem A_j, respectively. The probability of failure of the UVR or its failure index is given as

$$Q(t) = P(\bar{A}_1\bar{A}_2 \cup \bar{A}_2\bar{A}_3\bar{A}_4 \cup \bar{A}_2\bar{A}_5 \cup \bar{A}_6) \tag{3.9}$$

In order to evaluate the expression in equation 3.9 it will be assumed that the failures of the components or the subsystems of the UVR are independent. As defined earlier, $q_j = q_j(t) = P(\bar{A}_j)$ and $r_j = r_j(t) = P(A_j)$.

It follows from equation 3.9 that

$$\begin{aligned} Q(t) = {} & q_1 q_2 + q_2q_3q_4 + q_2q_5 + q_6 \\ & - q_1q_2q_3q_4 - q_1q_2q_5 - q_1q_2q_6 \\ & - q_2q_3q_4q_5 - q_2q_3q_4q_6 - q_2q_5q_6 \\ & + q_1q_2q_3q_4q_5 + q_1q_2q_3q_4q_6 + q_1q_2q_5q_6 \\ & + q_2q_3q_4q_5q_6 - q_1q_2q_3q_4q_5q_6 \end{aligned} \tag{3.10}$$

In equation 3.10 each

$$q_1 = 1-e^{-\lambda_j t} \tag{3.11}$$

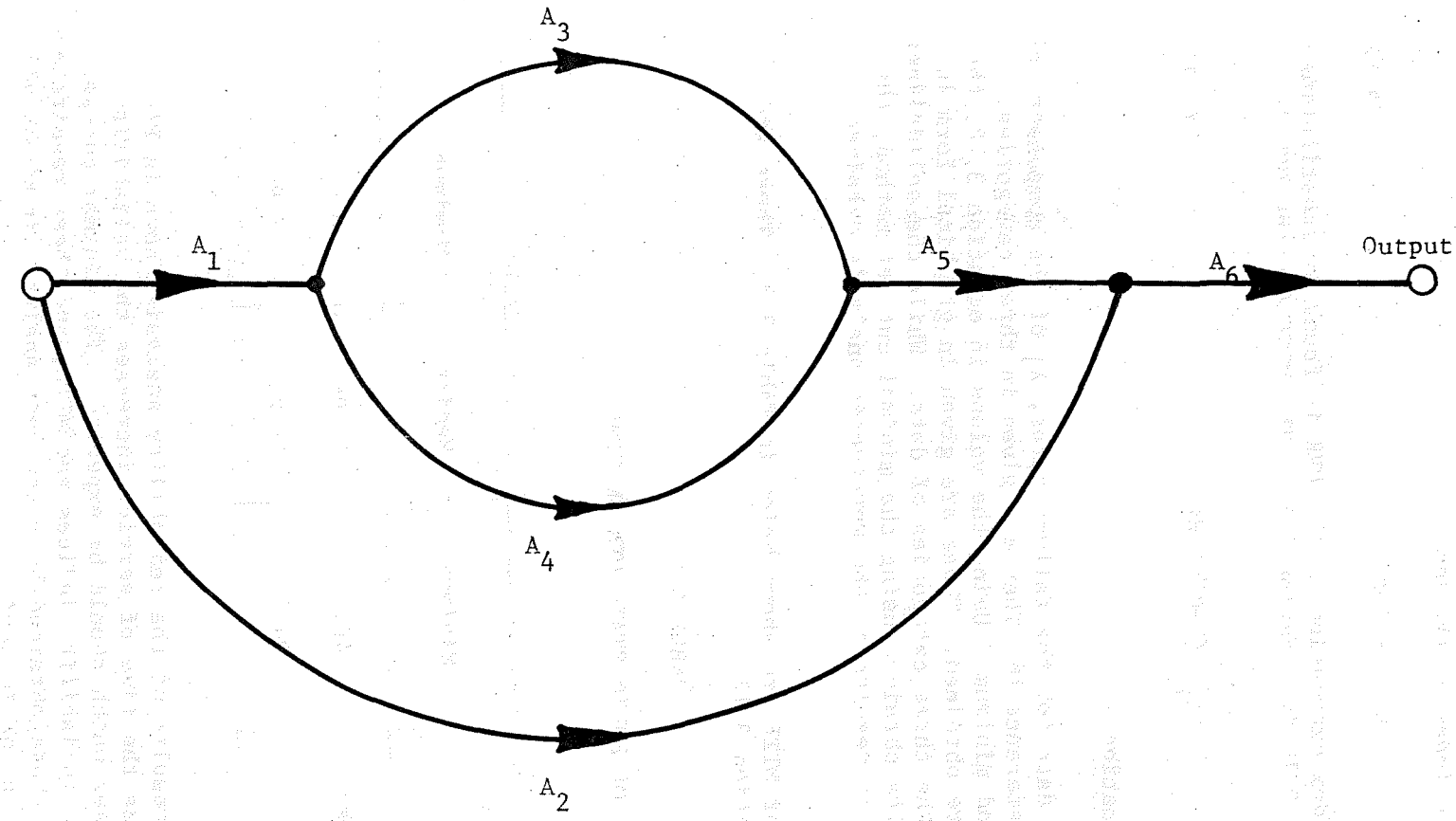

Fig. 3.16 Reliability Graph of the UVR.

and the reliability index of the UVR,

$$R(t) = 1-Q(t) \tag{3.12}$$

The reliability index expression of the UVR is found by substituting equations 3.11 and 3.10 in equation 3.12. The MTTF for the UVR is given as

$$T = \int_0^\infty (1-Q(t))dt \tag{3.13}$$

A. Numerical Application

The numerical data for the failure rates, λ_j of the components of the UVR are from Reference 18. They are given in three categories: maximum, median, and minimum. Using the values in equation 3.12, the specific results are obtained. These are given in graphical form in Fig. 3.17 for all the three categories of data. While the solid-lines represent the results obtained using the minimal cut-set method, the broken lines show the results of the worst-case analysis obtained earlier.

The results for MTTF are shown below in Table 3.3. These are obtained using equation 3.13.

TABLE 3.3

MTTF OF SOLID-STATE UVR IN YEARS

Method	Minimum	Median	Maximum
Minimal Cut-set	40.1	22.96	10.47
Worst Case	34.7	18.22	9.99

The graphical results of the reliability analysis shown in Fig. 3.17 revealed that as the time of service increases the reliability index of UVR decreases which should be expected. The minimal cut-set approach gave better reliability indices and MTTF, and these results are more realistic than those obtained by worst case analysis in which all components are taken to be in series.

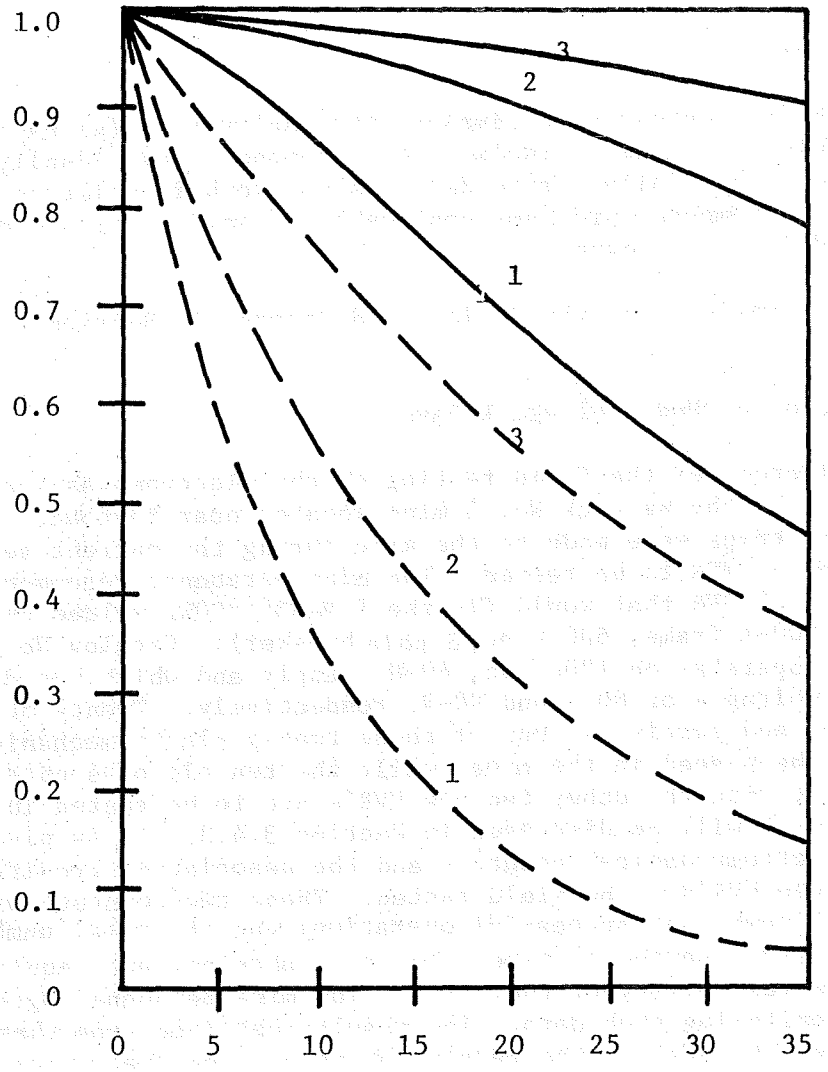

Fig. 3.17 Reliability Characteristics of Solid-State UVR.

'1' Indicates Maximum
'2' Indicates Median
'3' Indicates Minimum

——— Cut-Set Method

--- Worst Case Analysis

B. Work in Progress

Further work is in progress to improve the analysis by (a) expanding the reliability block diagram to include each component individually; (b) by using more recent failure rate data. Also, work is going on to develop generalized computer programs applicable to any protective device whose reliability is to be found.

The fail-safe analysis of the device is discussed in Section 4.5 of Chapter IV.

3.4.2 Field Testing of Undervoltage Relays

The mine selected for the field testing of the electromechanical undervoltage relay is the Warwick No. 3 mine located near Bobtown, Pennsylvania. Two trips were made to the mine during the current year to select the type of UVR to be tested. The mine personnel recommended the following type of UVR that would fit the TKMA836-800WL molded case circuit breaker (800-A frame, 600-V ac, 3 pole breaker): Catalog No. TKMA UVA1RB which operates on 120-V ac, 60-Hz supply and which has drop-out and pick-up voltages of 60-V and 90-V, respectively. Twenty of these UVR's were ordered and received. Out of these twenty electromechanical UVR's, ten are to be placed in the mine, while the ten old ones obtained from the mine along with the other ten new UVR's are to be tested in the laboratory, which will be discussed in Section 3.4.3. It is planned to install two electromechanical counters and the associated circuitry with each of the ten UVR's to be field tested. These two counters will register the total number of successful operations and the total number of operations over a given period of time. The data obtained are required for evaluating the reliability of the UVR's. The mine personnel agreed to cooperate in monitoring such data. The results obtained from these data will be correlated against the results obtained from theoretical analyses and laboratory tests.

The initial form of the circuit designed for counting the total number of successful operations was explained in Section 4 of the third quarterly report of the current project year. [19]

The circuit was fabricated and tested in the WVU Electrical Engineering Laboratory. While testing the circuit, it was found that microswitch S which was supposed to operate when the UVR deenergizes did not work properly. This was because the force exerted by the arm of the undervoltage release was not sufficient to make the microswitch operate, thus, preventing the counter circuit from operating. Because of this problem a new circuit was designed for this purpose. This circuit is shown in Fig. 3.18. The circuit works as follows:

The sensor part of the circuit contains an emitter and a detector. The emitter is an ultraviolet light emitting diode and the detector is a photo darlington transistor pair.

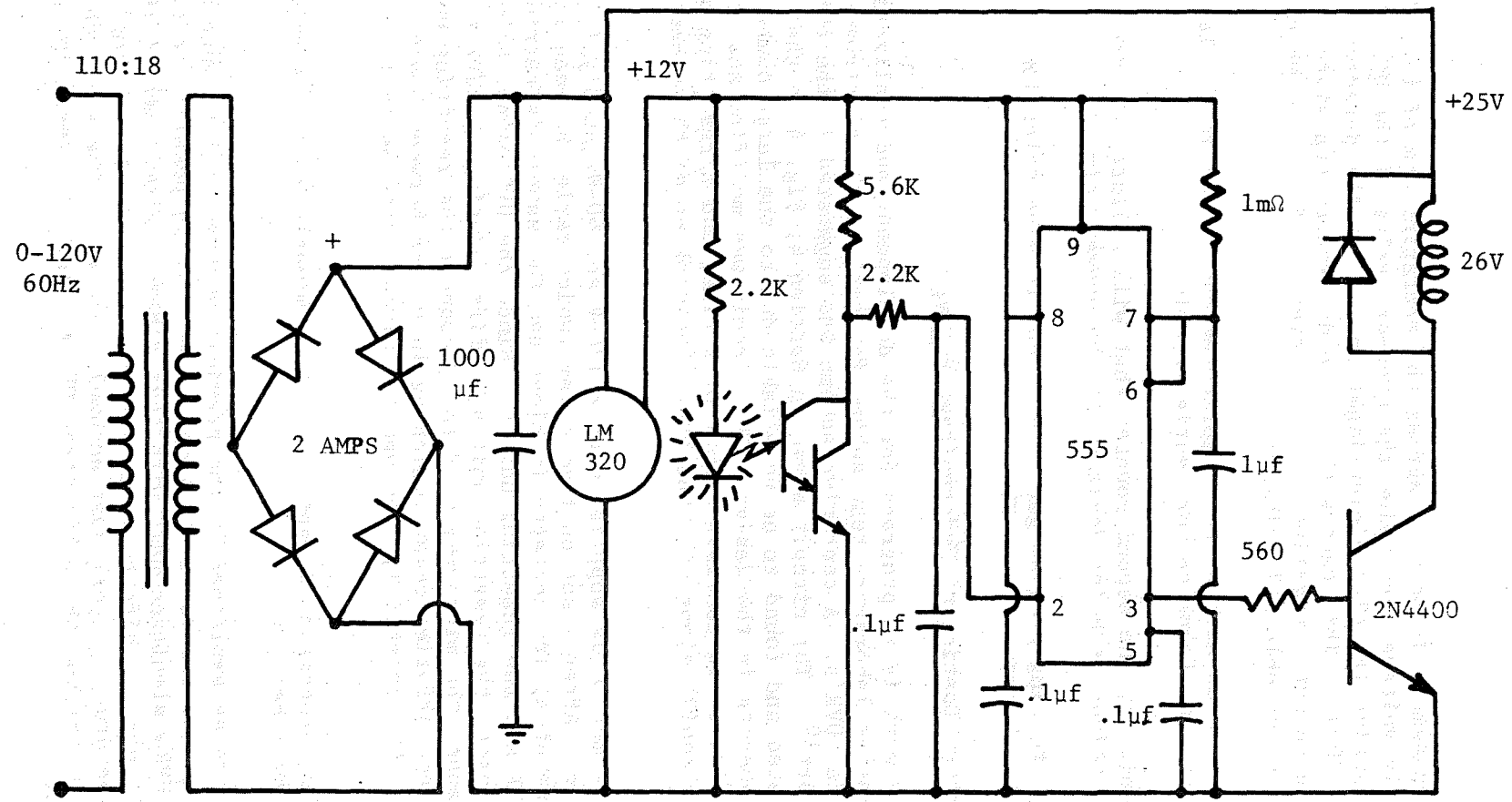

Fig. 3.18 Circuit for Counting the Number of Successful Operations of UVR.

This arrangement is mounted across the operating arm of the UVR. When the supply voltage goes below the drop-out value of the UVR, it deenergizes causing the ultraviolet light to fall on the detector for approximately 20 ms. This causes the photo darlington transistor to saturate and give out a negative pulse to trigger a 555 timer which operates as a monostable multivibrator.

This circuit has already been fabricated and tested in the laboratory and has been found to work satisfactorly.

The circuit for the second counter that will register the total number of operations is being designed at the present time.

The field testing program got delayed due to mine selection process and the shipment of the UVR

3.4.3 Laboratory Testing of Undervoltage Relays

Currently work is in progress for the development and realization of a comprehensive laboratory test scheme for testing the electromechanical and solid-state UVR's. A tentative scheme was suggested in the third quarterly report[19]. The circuit given in Section 4, Fig. 4 in that report was tested and found to be unreliable due to the large number of moving components in the design. The circuit was modified and is shown in Fig. 3.19. It consists mainly of a timer and a resetting unit (which is a solenoid) along with the UVR. The working of the scheme is as follows.

When the timer T is supplied with a 120-V ac, 60-Hz supply, it is fully energized. After a set on time delay (which varies between 1 minute and 3 minutes) its contacts T_1 close and the supply is carried over to the UVR and the resetting unit R. Since the UVR cannot hold in unless it is reset, the resetting unit acts first causing the UVR to hold. This causes the microswitch S to disconnect the resetting unit R. After a given off-time delay (which again varies between 1 minute and 3 minutes) the contacts T_1 open and the circuit returns to its original state.

This cyclic process of duration of 2 to 6 minutes continues unless the supply is switched off.

Two counters, as explained in the previous section will be incorporated with each UVR in the laboratory testing scheme. It is possible to test three to five UVR's simultaneously with this scheme. Simulation of the following environmental effects in this testing program are contemplated: humidity, temperature, coal dust accumulation, etc. The same scheme will be used for testing the solid-state UVR's except the resetting unit is not required.

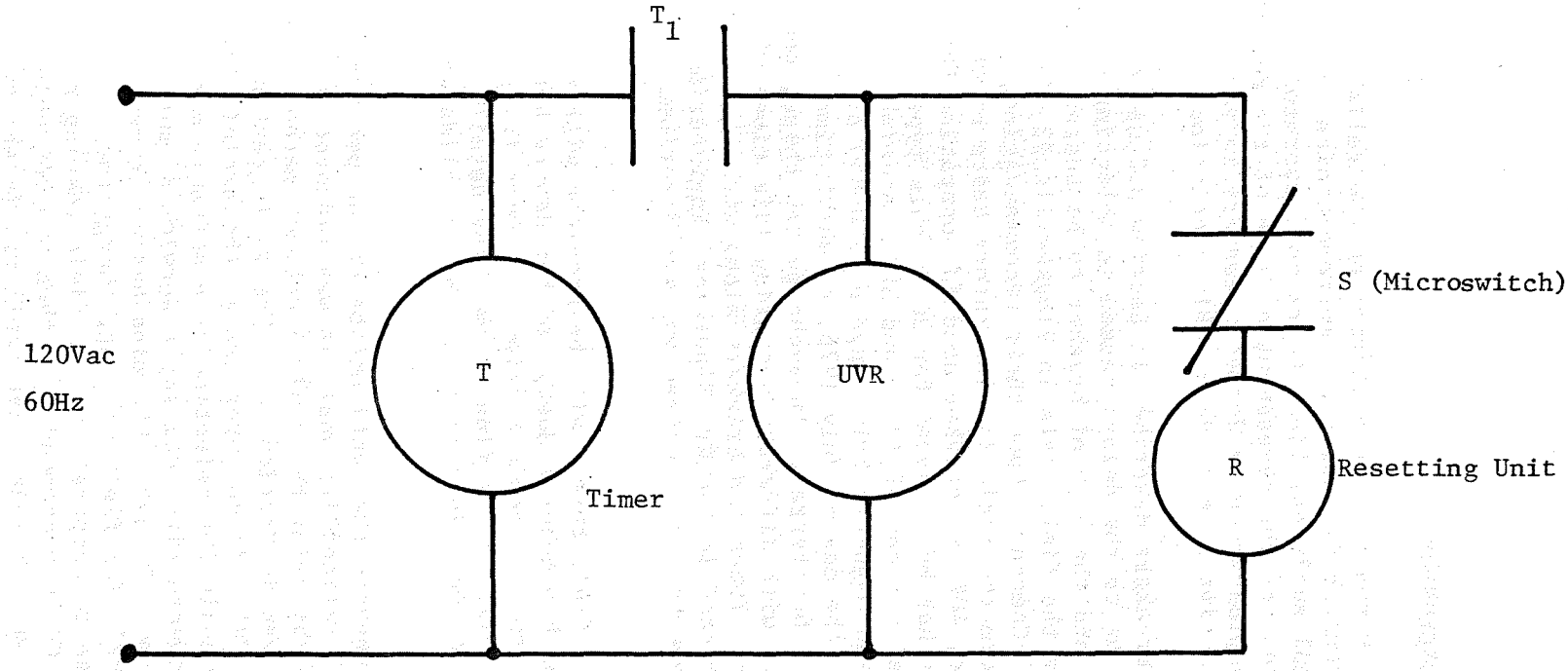

Fig. 3.19 Scheme for Laboratory Testing Of UVR's.

3.5 SUMMARY, RESULTS, AND CONCLUSIONS

This chapter entails the research work performed on the reliability assessment of molded case circuit breakers, and electromechanical and solid-state UVR's. Theoretical analyses, field tests and laboratory tests represent the three facets of the assessment of each of the devices mentioned above. All three approaches were deemed necessary to correlate the results and consequently arrive at more dependable conclusions.

The work on the circuit breakers described in Section 3.2 did not proceed at the expected rate due to the delays caused in selecting a suitable mine for field study and the type of breaker to be tested. It has been decided to perform the field tests in Blacksville #2 mine operated by Consolidation Coal Company. Upon their recommendation, it has also been decided to perform the field and laboratory tests on the Westinghouse LA-Frame, 600-Vac, 400-A breaker used for operating the loaders and bolters. An order has been placed for 20 of this type breaker which draws a full load current of 130 A and has a special thermal trip rating of 225 A and magnetic trip range of 350-850 A. It is expected to obtain these by the end of July 1976, at which time field tests on ten of them will be started. In exchange for these, ten old breakers of similar ratings with different operating life times will be offered by the coal company. These old breakers along with the remaining ten new ones will be tested in the WVU Electrical Engineering laboratory. The detailed scheme has been devised and was described in detail in Section 3.2.

Each of the breakers to be field tested will be provided with a threshold counting device. The bread-board design of the device has been completed and its details were given in Section 3.3. Once it is tested thoroughly, it will be built in the final form. The details of the development of this device were influenced by the Consolidation Coal Company.

The work on the UVR's represents the continuation of the previous year's effort. The theoretical reliability analysis was improved and realistic results were obtained by using the minimal cut-set method. The details of the analysis were given in Section 3.4. The field testing program for electromechancial UVR's did not progress at the anticipated rate. Initially, the problem was in the selection of a suitable mine. The mine selected (which is Duquense Light Company's Warwick #3 mine) has continuing operating problems. To date, the mine has not given clearance to install the ten UVR's for field testing, though they have indicated their willingness to cooperate in the field testing program. In the meantime, twenty UVR's recommended by them were purchased. These UVR's manufactured by GE, are the ones that would fit in the type TKMA, 600-Vac, 800-A, 3-pole breakers. Each of the ten UVR's to be field tested, will be provided with two counters, whose circuitry was described in detail in Section 3.4. The scheme for the laboratory testing program was also discussed in that section.

REFERENCES

1. Martin L. Shooman, Probabilitic Reliability: An Engineering Approach, New York, McGraw-Hill Co., pp. 1-488, 1968.

2. R. Billinton and M. S. Grover, "Reliability Evaluation in Distribution and Transmission Systems", Proc. IEE, Vol. 122, No. 5, pp. 517-523, May 1975.

3. Richard E. Barlow and Frank Proschan, Statistical Theory of Reliability and Life Testing, New York, Holt, Rinehart and Winston, Inc., 1975.

4. Richard E. Barlow, Fussel, and N. D. Singapurwalla, Reliability and Fault Tree Analysis: Theoretical and Applied Aspects of System Reliability and Safety Assessment, SIAM 1975.

5. Westinghouse Electric Corporation, Breaker Basics - File 29000, pp. 1-22, 31-56.

6. Westinghouse Electric Corporation, Instrument Transformers - Technical Data Sheet 44-060, pp. 1-25, Nov. 1971.

7. Westinghouse Electric Corporation, Current and Potential Transformers - Price List 44-020, Nov. 1976.

8. Jacob Millman and Christos C. Halkias, "Integrated Electronics: Analog and Digital Circuits and Systems", McGraw-Hill, pp. 568-574, 1972.

9. Radio Shack, Archer Technical Data Sheet, RS339 Quad Comparator, p. 4, 1976.

10. Texas Instruments Incorporated, The TTL Databook, 1973, pp. 82-134.

11. ibid, pp. 62, 86.

12. ibid, pp. 62, 88.

13. ibid, pp. 64, 96.

14. ibid, pp. 64, 86.

15. Redington Counters Incorporated, Electrical and Mechanical Counters, RCI-35, pp. 22-23, Nov. 1972.

16. Redington Counters Incorporated, Conseemer Price List - Model 300 Counters, RCI-6, p. 1, Nov. 1974.

17. USBM Grant No. G0122088 (1974-75), Final Report, August 1975.

18. D. R. Earles, "Reliability Growth Prediction During the Initial Design Analysis", Proceedings of Seventh National Symposium on Reliability and Quality Control, pp. 380-388, Jan. 1961.

19. USBM Grant No. G0144137 (1975-76), Third Quarterly Report.

CHAPTER IV

SAFETY ASSESSMENT OF SOLID-STATE PROTECTIVE DEVICES

4.1 INTRODUCTION

This chapter deals with the safety assessment of several solid-state protective devices used in coal-mine power systems. The fail-safe analysis of these devices was performed theoretically using two canned software programs: Electronic Circuit Analysis Program (ECAP) and Systems of Circuit Analysis Program (SYSCAP). The practical part of the analysis was performed by suitable laboratory tests. These tools were applied to the following solid-state devices: 1) Lee Trip (over-current relay). These tools will be used in the future to test 1) EEEI ground monitor, 2) two different PEMCO overcurrent relays and 3) Christy Laboratory's meter relay.

Before proceeding with the description of the analytical tools and their application to the devices, the term fail-safe performance is defined first:

4.1.1 Definition of "Fail-safe" Performance[1]

"A component failure shall not negate the ability of the device to perform properly its intended function or shall open the circuit interrupting devices. (For example, circuit breaker)".

The use of "redundant components or circuitry" will not be accepted as a method of complying with the requirements of the above definition. This definition accepted by Mining Enforcement and Safety Administration (MESA) is kept in mind in carrying out the fail-safe analysis of solid-state protective devices and in interpreting the results.

4.2 SOFTWARE PROGRAMS FOR THEORETICAL FAIL-SAFE ANALYSIS

4.2.1 Electronic Circuit Analysis Program (ECAP)

The theoretical fail-safe assessment of some solid-state devices was initially conducted using the ECAP canned software package available in West Virginia University's Computer Center Library.

Description of ECAP

ECAP is a set of computer programs which have been integrated to form a system capable of analyzing an electronic circuit from a description of its topology. Three forms of analysis are possible with ECAP. They are a direct current (dc) analysis, an alternating current (ac) analysis, and a transient (TR) analysis. Each of these analysis programs will recognize the standard linear circuit elements with some few exceptions. The most outstanding feature of ECAP is its ability, in the transient mode of analysis, to handle nonlinear elements in a piecewise fashion through the use of switches.

ac Analysis

This program provides the steady-state solution for linear circuits which contains resistors, fixed voltage sources, fixed current sources, and dependent current sources. Circuit parameters can be modified in this analysis very simply by just inserting a modify statement and the intended modifications.

dc Analysis

This program provides dynamic solution for linear circuits subject to sinusoidal excitation at a fixed frequency. The circuits may be composed of the following elements: resistors, capacitors, inductors, voltage and current sources, dependent current sources, and mutually coupled inductors. In addition to modifying parameters as in the dc analysis, frequency may also be changed.

TR Analysis

The transient analysis program provides the time response of a circuit subject to user-specified driving functions. The circuits may consist of resistors, capacitors, inductors, fixed or time dependent voltage and current sources, dependent current sources and switches. There are two possible responses from the program. The transient response provides the node voltages, element currents, and switch actuation times as outputs. The voltage and currents are computed at the start of a transient solution and at uniform intervals of time until the solution is reached. The equilibrium response provides a final dc steady-state solution with capacitors automatically open-circuited and inductors short-circuited.

In all of these analyses, each element can be opened and shorted within the program. Input voltages can be applied to the devices to simulate their operating conditions, complete with fluctuations and transients. The transient analysis program was used exclusively in this study, since it met all requirements.

Modeling of Components

Any solid-state devices usually contains resistors, inductors, capacitors, diodes, transistors, operational amplifiers, etc. While it is obvious how to model the first three passive components, it is not clear how to model the active and nonlinear elements or subsystems. This section deals with the modeling of diodes, transistors, and operational amplifiers of the solid-state devices.

Diodes

Diodes can be handled as switches. The switches are current sensitive branches in the circuit. Fig. 4.1 shows the diode model used for the fail-safe assessment of solid-state overcurrent relays. Any branch can be assigned as a switch. The branches so designated have

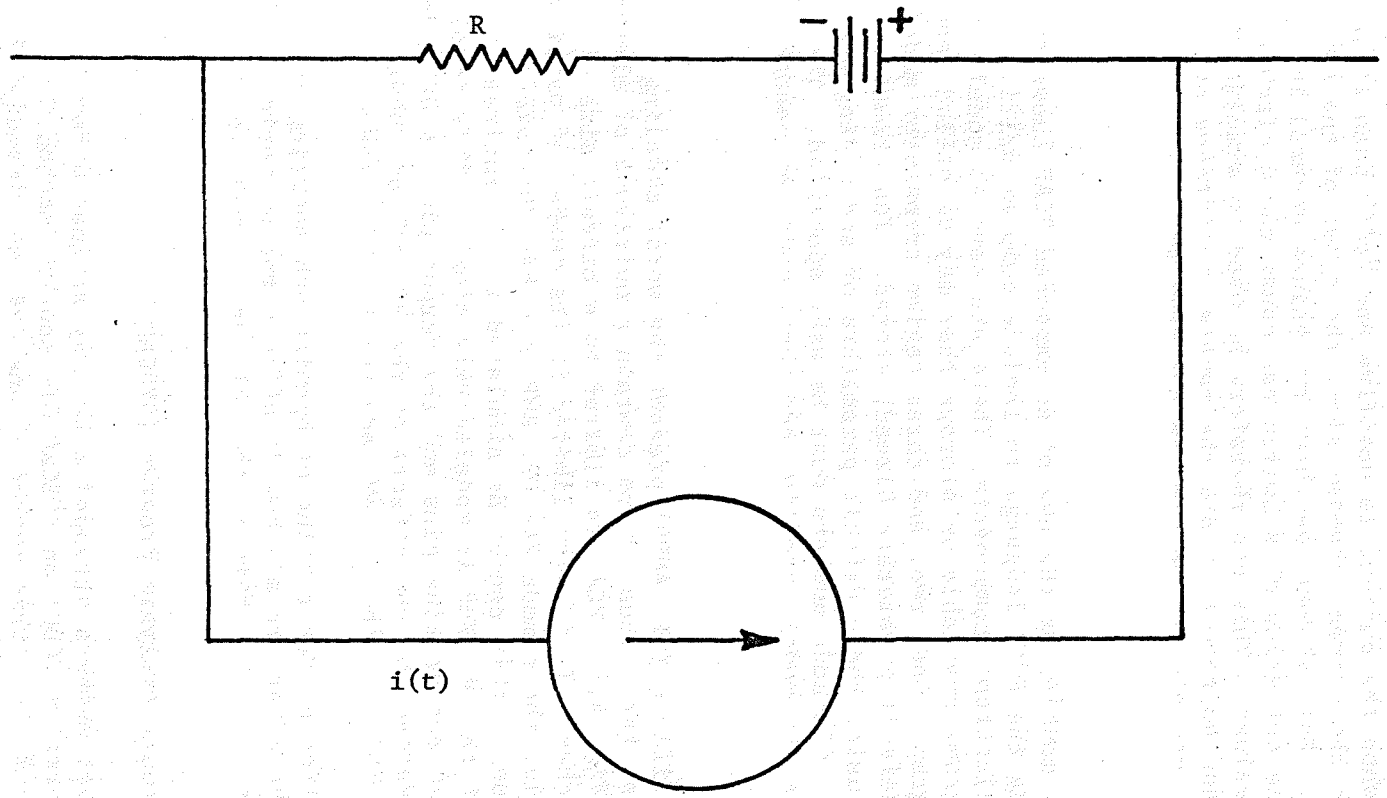

Fig. 4.1. Switch Circuit to Replace Diode.

their current monitored throughout the transient solution. The switch is considered "on" when the current is positive and "off" when it is negative. Thus when the current changes sign, the sense of the switch changes accordingly. Each element can have two values entered in its input data. Then the actuation of a switch can cause these circuit elements to change values. This can therefore be used to simulate the forward conduction and voltage drop and the reverse resistance of a diode. Zener diodes can also be modeled in the same way.

Transistors

A transistor is modeled by the use of an expanded ECAP known as PRECAP, which extends the ECAP language to include complex multi-element models for electronic components. There are several models in the form of sub-programs available on storage that may be called upon within the ECAP program. One, two, and three region transistor models are available with default parameters already stored. The transistor model may be called using these default parameters or specifying new ones. The transistor pin-node numbers must be user specified. The computer then inserts the model, creating additonal nodes as needed.

Operational Amplifiers

Operational amplifiers (OP. AMPS) present the worst modeling problem encountered so far. These chips contain a multitude of elements in themselves. See Fig. 4.2. ECAP is limited to a circuit size of 20 nodes and 60 branches. It is also limited in its number of particular elements. For example, the common 741 OP. AMP chip has 20 transistors and 23 nodes. Obviously, this cannot be simulated in its entirety. Instead the effect of the OP. AMP is modeled very simply. This involved only the inverting and noniverting pins and the output pin. A dependent current source is inserted and the effects of the OP. AMP are observed. Fig. 4.3 depicts the model of the OP. AMP adopted in this paper.

This does not allow proper testing of opening and shorting each and every pin with the others to see how it affects the operation. This is a serious drawback, but this is the only way to model such a device on ECAP.

4.2.2 Systems of Circuit Analysis Program (SYSCAP-II)

One of the project members attended a two-day seminar offered by Control Data Corporation (CDC) on SYSCAP-II, another method for electronic circuit analysis. This method of analysis was immediately put to use to evaluate the Westinghouse undervoltage relay described in the previous chapter.

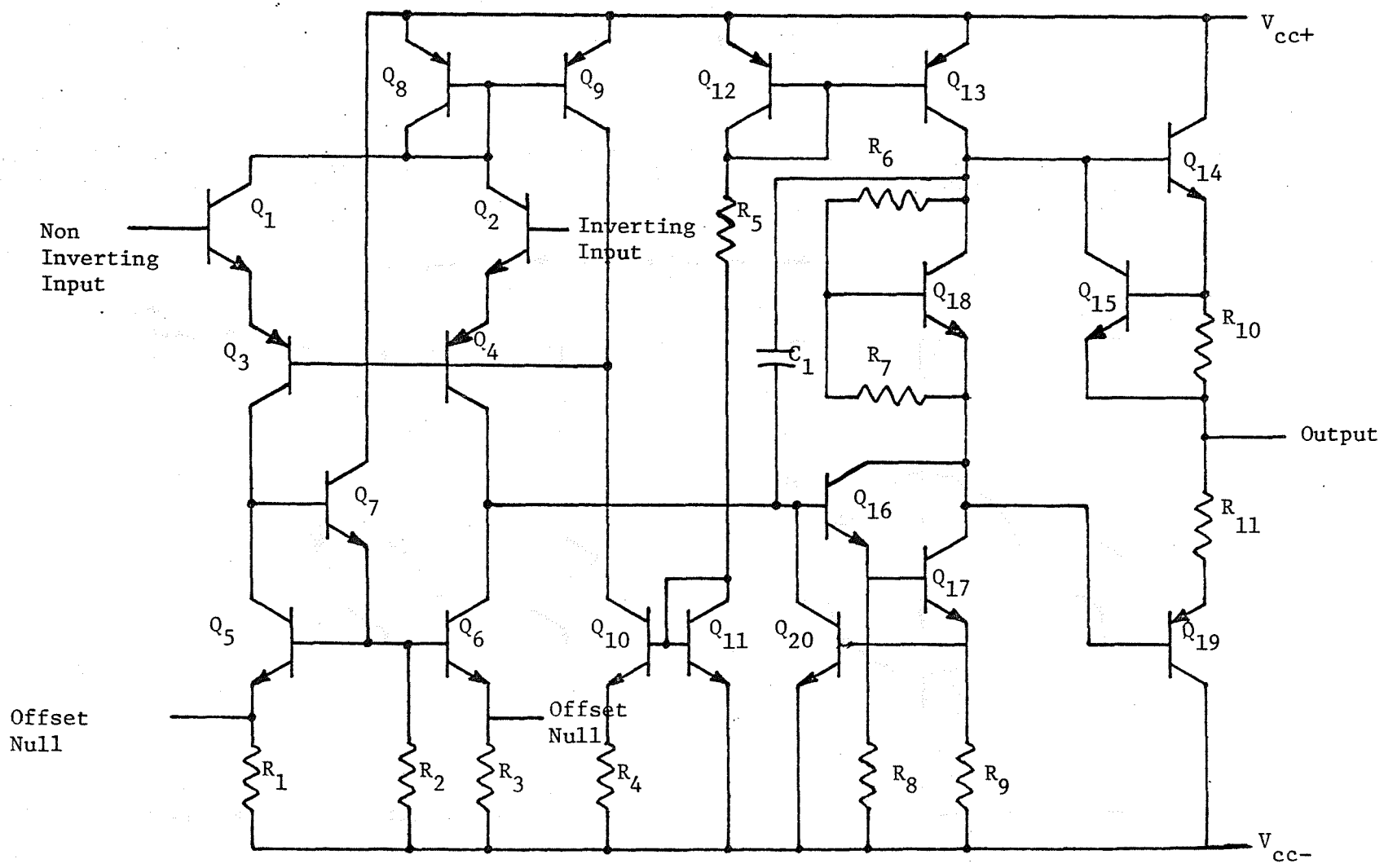

Fig. 4.2. Schematic Diagram of LM741C OP. AMP Chip.

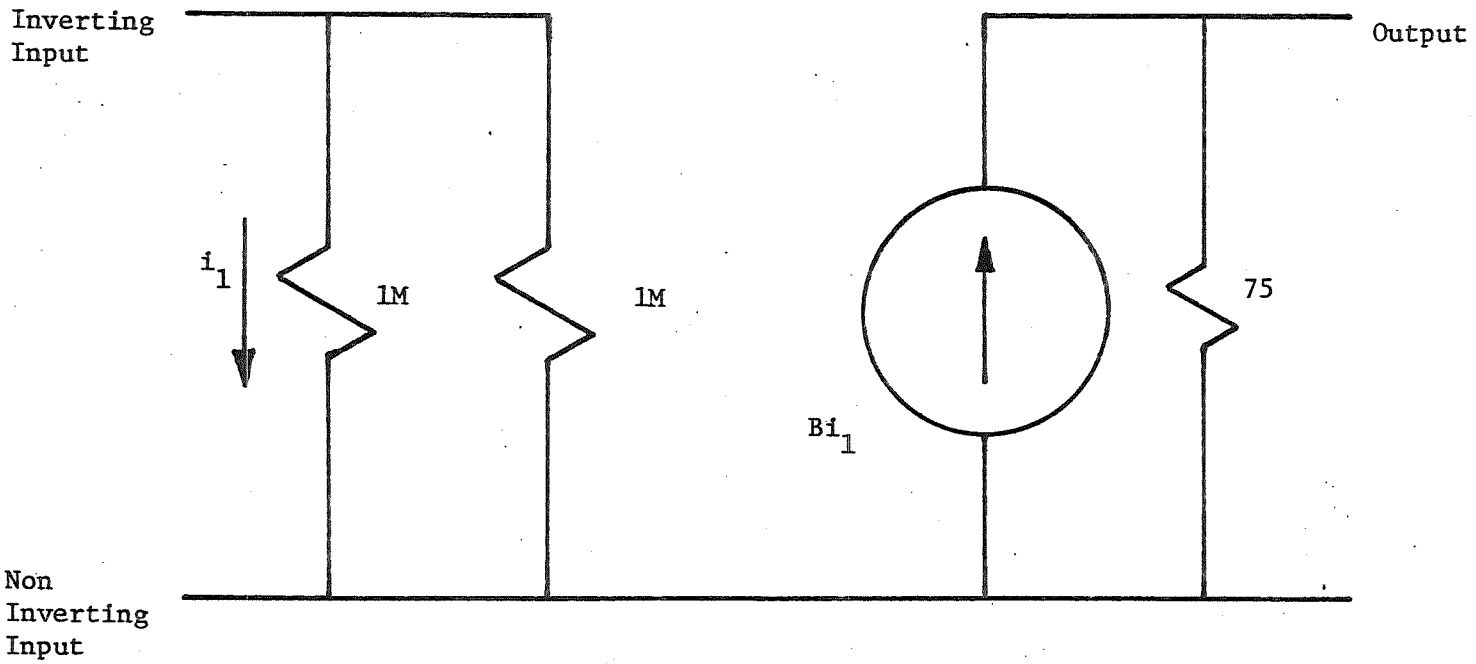

Fig. 4.3. Basic Model for LM741C OP. AMP. $B=-1.33\times10^{9}$.

The system consists of a set of programs that perform static/dynamic and linear/nonlinear analyses of electronic circuits. Basically an electronic circuit is simulated by creating a mathematical model of that circuit's topology. The model usually consists of a series of nodes which are interconnected by circuit elements and devices and are driven by signal sources and power supplies. The topology of the circuit is coded into a form compatible with the SYSCAP system. The system also includes a built-in semi-conductor device parameter data base (DATA BANK) which simplifies the semiconductor coding for the user.

This input data is then submitted to one (or more) of the SYSCAP systems' analysis programs that is, ALCAP, DICAP and TRACAP. These programs write the model equations for the circuit and respectively perform linear ac, dc, and transient analyses on the user's circuit. From the user point of view this canned program is simpler than ECAP. Also, it can handle larger size of systems and the entire fail-safe performance results can be obtained with one computer run, whereas, ECAP requires one run for each mode of failure.

4.3 LABORATORY TESTS FOR PRACTICAL FAIL-SAFE ANALYSIS

While the programs described in the previous section simulate the opening and shorting of every component in the devices, the two modes of failure can be physically done by conducting open-circuit and short-circuit tests in the laboratory. The laboratory results will be useful in verifying the theoretical results of the device. In the open-circuit tests on a solid-state device, each component of it is physically removed from the board. Similarly every component of the device is physically shorted in the short-circuit test. By monitoring the level of current in the holding coil or similar component of the device, the decision on the fail-safe performance can be made.

Before performing the destructive open- and short-circuit tests, it is desirable to test the calibration of the device. Also, the device should be subjected to transient voltages of different frequencies to test its dynamic behavior.

4.4. FAIL-SAFE ANALYSIS OF LEE TRIP

The Lee Trip is a solid-state overcurrent relay. Fig. 4.4 shows the circuit of the device.

4.1.1 Theoretical Analysis:

The two operational amplifiers were broken down to their simplest linear form and modeled with resistors and voltage sources. The transistor was modeled using a different software package called PRECAP, which is compatible with ECAP. All diodes were represented as switches. Two portions of the device's circuit were not modeled: the power supply including transformer and a thyristor resetting circuit, since these play secondary roles in the successful operation of the device. All other elements (linear and passive) were modeled without much difficulty.

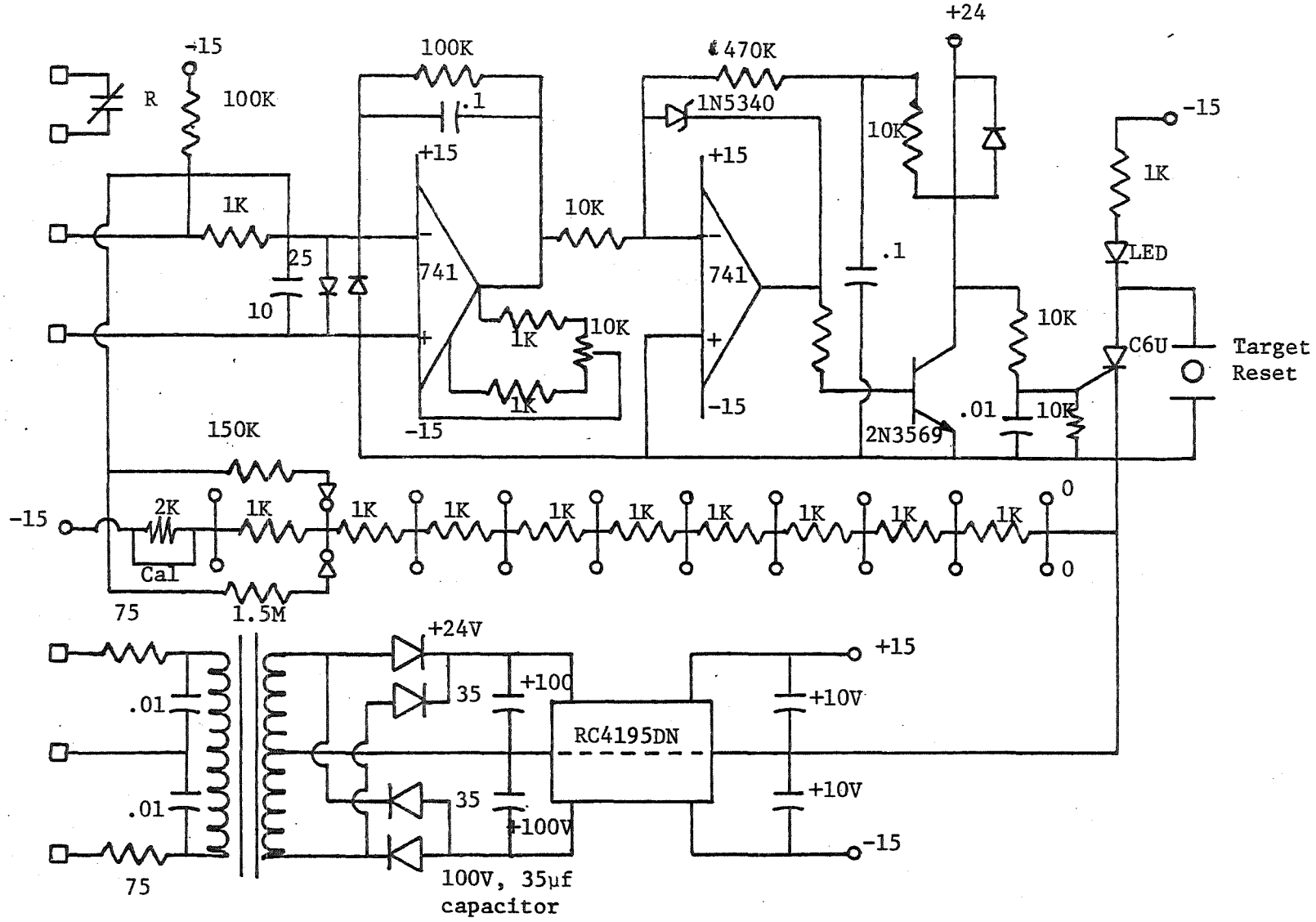

Fig. 4.4. Lee Overcurrent Relay (Solid State).

After a few trial (and error) runs were made, the model for the device took shape and efficiently represented the circuit. After that goal was reached, a control program, with all inputs and elements normal, was run with varied trip settings to determine the validity of the model. Then the device was systematically tested, element by element, to determine theoretically if the device was fail-safe. This was done by simulating the shorting and opening of all the important components, keeping the trip setting constant at 40 mV. The results are shown in concise form in Tables 4.1 and 4.2, which show four different types of response of the relay: normal operation, degraded operation (that is the relay operates successfully, but above or below 40 mV), fail-safe and fail-unsafe operations.

A sample of the ECAP listings and plots are given in Appendix A.

TABLE 4.1

CONCISE RESULTS OF THEORETICAL ANALYSIS OF OCR (OPENING OF COMPONENTS)

Opening of Components Resulted in				
Normal Operation	Degraded Operation		Fail-safe (Relay de-energized)	Failed Unsafe (Relay does Not deenergize)
		Drop Out Voltage		
R_3 R_{14} R_2 R_5 R_{12} R_{15} C_7 C_8 C_9 C_{10} D_6 D_5	R_8	68mV	R_9 R_6 R_4	R_7

TABLE 4.2

CONCISE RESULTS OF THEORETICAL
ANALYSIS OF OCR (SHORTING OF COMPONENTS)

Nornal Operation	Shorting of Components Resulted in			
	Degraded Operation		Fail-safe (Relay de-energized)	Failed Unsafe (Relay does Not deenergize)
		Drop Out Voltage		
R3			R_7	R_2
			R_{12}	R_6
R_9			R_5	
R_4			R_{14}	
R_{15}			R_8	
C_9				
D_6			C_7	
C_{10}			C_8	

4.4.2 Practical Analysis

While the theoretical investigation was being carried out, the device was subjected to several laboratory tests. A brief description of the tests along with the results are given below.

A. Calibration Test The results of the calibration test show that the relay trips with an error of about $\pm$2% of the trip setting. The results are given below.

Trip setting voltage in mV	Relay drop-out voltage in mV	Relay pull-in voltage in mV
10	10	5.2
15	15	10.2
20	20.1	15.3
25	25.2	20.4
30	29.9	25.2
35	35.0	30.2
40	40.0	35.3
45	45.0	40.3
50	50.0	45.2
55	54.9	50.2
60	60.1	55.1
65	65.6	60.3
70	70.4	65.6
75	75.2	70.6
80	80.6	76.6
85	85.7	81.0
90	92.6	86.5

The setting device or the test equipments might have introduced the error, which is the difference between the trip setting and actual relay drop-out voltages.

B. Transient Voltage Test Both triangular and square wave voltages were applied to the relay at two different frequencies, namely 0.1 and 1 Hz. The inputs as well as the contact responses were recorded. The relay did not show any malfunctioning in all the cases, when the output from the strip chart recorders were observed.

C. Open Circuit Test The relay coil performance was observed by opening one component at a time, while keeping all others in their normal condition. The test was repeated for most of the components. Throughout the tests the trip setting was kept constant at 40 mV. The results are given in the same form as Tables 4.1 and 4.2, the theoretical results.

TABLE 4.3

CONCISE RESULTS OF OPEN CIRCUIT TEST ON OCR

Normal Operation	Opening of Components Resulted in				
	Degraded Operation			Fail safe (Relay de-energized immediately as the component was opened)	Fail unsafe (Relay remained energized from the instant of opening the component)
		Drop out voltage (mV)	Pull in voltage (mV)		
R_1	R_8	43.0	37.8	Dual Decade Switch	R_7
R_2	R_{10}	43.5	39.1	R_4	
R_3	R_{11}	42.0	36.7	R_9	
R_{12}	R_{13}	34.4	33.7	R_{16}	
R_{14}	D_1, D_2	Vibration of contacts at 34.0 and drop out at 35.0		R_{17}	
R_{15}				Transformer	
C_1				Transistor	
C_2				Relay Coil	
C_3		39.5	33.8		
C_4	D_3	39.5	34.2		
C_5	D_4		34.2		
C_6					
C_7					
C_8					
C_9					
C_{10}					
SCR					
LED					
D_5					
D_6					
D_7					
D_8					

It was not certain whether the components that did not affect the normal operation of the relay would not have done so if left open for a longer time.

D. Short-Circuit Tests This test was similar to the open-circuit test. All components were shorted one at a time. The detailed results are shown in Table 4.4.

TABLE 4.4

CONCISE RESULTS OF SHORT-CIRCUIT TEST ON OCR

Shorting of Components Resulted in				
Normal Operation	Degraded Operation		Fail safe (Relay de-energized immediately as the component was shorted).	Fail unsafe (Relay remained energized from the instant of shorting the component).
	Drop-out voltage (mV)	Pull-in voltage (mV)		
R_3	R_{10} 38.8	34.3	R_1	R_2
R_4			R_7	R_5
R_9			R_8	R_6
R_{10}			R_{12}	R_{14}
R_{13}			C_5	C_6
R_{15}			C_8	C_7
R_{16}			D_1	D_3
R_{17}			D_2	D_4
C_1			D_5	D_7
C_2			D_6	D_8
C_9			Transformer	Transistor
C_{10}			Relay Coil	

4.4.3 Results and Conclusions

Close observation of Tables 4.1 to 4.4 reveals that the theoretical results of the OCR were 87% consistent with the laboratory results. While the entire circuit was tested in the laboratory, the power supply subsystem shown in the bottom part of Fig. 4.4 of the circuit could not be modeled in the theoretical analysis due to the dimensional limitation of the ECAP software. This is one of the possible reasons for the 13% inconsistency. Another reason for the disagreement in both the results could be due to the differences in parameter values used in the theoretical analysis and their actual values when the laboratory tests were done.

From the results of these two investigations it was observed that the resistor R_7 failed unsafe in the open mode of failure and the resistors R_2 and R_6 failed unsafe in the shorted mode. These components are therefore the critical parameters. The other nine components which failed unsafe in the short-circuit test should be examined closely. If the Lee-Trip were to be a perfect fail-safe device, considerable modification in the circuitry would be required. It was learned from the Lee Engineering personnel that some modifications are in progress as of this date.

4.5 FAIL-SAFE ANALYSIS OF SOLID-STATE UVR

The functions of this solid-state UVR along with its schematic diagram are given in Section 3.4 of Chapter III.

4.51 Theoretical Analysis

The undervoltage relay circuit is modeled following the standard format as outlined in the SYSCAP-II manual. All parameters in the circuit except the transformer, bridge and SCR are modeled to simplify the analysis. Then all the desired component failures are simulated in both the open and short modes systematically using the Circuit Failure Simulation (CFS) option. It is assumed in the analysis that neither simultaneous nor sequential failure of components occur. The current through the resistor R_{13} is monitored, since this is the current which would control the SCR, which in turn controls the indicator. For the UVR to be fail-safe whenever a component fails, (see the definition given earlier in this chapter) the current through R_{13} must decrease from several milliamperes (necessary to turn on the SCR) to microampere level and turn off the indicator, if not the component has failed unsafe.

Appendix B shows a sample of the SYSCAP-II listings. Appendix B shows a sample of the SYSCAP-II listings. Table 4.5 is a plot of the "change in the current through R_{13} vs. failure number" for all component failures obtained from the program. From this graphical plot,

Table 4.6 is generated which shows the concise results. From this table it can be observed that only the resistor R_2 failed-unsafe in both the short and open mode. 13 components as listed in the table totally failed-safe. The remaining components failed safe or unsafe in either open mode or short mode.

4.5.2 Practical Analysis

In order to verify the theoretical results of the fail-safe analysis. the failure of each of the components is simulated in the laboratory, Each component is physically opened and shorted and the device performance is observed for each of the failures. For the device to be fail-safe it is expected to drop out at the drop-out value (70% of 120 volts) $\pm$5% tolerance value. That means if the device drops out between 63 volts and 77 volts for each failure condition, it is considered to fail-safe. The detailed results of the tests performed on the UVR are tabulated in Table 4.7 in the same format at Table 4.6. In this case also, R_2 failed totally unsafe. 22 components failed safe in both the open and short mode. The other remaining components failed safe in one mode and unsafe in the other mode.

Comparing Tables 4.5 and 4.7, it is evident that resistor R_2 is the only component that failed unsafe and is therefore the critical component. The device needs to be redesigned with respect to this component. The following components failed safe: Resistors R_3, R_5, R_{10}, R_{11}, POT1, POT2, capacitor C_3, and diodes D_3, D_4, and D_5. The results for the other components did not agree between the theoretical and practical approaches. Some of the possible reasons are (a) the entire subsystem C, the transformer and the input capacitor C_1 are not included in the theoretical analysis, whereas they are present when the laboratory tests are done on the UVR, and (b) the inadequancy of modeling the active components of the device.

4.6 OHIO BRASS OVERCURRENT RELAY

4.6.1 Theoretical Analysis

Another overcurrent relay which is being studied and tested is the Ohio-Brass overcurrent relay. The Ohio Brass overcurrent relay is similar in design to the Lee Trip. The circuit is more complicated due to an additional operational amplifier and several diodes. Since diodes are represented as switches, this greatly increases the complexity of the ECAP model. Because of this complexity, the ECAP program had to be completely rewritten. The model previously used was the basic 741 operational amplifier model with two inputs and one output. There is no provision for simulating the offset or bias voltages in the fail-safe design. A new model is under consideration. This one simulates all the internal connections and the external pin connections of the 741 operational amplifier. There are twenty transistors which are called from the PRECAP program.

TABLE 4.5

RESULTS OF THEORETICAL FAIL-SAFE ANALYSIS FROM SYSCAP PROGRAM

Failure Number	Component Failed/Mode	Change in current level through R_{13} in milliamps: When normal voltage is detected (0 to 13)	Change in current level through R_{13} in milliamps: When under-voltage is detected (0 to 7)	Failed: Safe(S) or Unsafe(U)
1	T_1/open(O)		→	U
2	T_1/short(S)	←		S
3	T_2/O	←		S
4	T_2/S		→	U
5	T3/O		→	U
6	T3/S	←		S
7	T_4/O	←		S
8	T_4/S		→	U
9	DZ/O	←		S
10	DZ/S		→	U
11	D_1/O			U
12	D_1/S	←		S
13	D_2/O	←		S
14	D_2/S	←		S
15	D3/O	←		S
16	D3/S	←	→ 1.2	S
17	C1/O	←		S
18	C1/S	←		S
19	C_2/O	←		S
20	C_2/S	←		S
21	R10/O	←		S
22	R10/S	←		S
23	R_{11}/O	←		S
24	R_{11}/S	←	→ 2.4	S
25	R_{12}/O	←		S
26	R_{12}/S	←		S
27	R_{13}/O	←		S
28	R_{13}/S	←		S
29	R_{14}/O	←		S
30	R_{14}/S	←		S
31	R_{15}/O	←		S
32	R_{15}/S	←		S
33	R_1/O	←		S
34	R_1/S		→	U
35	R_2/O		→	U
36	R_2/S		→	U
37	R_3/O	←		S
38	R_3/S	←		S
39	R_4/O		→	U
40	R_4/S	←		S
41	R_5/O	←		S
42	R_5/S	←		S
43	R_6/O		→	U
44	R_6/S			U
45	R_7/O			U
46	R_7/S		→	U
47	R_8/O		→	U
48	R_8/S	←		S
49	R_9/O	←		S
50	R_9/S	←		S

TABLE 4.6

CONCISE RESULTS OF THEORETICAL FAIL-SAFE ANALYSIS OF UVR

Components that totally failed unsafe	Components that totally failed safe		Components that failed safe in open mode and unsafe in short mode	Components that failed safe in short mode and unsafe in open mode
R_2	R3	C_2	R_1	R_4
	R5	C_3	R_7	R_6
	R9	D_3	DZ	R_8
	R_{10}	D_4	T_2	T_1
	R_{11}	D_5	T_4	T_3
	R_{12}			
	POT1			
	POT2			

TABLE 4.7

CONCISE RESULTS OF PRACTICAL FAIL-SAFE ANALYSIS OF UVR

Components that totally failed unsafe	Components that totally failed safe		Components that failed safe in open mode and unsafe in short mode	Components that failed safe in short mode and unsafe in open mode
R_2	R_1	C_1	NONE	D_1
	R_3	C_3		D_2
	R_4	D_2		C_2
	R_5	D_3		T_2
	R_6	D_4		
	R_7	D_5		
	R_8	T_1		
	R_9	T_3		
	R_{10}	T_4		
	R_{11}			
	R_{12}			
	POT1			
	POT2			

However, this new model proved too complicated for ECAP to handle. When PRECAP transistor model is used, several switches are added to the circuit. Therefore, with 20 transistors for just one section of the circuit (the op amp), 60 switches were introduced. There was just too much switch chatter to solve the circuit. The timed increment of calculations never got past zero time becuase of the switch chatter. Switch chatter is a result of the circuit variables (current and voltage) taking one value at the initial switchpolarities and then changing when certain switches change. This causes certain other switches to change again. The more switches there are, the worse the chatter problem is. SYSCAP is being tried in place of ECAP to alleviate the problem.

4.7 RESULTS, SUMMARY, AND CONCLUSIONS ON FAIL-SAFE ASSESSMENT

The fail-safe assessment of three solid-state protective devices is presented in this chapter. The assessment was made by conducting both the theoretical and practical analyses. The recourse to the two approaches was taken to verify each other's results and strengthen them so that they are more dependable.

The analyses and the results of the Lee Trip overcurrent relay and the Westinghouse UVR are given in sections 4.4 and 4.5, respectively. The components which failed unsafe were identified from the results and it was found that both the circuits need design modifications with respect to these critical components. In fact, it has been learned that these devices are undergoing several modifications. (Before the final versions of these devices are allowed into the mines, their fail-safe behavior should be evaluated using the techniques outlined in this Chapter).

The Lee Trip was theoretically analyzed by the ECAP software, whereas the UVR was analyzed using the SYSCAP-II canned program. During the course of the investigation it was found that ECAP is limited in scope and can be applied to smaller size circuits only. On the other hand, the SYSCAP program is versatile, faster in execution, and can easily be used for modeling larger size devices. In fact, it is being used to back up the ECAP results on the Lee Trip.

SYSCAP is also being used for analyzing the Ohio-Brass overcurrent relay, which has been suceessfully modeled; but the final results have not yet been obtained. The work on the Pemco overcurrent relay, and the Christy Laboratory's meter relay have started. Some of the details on the circuitry are not available and proper contact has been established to get all the required information. Work is also underway to perform the laboratory tests on these devices.

A solid-state ground monitor manufactured by EEEI is also being investigated for its fail-safe performance using the SYSCAP program and the laboratory tests. This task was undertaken upon the request of the research team working on U.S.B.M. Grant G0144138. This circuit has several redundancies. This means that there are several repeatable segments of the circuit. This is very conveniently handled by the SYSCAP's modeling system.

REFERENCES

1. Mining Enforcement and Safety Administration, Guidelines for Evaluation of Metered Relays and Solid-State dc Overcurrent Devices for Protecting dc Trolley Feeder Wires, (document).

2. IBM, 1620 Electronic Circuit Analysis Program, Users Manual, General Systems Division, Atlanta, Georgia, April 1970.

3. Control Data Corporation, Cybernet Services, User Information Maunal, Data Services Publications, Minneapolis, Mn., 1975.

APPENDIX A

SAMPLE OF ECAP LISTINGS AND RESULTS OF LEE TRIP

```
*** VU ECAP PREPROCESSOR RUN 09/01/76 AT 10:21:15  VERSION 2.0

001           TRANSIENT ANALYSIS
002     QS*2B.BASE=17,COLL=15,VCX=24
003     B1      N(1,0),R=1000
004     B2      N(2,1),R=1000
005     B3      N(3,2),R=1000
006     B4      N(4,3),R=1000
007     B5      N(5,4),R=1000                          FORTRAN STATEMENTS FOR ECAP
008     B6      N(6,5),R=1000
009     B7      N(7,6),R=1000
010     B8      N(8,7),R=1000
011     B9      N(9,8),R=1000
012     B10     N(0,9),R=2000,E=15
013     B11     N(7,10),R=1.5E6
014     B12     N(2,10),R=1.5E5
        C THIS TRIAL HAS A TRIP SETTING OF 20 MILLIVOLTS
015     B13     N(10,11),R=1E3
016     B14     N(11,0),R=1E5,E=15
017     B15     N(10,0),R=1E6
018     B16     N(10,0),R=1E6
019     B17     N(10,12),R=1E5
020     B18     N(0,12),R=75
021     B19     N(12,13),R=1E4
022     B20     N(13,0),R=1E6
023     B21     N(13,0),R=1E6
024     B22     N(14,13),R=(1E4,5),E=(0,-10.5)
025     B23     N(13,18),R=4.7E5
026     B24     N(0,14),R=75
027     B25     N(14,17)R=3.3E3
028     B26     N(15,19),R=1E4
029     B27     N(15,16),R=(1E6,1E2),E=(0,-0.8)
030     B28     N(20,15),R=300
031     B29     N(0,11),C=500E-6,I=2.5E-4
032     B30     N(0,16),R=0.1,E=24
033     B31     N(10,0),C=1.0E-5
034     B32     N(10,12),C=0.1E-6
035     B33     N(18,15),R=1E4
036     B34     N(18,0),C=0.1E-6
037     B35     N(19,0),R=1E4
038     B36     N(19,0),C=0.1E-7
039     B37     N(16,20),L=0.824
040     T1      B(15,18),BETA=-1.33E9
041     T2      B(20,24),BETA=-1.33E9
042     S1      B=22,(22),OFF
043     S2      B=27,(27),ON
044           TIME STEP = 1E-3
045           OUTPUT INTERVAL = 3
046           FINISH TIME = 200E-3
047           PRINT,VOLTAGES,CURRENTS
        C*    LIST(TIME,VO(11),VO(10),VO(12),VO(13),VC(14),CL(28),CU(37))
        C*    PLOT(TIME,VO(11))
        C*    PLOT(TIME,VO(14))
        C*    PLOT(TIME,CU(28))
        C*    PLOT(TIME,CU(25))

*** EXPANSION OF MODEL QS*2B   USED IN LINE 002 :
```

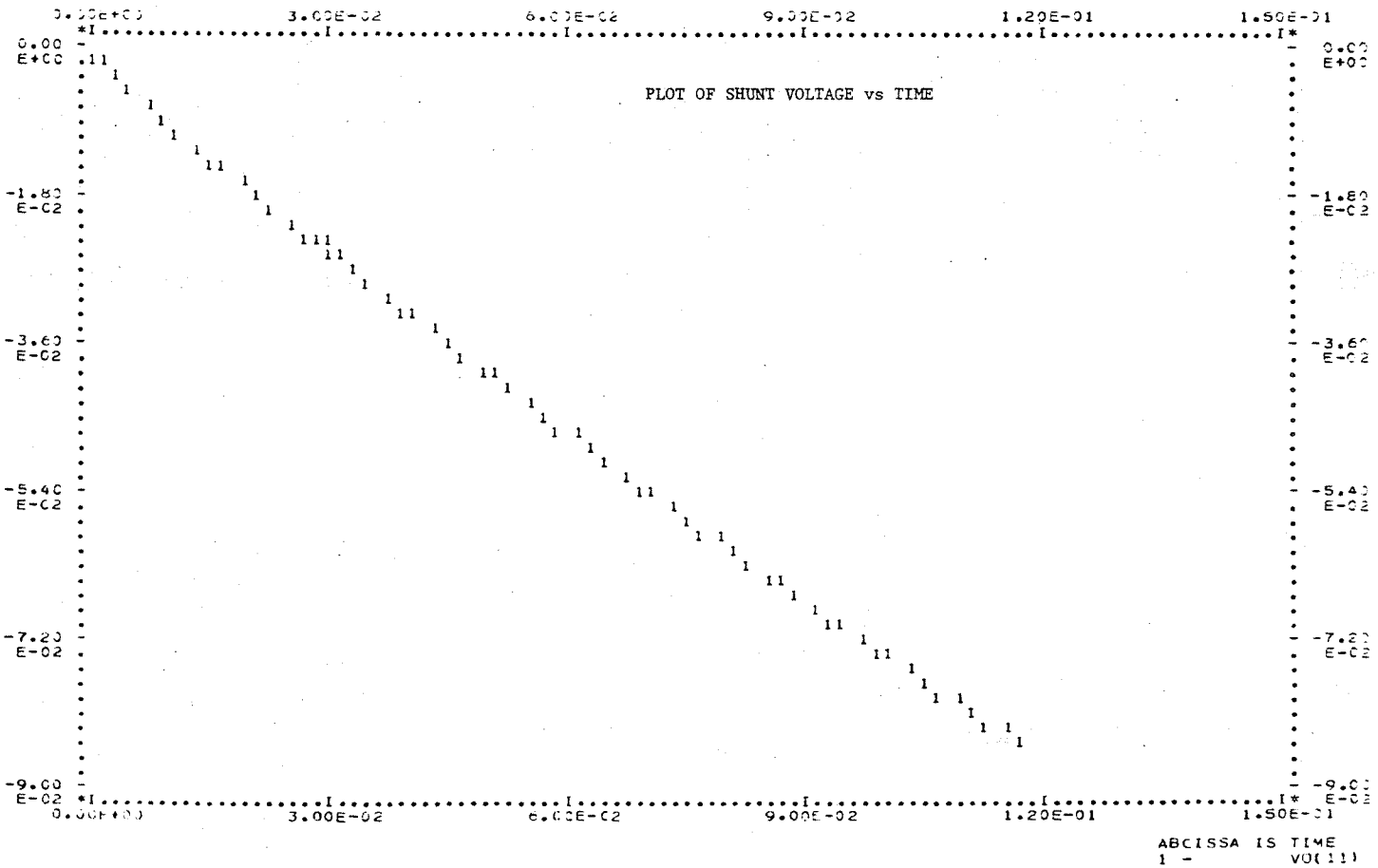
PLOT OF SHUNT VOLTAGE vs TIME
0.00E+00
3.00E-02
6.00E-02
9.00E-02
1.20E-01
1.50E-01
0.00 E+00
-1.80 E-02
-3.60 E-02
-5.40 E-02
-7.20 E-02
-9.00 E-02
ABCISSA IS TIME
1 - V0(1 1)

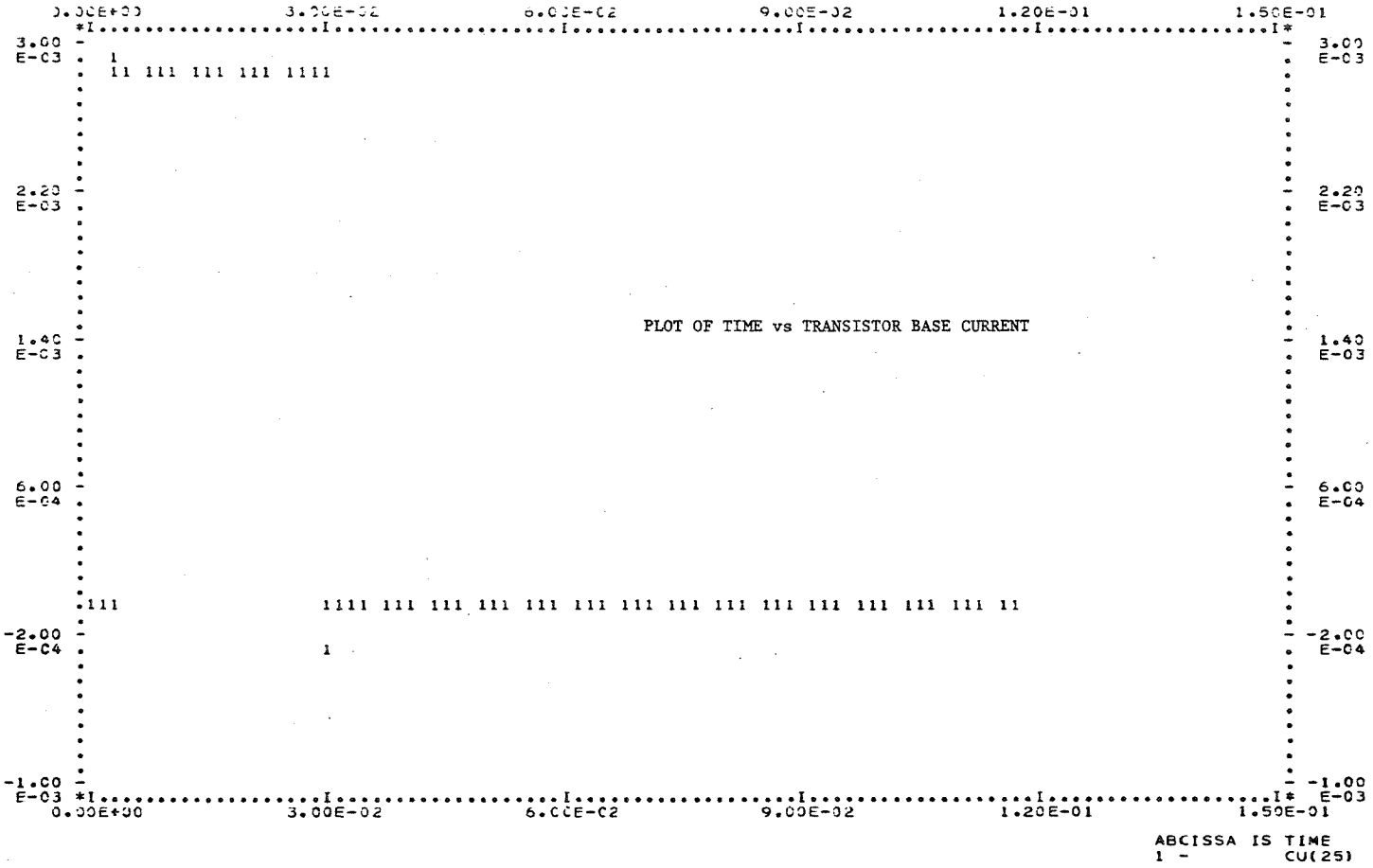
0.00E+00
3.00E-02
6.00E-02
9.00E-02
1.20E-01
1.50E-01
3.00 E-03
2.20 E-03
1.40 E-03
6.00 E-04
-2.00 E-04
-1.00 E-03
PLOT OF TIME vs TRANSISTOR BASE CURRENT
ABCISSA IS TIME
1 - CU(25)

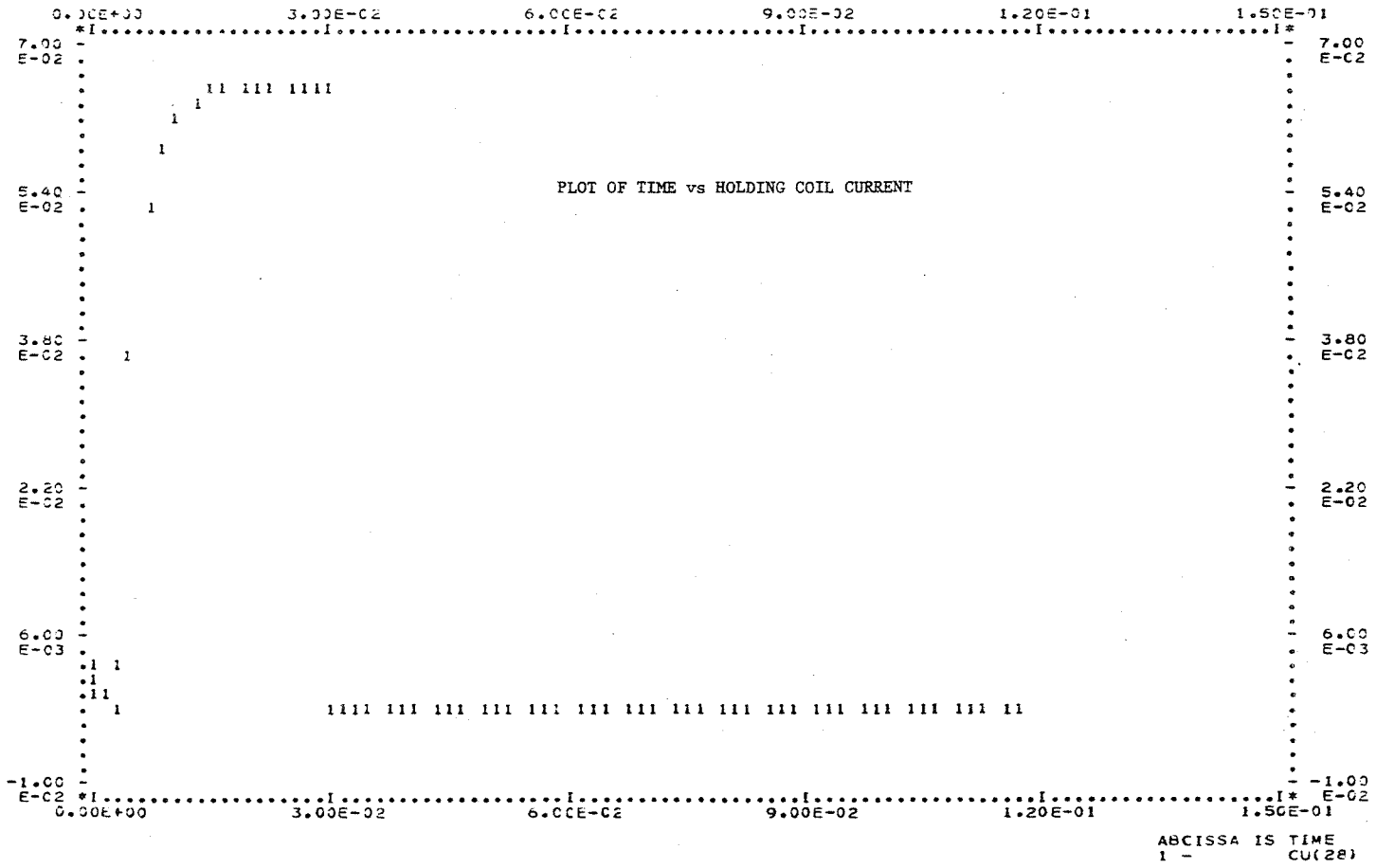
PLOT OF TIME vs HOLDING COIL CURRENT
0.00E+00
3.00E-02
6.00E-02
9.00E-02
1.20E-01
1.50E-01
7.00 E-02
5.40 E-02
3.80 E-02
2.20 E-02
6.00 E-03
-1.00 E-02
ABCISSA IS TIME
1 - CU(28)

APPENDIX B

SAMPLE OF SYSCAP-II LISTINGS

AND RESULTS OF WESTINGHOUSE SOLID-STATE UVR

```
DICAP
CFS
RELEASE
C1(0,1)250U
R1(3,1)1K
R2(0,3)1K
R3(3,7)560
R4(1,10)1K
R5(11,12)220
R6(10,13)560
R7(1,9)3.7K
R8(8,0)3,9K
R9(6,0)2.2K
R10(5,4)470
R11(2,3)120K
R12(2,14)400
R13(14,0)I,150
R14(10,11)300
R15(3,5)300
C2(13,7)0.1U
E1(+1,-0)9
D1(A13,C3)1N456
D2(A3,C13)1N456
D3(A2,C4)1N456
DZ1(A0,C12)1N751A
Q1,NPN(B13,C9,E8)2N2222
Q2,NPN(B7,C1,E8)2N2222
Q3,PNP(B9,C6,E1)2N3637
Q4,PNP(B6,C2,E1)2N2945 3638
FINIS
PLOT=NODE14,R13IR
SPECIAL
RALL,DALL,QMIN,QALL,N1/0,N13/7,STOP
END OF DATA
END OF DECK SETUP PHASE
```

CHAPTER V

RELAY/FUSE COORDINATION PROGRAMS

5.1 INTRODUCTION

A very limited effort that was started during 1974-75 was continued during 1975-76 to develop programs for use in the field by MESA inspectors for checking the settings or selection of relays and fuses. During the first year, the Coordination Program was developed, largely by combining various existing programs available at West Virginia University or from electric utilities. This program seemed to work reasonably well but did not have the ease of data input desired. Further testing of the program revealed that its results were exceedingly data dependent. In fact, the order of data input could change the results radically. Thus, two goals were established:

1) to remove all problems with the reliability of the program and

2) to provide free-format input capability .

Both of these goals have been achieved.

A second area of effort has been to further develop the HP-65 programming forfuse coordination. This was done by extending the program to allow N-link fuses. In addition, an HP-65 program was acquired from MESA to calculate the short circuit currents necessary to properly coordinate the fuses. This program is limited to radial systems but this is not a severe restriction for mine power systems which are largely radial.

5.2 COORDINATION PROGRAM RELIABILITY

A major fault was observed in the execution of the Coordination Program. Successive runs indicated that the program was data dependent, yielding solutions that were only sporadically correct. Solutions were either entirely correct or wild and unpredictable. The problem was traced back, not to the data themselves but rather to how they were entered. This applied specifically to the order in which the bus numbers for a given element (track section, breaker, or rectifier) were entered. The building algorithm in the subroutine FAULT did not allow for certain cases causing wrong values to be used in forming the bus impedance matrix. Since the building process was cumulative, the error effects were compounded and subsequently the results bore no resemblance to the correct answers.

To correct the error the subroutine FAULT was expanded to account for the additional possible cases. Further computer runs of the Coordination Program with the bus number order changed yielded consistent and sound results.

5.3 FREE-FORMAT FEATURE

One of the original requirements of the Coordination Program was that the data be easy to enter. It's use in the interactive mode was a worthwhile move in that direction. There still existed a problem, however, in that there was a need to adhere to a strict format which had to be defined with each query for new data. An individual loading the program had to take care in entering the data, because keying an invalid character did not trigger a "reenter data" request and would usually result in an abnormal termination to the program's execution requiring the reentry of the data from the beginning. The error trigger of the program was very limited, namely it would only act for a character outside the expected data field (a shift-right in the data).

In preparing to adapt the Coordination Program to become more flexible in accepting its input some investigation was conducted along the lines of available free-format routines. One stipulation was that the routine should be coded in Fortran so that the entire program could be run at other computer installations that accept Fortran. For this reason, the free-format routines which may have been available had to be discarded, since most of them were written in an assembler or machine language which may not always be operational at other installations.

To free the input to the Corrdination Program from its present format, and improve the error detection procedure of the program, three subroutines were developed. The main program first reads in the data as a string of characters and then the appropriate subroutine is called.

Subroutine IND determines if a particular string (e.g. MCM, YES, NONE, etc.) exists within the input string.

Subroutine EVAL evaluates the floating point value of a number found within the input string. The number may be entered in a variety of ways (discussed later). This applies to a single number which may or may not have additional character data in the same entry (e.g. codes).

Subroutine INTG is capable of returning any number of integer values found within the input string but in this program delivers no more than two. When two values are to be entered, a comma and/or blanks serve as delimiters.

The free-format feature eliminates the need for entering leading zero's and can allow entry of a number using an exponential or E format in several variations. The use of a decimal point is optional and if left out is understood to be to the right of the rightmost digit. An illustration of some allowed entries is shown in Fig. 5.1, a sample read-in to the Coordination Program. The input directly follows the query; the value as used by the computer follows the three asterisks in the next line.

```
THIS PROGRAM DETERMINES IF EXISTING RELAY SETTINGS AND
FUSE SIZES ARE CAPABLE OF ISOLATING FAULTS.
ENTER THE NAME OF THE MINE UNDER STUDY.
***W. VA.
ENTER LOCATION OF THE MINE.
***MORGANTOWN
PLEASE SPECIFY AC OR DC ANALYSIS.  ENTER 1 FOR DC
 OR 2 FOR AC.
1
***1
YOU ARE NOW IN THE DC MODE.  PLEASE ENTER THE NUMBER
 OF BUSSES IN THE SYSTEM.
05
***5
NOW ENTER THE BASE VOLTAGE OF  THE SYSTEM.
3E2
***300.
NOW ENTER THE BASE POWER OF THE SYSTEM IN KW.
1.5E2
*** 150.
ENTER THE NUMBER OF TRACK, TROLLEY SECTIONS
   3
*** 3
NOW ENTER THE BUS NUMBERS FOR TROLLEY SECTION NUMBER
  1
3 2
*** 3  2
NOW ENTER THE LENGTH OF  THE SECTION IN FEET.
520.
*** 520.
NOW ENTER THE TROLLEY SIZE AND CODES FOR
ELEMENT   1
400 MCM CU
*** 400. MCM CU
NOW ENTER THE TROLLEY PARALLEL FEEDER SIZE AND
CODES.  IF NONE EXISTS ENTER NONE.
1E3,MCM,CU
***1000. MCM CU
NOW ENTER THE DATA FOR RETURN FEEDER IN ELEMENT
  1 IF NONE EXISTS ENTER NONE
1E3 MCM CU
***1000. MCM CU
NOW ENTER THE WEIGHT OF TRACK IN THIS SECTION.  AND THE BONDING CODES
85 B
*** 85.B
NOW ENTER THE BUS NUMBERS FOR TROLLEY SECTION NUMBER
  2
 4  2
*** 4  2
NOW ENTER THE LENGTH OF THE SECTION IN FEET.
250.
*** 250.
IF THE WIRE AND TRACK DATA IS THE SAME
AS IN THE PREVIOUS SECTION ENTER YES. IF NOT ENTER NO
NOW ENTER THE BUS NUMBERS FOR TROLLEY SECTION NUMBER
  3
 3   4
*** 3  4
```

Fig. 5.1. Illustration of the Use of the Coordination Program with Free Format Input.

```
NOW ENTER THE LENGTH OF THE SECTION IN FEET.
50.
***  50.
IF THE WIRE AND TRACK DATA IS THE SAME
AS IN THE PREVIOUS SECTION ENTER YES.IF NOT ENTER NO
ENTER THE NUMBER OF RECTIFIERS
 1
*** 1
NOW ENTER THE BUS NUMBERS FOR RECTIFIER NUMBER  1
1,0
*** 1  0
ENTER KW RATING OF RECTIFIER   1
1.5 E 2
*** 150.
ENTER THE PERCENT IMPEDANCE OF RECTIFIER   1
7
*** 7.
ENTER THE DC OVERCURRENT RELAY SETTING FOR RECTIFIER    1
2.8E+3
***2800.
ENTER NUMBER OF BREAKERS IN THE SYSTEM
 1
*** 1
ENTER BUS NUMBERS FOR BREAKER  1
 2 1
*** 2  1
ENTER SETTING FOR BREAKER  1
25E 2
***2500.
```

Fig. 5.1. Illustration of the Use of the Coordination Program with Free Format Input.

The three subroutines also provide a more efficient input-error detection for the program. Keying an invalid (non-numeric or unexpected code) character will trigger a request to reenter data.

There are some limitations to this new free-format feature. The principal one is that a floating point entry should not be keyed in for integer data. This means that when the program queries for an integer number (i.e. number of busses, track sections, rectifiers or breakers or the bus numbers for an element) that the individual should respond with a pure number, or numbers. When the program queries for a measurement or a rating then the floating point options may be used.

The overall effect of the free-format feature has been to make the entry of input data much easier than it previously had been.

5.4 COORDINATION PROGRAM - IBM COMPATIBILITY

Proximity and ease of access to West Virginia University's IBM 360/75 computer served as justifiable reasons for checking into the possibilities of a conversion of the Coordination Program as it exists on the Control Data Corporation (CDC) system at Rockville, Md. into an executable version on IBM.

Most of the changes essentially involved some special character conversion (e.g. equal signs and parentheses) because of the difference in data card punch machines. Realignment of the program's text and some command changes were also necessary. The final change was replacement of the Job Control Language since it varies with the installation site.

The drawback to the use of the Coordination Program on the IBM machine is that it cannot be run in an interactive mode. Accordingly, the Coordination Program must run as batch, i.e. the data must follow the program directly and the program executes only once rather than executing continuously as it queries for data. However, despite this inconvenience the program's use is no longer confined to CDC operation.

5.5 ADDITIONAL DETAILS RELATED TO COORDINATION PROGRAM

In the 1974-75 annual report most of the details of the Coordination Program were presented. In this section a few of the other details of the program will be presented including the manner in which data for trolleys, track, and feeders is generated from AWG sizes and track weights, as well as the models used for circuit breakers.

5.5.1 Generation of Circuit Data

In order to keep data preparation as simple as possible it is desirable to be able to enter trolley and feeder sizes in a manner similar to the way it is specified in handbooks or application manuals. In order to do this the resistance of the conductors must be generated inside the program from the AWG size or size in circular mils. In addition, track sizes are normally specified in terms of lbs. per yard. These data should also be converted into resistance internal to the program.

The two basic materials used for electrical conductors in mine power systems are aluminum and hard drawn copper. Based on available data[1,2], the following resistivities can be used for these two materials.

Resistivity of Al = 17349.05 ohm-cmil/1000ft.

and

Resistivity of Cu = 10742 ohm-cmil/1000ft.

The error in using the figure given for copper is less than 2 percent for feeders or any shape of trolley wire.

Since the track is also a part of the electrical system, its resistivity is also important. A figure for medium carbon steel can be developed for the track resistance by using the density of medium carbon steel and its volume resistivity. The final result is

$$\text{Resistance of track} = \frac{1.0895 \text{ ohm/1000ft.}}{w}$$

where w is the weight per yard of the track.

From the above discussion it is clear that all resistances can be easily calculated if the trolley and feeder sizes can be found in circular mils. This presents no problem when the size is given in MCM or thousands of circular mils. But when AWG sizes are specified some method must be used to convert AWG sizes to circular mils.

The AWG size designation was formed by specifying two sizes, 4/0 and 36, and then determining the 38 intermediate sizes by geometric progression.

The 4/0 size is 0.4600 inch in diameter and size 36 is 0.00500 inch in diameter. From this the ratio of any diameter to the next smaller diameter is given by the following relationship:

$$r = \sqrt[39]{0.46/0.005} = 1.1229322$$

Using this ratio, one can now convert AWG size to circular mils using the following equation.

$$\text{cmils} = (460 \text{ mils}/1.1229322^{n})^{2}$$

Where n-1 is the number of intermediate sizes between 4/0 and the size to be converted.

The FORTRAN statements used to accomplish the conversion are listed below. It should be noted that in the program, 4/0 is entered as 400, 3/0 as 300, 2/0 as 200 and 1/0 as 100.

```
58 IF (SIZE. EQ. 400) GO TO 60
   IF (SIZE. EQ. 300) GO TO 61
   IF (SIZE. EQ. 200) GO TO 62
   IF (SIZE. EQ. 100) GO TO 63

60 SIZE = 1
   GO TO 65

61 SIZE = 2
   GO TO 65

62 SIZE = 3
   GO TO 65

63 SIZE = 4

65 N = SIZE - 1
   SIZE = 460/(1.1229322**N))**2
```

These few statements are much more efficient from both a computational and storage point of view than table storage and table searching.

5.5.2 Circuit Breaker Model

The circuit breakers could be modeled in the program as short and open circuits depending upon whether their contacts were closed or open, respectively. The problem with this model is that the subroutine that calculates short circuits computes only the current through an element and not into and out of nodes. Thus, it would be necessary to keep track of all the elements connected to the breaker and algebraically sum the elemental currents to find the breaker current. This is rather cumbersome so it was decided to use a very small resistance to model a breaker Actually the breaker's contacts do have a contact resistance so that thi is not a purely mathematical "model of convenience". The value selected for the breaker resistance is 0.001 ohm. This value is small enough that it will not affect the short circuit calculation but not so small that it causes round-off problems. With this model the required breaker currents are merely equal to the element currents for the 1 milliohm resistors that they are represented by. These currents are found along with all other currents in the network by the fault subroutine.

5.6 HP-65 FUSE COORDINATION PROGRAM

In the 1975 annual report, HP-65 programs were described for the coordination of type K and type T fuse links. These two fuse types are the fast and slow speed links. The third important fuse type is the N link which is the normal speed link. The HP-65 program has now been expanded to include coordination of type N fuse links.

Because the continuous current capacity of N-type fuses is somewhat different than K or T type fuses, extensive new programming was necessary. In fact, a new version of the program called "FUSES" was written. The new program is called "N-FUSES". This program basically selects fuse sizes on the basis of continuous current capacity and the full-load current at the fuse location. It doesn't factor in coordination of protective devices in series with each other. This problem is handled by the program called "N-COORD" which is used in place of "COORD", The latter being used with T and K links. The program "N-COORD" uses coordination tables to determine the minimum size fuse link which will coordinate with a specific size protective link for a given level of fault current. A different program is required by N links because they come in different standard ratings than K and T links.

Of course, programs containing the information in the coordination tables for type N fuses are needed. These three programs are called 5-15 N-DATA, 20-50 N-DATA and 60-150 N-DATA.

The requirement that the fault current level be used with the programs called "COORD" and "N-COORD" means that a method for computing fault current levels is needed. For radial systems, the required fault currents can be calculated using a separate HP-65 program written by George Fesak of MESA . This program computes the current when a fault occurs at the end of a radial system that consists of a source voltage in series with the source impedance and an unlimited series of transformers (with known percent resistance and reactance) and conductors (also with known resistance and reactance). The program computes the current magnitude and phase as well as the total system impedance, resistance and reactance. This program along with the coordination programs developed by WVU provide a very useful means of selecting fuses.

5.7 SUMMARY AND CONCLUSIONS ON RELAY/FUSE COORDINATION PROGRAMS

These programs have been developed rather slowly over a period of about eighteen months in a rather low-keyed effort. They are now sufficiently polished and reliable, as well as easy to use, that they can be tested by MESA inspectors. The principal investigator will participate in a MESA training school for electrical engineers in August of 1976. At that time, material will be distributed to these engineers to acquaint them with the programs that have been developed.

Participants at a short course conducted at West Virginia University during the summer of 1976 have also been made aware of this available software and have been supplied with program materials. Via these two continuing education programs, materials have or will be provided to about 30 practicing engineers either in MESA or in coal operating companies.

REFERENCES

1. United States Department of the Interior, Bureau of Mines, "Coal Mine Safety Electrical Inspectors Manual."

2. Donald G. Fink, "Standard Handbook for Electrical Engineers," McGraw Hill Book Company, New York, N.Y., 1969.